A TEST METHODOLOGY FOR MEASURING GASEOUS CONTAMINANT TRANSFER IN ENERGY WHEELS

A Thesis Submitted to the
College of Graduate and Postdoctoral Studies
In Partial Fulfillment of the Requirements
For the Degree of Master of Science
In the Department of Mechanical Engineering
University of Saskatchewan
Saskatoon

By

Mehrdad Torabi

PERMISSION TO USE

In presenting this thesis in partial fulfillment of the requirements for a Postgraduate degree from the University of Saskatchewan, I agree that the Libraries of this University may make it freely available for inspection. I further agree that permission for copying of this thesis in any manner, in whole or in part, for scholarly purposes may be granted by the professor or professors who supervised my thesis work or, in their absence, by the Head of the Department or the Dean of the College in which my thesis work was done. It is understood that any copying or publication or use of this thesis or parts thereof for financial gain shall not be allowed without my written permission. It is also understood that due recognition shall be given to me and to the University of Saskatchewan in any scholarly use which may be made of any material in my thesis.

DISCLAIMER

Reference in this thesis/dissertation to any specific commercial products, process, or service by trade name, trademark, manufacturer, or otherwise, does not constitute or imply its endorsement, recommendation, or favoring by the University of Saskatchewan. The views and opinions of the author expressed herein do not state or reflect those of the University of Saskatchewan, and shall not be used for advertising or product endorsement purposes.

Requests for permission to copy or to make other uses of materials in this thesis in whole or part should be addressed to:

Head of the Department of Mechanical Engineering
57 Campus Drive
University of Saskatchewan
Saskatoon, Saskatchewan S7N 5A9 Canada

OR

Dean
College of Graduate and Postdoctoral Studies
University of Saskatchewan
116 Thorvaldson Building, 110 Science Place
Saskatoon, Saskatchewan S7N 5C9 Canada

ABSTRACT

This thesis meets some of the objectives of ASHRAE Research Project 1780, titled "Test method to evaluate cross-contamination of gaseous contaminants within total energy recovery wheels" and contains a literature review and experimental measurements of contaminant transfer in energy wheels. The literature review showed that there is no established test methodology for measuring the contribution of adsorption/desorption to gaseous contaminant transfer in energy wheels. Furthermore, most of the studies lacked a rigorous uncertainty analysis. Analysis of the data in the literature revealed that the energy wheel design parameters such as face velocity have a more significant effect on the contaminant transfer rate, i.e., Exhaust Air Transfer Ratio (EATR), than operating conditions such as temperature and humidity. Furthermore, the EATR due to adsorption/desorption was higher for acetic acid, phenol, and acetaldehyde than for other contaminants, which may be due to the high water solubility and small molecular size of acetic acid, phenol, and acetaldehyde.

The thesis shows that the test facility used to measure gaseous contaminant transfer in energy wheels conserved mass and energy, provided steady state flow parameters and satisfied ASHRAE Standard 84 (2020) requirements. Experimental data showed that EATR consistently decreased with increasing air flow rate and did not change significantly with changes in outdoor air temperature. The EATR values for carbon dioxide and sulfur hexafluoride were nearly equal, indicating that carbon dioxide does not transfer by adsorption/desorption. A proposed test method for determining the contribution of adsorption/desorption in gaseous contaminant transfer in energy wheels was applied for ammonia, methanol, isopropyl alcohol, and carbon dioxide. The EATR values due to adsorption/desorption were highest for ammonia, followed by methanol, isopropyl alcohol, and carbon dioxide. The reason for the high adsorption/desorption of ammonia might be because its physical properties are similar to water.

ACKNOWLEDGEMENTS

First, I would like to sincerely thank my supervisor, Professor Carey Simonson, for his support and patience during the last few years. I have learned a lot of valuable lessons during my MSc program from my supervisor. I would also like to thank Professor Jafar Soltan, co-investigator on ASHRAE RP-1780, for his input on my research.

I would like to thank my advisory committee members, Prof. Donald Bergstrom and Prof. David Sumner, for their valuable comments and constructive feedback.

I would like to acknowledge technical assistance that I received from the departmental assistants, Mr. Hayden Reitenbach, Dr. Melanie Fauchoux, and Mr. Shawn Reinink. I specially acknowledge my fellow graduate students and post-doctoral fellows, Dr. E. Krishnan, Mr. H. Ramin, Dr. W.O. Alabi, Dr. G. Annadurai, Mr. B. Xing, Mr. A. Razmavar, Mr. T. Okolo, and Mr. M. Mostafavi Sani, for their encouragement, valuable comments, and support.

I also wish to thank my friends, Mr. Iman Jamali and Mr. Kharazm Khaledi, for their spiritual words which supported me throughout my program.

The financial assistance from American Society of Heating Refrigerating and Air-conditioning Engineers (ASHRAE), a Dean's scholarship, Russell Haid Memorial Award, Graduate Devolved Scholarship, and the Natural Sciences and Engineering Research Council of Canada (NSERC), is greatly appreciated.

TABLE OF CONTENTS

LIST OF TABLES

LIST OF FIGURES

NOMENCLATURE

ACRONYMS

AAEEs	Air-to-air energy exchangers
ASHRAE	American Society of Heating Refrigerating and Air-conditioning Engineers
CFM	Cubic feet per minute
EA	Exhaust air
EATR	Exhaust air transfer ratio
FTIR	Fourier transform infrared
HPLC	High performance liquid chromatography
HVAC	Heating, ventilating and air conditioning
IER	Ion exchange resin
ISO	International Organization for Standardization
LAMEE	Liquid-to-air membrane energy exchanger
MIBK	Methyl isobutyl ketone
NI	National Instruments
OA	Outdoor air
OACF	Outdoor air correction factor
P	Liquid circulating pump
ppb	Parts per billion
ppm	Parts per million
PVC	Polyvinyl Chloride
RA	Return air
RAMEE	Run-around membrane energy exchanger

RFP	Request-For-Proposal
RP	Research project
SA	Supply air
SG	Silica gel
VOCs	Volatile organic compounds

SYMBOLS

a	Absorptivity (m^2/mol)
A	Absorbance
b	Optical path length (m)
c	Concentration (ppm)
C	Heat capacity rate (J/K)
Cr*	Heat capacity rate ratio
C_p	Specific heat capacity (J/kg.K)
dT	Maximum deviation from time-averaged temperature (°C)
dW	Maximum deviation from time-averaged humidity (g_w/kg_a)
fpm	feet per minute (ft/min)
h	Specific enthalpy (kJ/kg)
I	Intensity of infrared radiation that has passed through the sample gas (W/m^2)
I_0	Intensity of infrared radiation for background measurement (W/m^2)
$\dot{m}$	Air mass flow rate (kg/s)
NTU	Number of transfer units on the supply or exhaust side of the wheel
P	Static pressure (Pa)

q	Heat transfer rate (W)
RH	Relative humidity (%)
rpm	Revolutions per minute (rev/min)
T	Temperature (°C)
TR	Transmittance
U	Total uncertainty
V	Face velocity (m/s)
W	Humidity ratio (g_w/kg_a)

GREEK SYMBOLS

ε	Effectiveness (%)
ω	Rotational speed (rad/s)

SUBSCRIPTS

a	Measured results for EATR and face velocity
ad	Adsorption
b	Calculated EATR and face velocity due to dilution
exhaust	Exhaust airstream
high	High
inert	Inert gas (sulfur hexafluoride in this thesis)
l	Latent
low	Low
matrix	Matrix in energy wheel
min	Minimum
non-inert	Non-inert gas

s	Sensible
supply	Supply airstream
tot	Total

CHEMICAL SYMBOLS

CO_2	Carbon dioxide
C_3H_8	Propane
C_3H_8O	Isopropyl alcohol
CH_3OH	Methanol
CHOH	Formaldehyde
N_2	Nitrogen
N_2O	Nitrous oxide
NH_3	Ammonia
SF_6	Sulfur hexafluoride

CHAPTER 1
INTRODUCTION

1.1 Overview

People spend 90% of their time in buildings and the air quality in buildings plays an important role in occupants' health and productivity [1]. The air quality in buildings can be diminished by increasing the indoor concentration of gaseous and particulate contaminants. Studies have shown that if the concentration of gaseous contaminants increases (due to insufficient fresh air), the productivity of the occupants will decrease [2]. Therefore, fresh air (i.e., ventilation) should be continuously supplied to occupied buildings in order to maintain adequate indoor air quality (IAQ).

To provide fresh air to buildings and maintain thermal comfort conditions, Heating, Ventilating and Air-Conditioning (HVAC) systems are needed to condition the fresh outdoor air [3]. One way to reduce energy consumption for conditioning the outdoor air is to use air-to-air energy exchangers (AAEEs) that exchange heat and moisture between the building exhaust and supply airstreams.

Figure 1.1 shows a schematic of an HVAC system that provides conditioned air to a building. The supply fan provides fresh outdoor air to the building and the exhaust fan removes stale/contaminated air from the building. The outdoor air will be heated or cooled by the exhaust air depending on the outdoor climatic conditions. The energy exchanger is used to transfer energy between the return airstream and supply airstream.

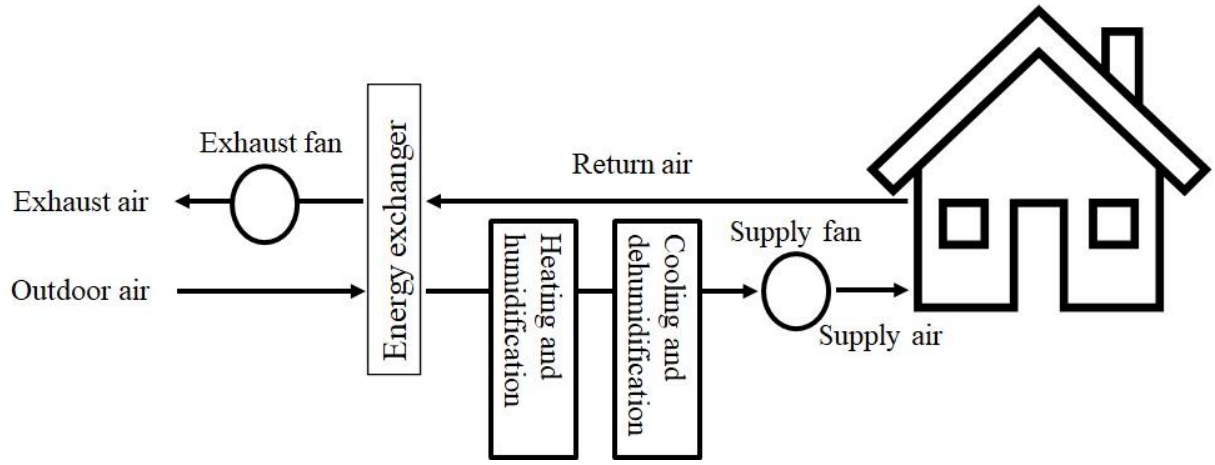

Figure 1.1. Schematic of an HVAC system providing conditioned (heated/cooled) outdoor air to a building.

As the energy exchanger exchanges heat and moisture between the supply and return airstreams, contaminants in the return airstream may also be transferred to the supply airstream. Over the past decades, researchers and engineers have investigated gaseous contaminant transfer in different AAEEs [4]–[8]. However, there is no established test methodology or systematic procedure with quantified uncertainty for measuring gaseous contaminant transfer in energy wheels reported in the literature.

Developing a test methodology for measuring gaseous contaminant transfer in energy wheels will be useful for quantifying the percentage of gaseous contaminants that return to the building. To address this gap, the American Society of Heating, Refrigerating and Air-conditioning Engineers (ASHRAE) initiated a research project on this topic. The project is ASHRAE RP-1780: Test method to evaluate cross-contamination of gaseous contaminants within total energy recovery wheels, and Professors Carey Simonson and Jafar Soltan of the University of Saskatchewan were selected by ASHRAE to complete this research project. The request for proposal for ASHRAE

RP-1780 is available in Appendix A. This MSc research is part of ASHRAE RP-1780 and the findings of this MSc research will be included in the final report for ASHRAE RP-1780.

1.2 Energy wheels

A schematic of an energy wheel operating as an AAEE that rotates between the supply and return airstreams of a building is shown in Figure 1.2. Energy wheels contain numerous tiny flow channels (hydraulic diameter of a few mm), and are typically made of aluminum, and coated with a desiccant. Some well-known desiccants are silica gel, molecular sieve, and zeolites. If the wheel is not coated with a desiccant, the wheel only transfers heat and is called a heat wheel.

During the operation of an energy wheel, one half of the wheel is exposed to the supply/outdoor airstream while the other half is exposed to the exhaust/return airstream. When hot and humid air passes through the flow channels of an energy wheel, heat and moisture transfer from the air to the energy wheel. Heat is stored in the aluminum matrix and moisture is adsorbed by the desiccant. As the wheel rotates, heat and moisture are released from the desiccant-coated wheel to the cold and dry outdoor airstream entering the building.

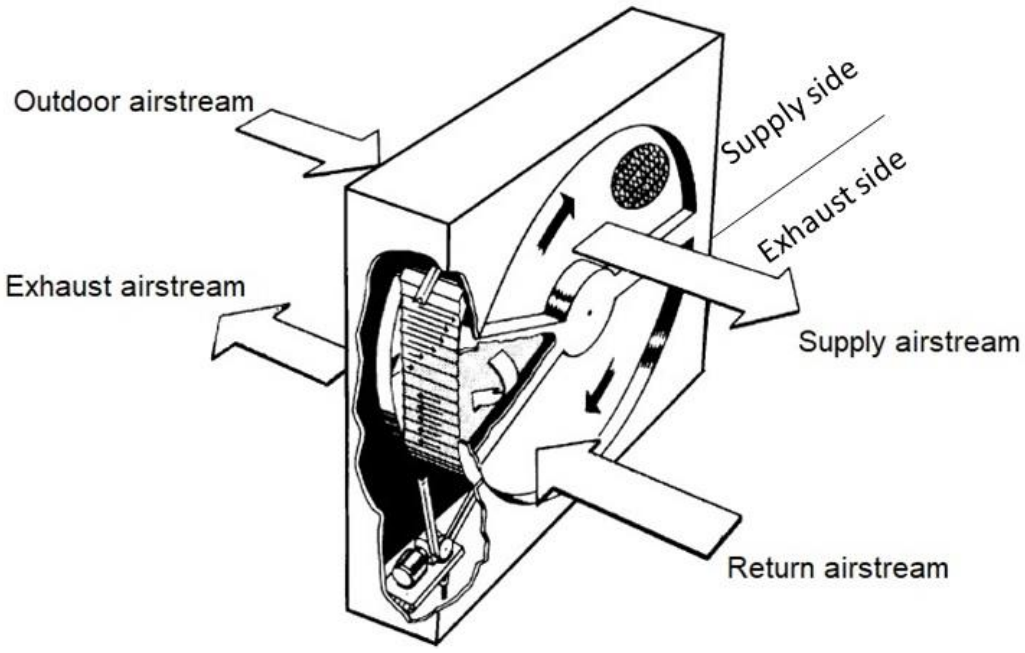

Figure 1.2. Schematic of an energy wheel rotating between the supply side (outdoor/supply airstreams) and the exhaust side (return/exhaust airstreams) [9].

In addition to energy exchange between the airstreams, gaseous contaminants may transfer between the two airstreams. There is a possibility of transferring contaminants from the return air (i.e., building exhaust air) to the supply air via three mechanisms: (1) air leakage, (2) carryover, and (3) adsorption/desorption [10].

Contaminant transfer from the return airstream to the supply airstream by air leakage can be reduced or eliminated by improving the sealing between the ducts and the exchanger and by having a higher pressure on the supply side than on the exhaust side. Carryover occurs because return air entrained in the flow channels is transferred to the supply side as the energy wheel rotates. Carryover can be reduced by installing a purge section which diverts the entrained return air to the exhaust airstream rather than to the supply airstream. Contaminant transfer due to adsorption/desorption occurs when the contaminant is adsorbed by the desiccant in the retum

airstream and desorbed in the supply airstream. These mechanisms will be discussed and described in more detail in the next section.

1.3 Contaminants and contaminant transfer

There are numerous indoor airborne contaminants including particulates, vapors, and gases. Particulate contaminants are solid particles with physical sizes ranging from nanometers to micrometers. ASHRAE [11] defines a vapor as a substance that is in a gaseous form but would be in in liquid or solid state under natural atmospheric conditions. A gas is a substance that is in the gaseous state under natural atmospheric conditions [11]. Vapor and gaseous contaminants are as small as air molecules and are found in indoor and outdoor environments. Gaseous contaminants can be divided into organic and inorganic compounds. The organic compounds, which contain carbon molecules, are found in higher concentrations in buildings than inorganic compounds. Volatile organic compounds (VOCs) are common contaminants in building indoor air and are organic compounds.

The ASHRAE RP-1780 (lists 11 specific contaminants that must be tested in the project. These contaminants are listed in Table 1.1 and were selected based on their relevance to building indoor air and their chemical properties (e.g., water solubility, molecular size, polarity (i.e., existence of positive and negative electrical charges in a molecule), and toxicity).

Table 1.1. List of the selected gaseous contaminants for ASHRAE RP-1780. The contaminants that will be tested in this thesis are highlighted.

Propane or hexane	Xylene	Acetaldehyde
Sulfur hexafluoride (SF_6)	Acetic acid	Methyl isobutyl ketone (MIBK)
Phenol	Carbon dioxide (CO_2)	Methanol (CH_3OH)
Ammonia (NH_3)	Isopropyl alcohol (C_3H_8O)	

In this MSc research, experiments will be conducted with carbon dioxide, sulfur hexafluoride, ammonia, isopropyl alcohol, and methanol as highlighted in Table 1.1. It should be noted that sulfur hexafluoride is often used as an inert (non-reacting) tracer gas, while there are some bans on sulfur hexafluoride due to its high global warming potential [12]. Ammonia and water have very similar chemical properties (molecular size and polarity) which will be discussed in detail in Chapter 3. It is expected that ammonia may show similar transfer rates as water vapor.

All gaseous contaminants will transfer in an energy wheel when air is transferred between the airstreams due to air leakage or carryover. However, only certain gaseous contaminants will transfer due to adsorption/desorption, as will be discussed in the subsequent sections.

1.3.1 Carryover

The contaminant transfer due to carryover occurs when return air flows through the energy wheel and part of the air is transferred to the supply airstream as the wheel rotates. Figure 1.3 presents a schematic of carryover in an energy wheel. As shown in Figure 1.3, the flow channels of the energy wheel are full of air from the exhaust side when the wheel rotates from the exhaust side to the supply side. This exhaust air, which contains gaseous contaminants, mixes with fresh incoming outdoor air resulting in contaminant transfer and these contaminants are returned to indoor space of the building.

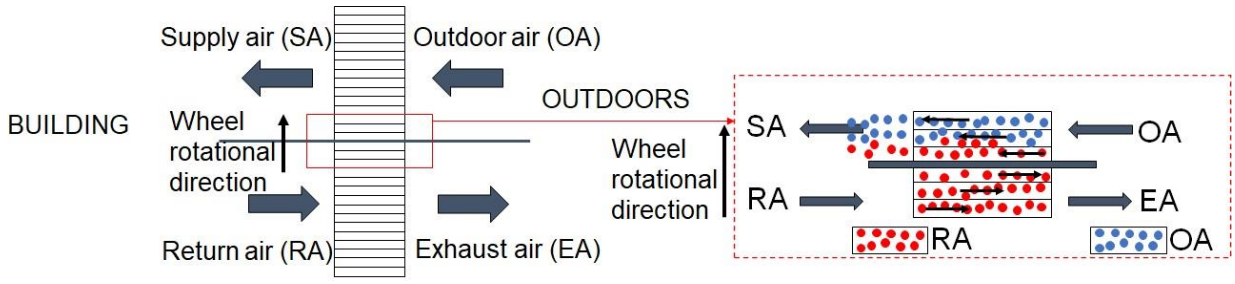

Figure 1.3. Schematic showing gaseous contaminant transfer by carryover in an energy wheel.

The carryover can be limited by using a purge section in the energy wheel and through a good installation and proper maintenance of the energy wheel [6], [9]. Figure 1.4 shows a schematic of a purge section in an energy wheel that prevents carryover from return airstream to supply airstream. The purge isolates a section of the wheel on the boundary between the supply and return airstreams and displaces the entrapped return air (from the exhaust side) along with some outdoor air to the exhaust side. Contaminant transfer due to carryover is independent of the gas since contaminants are simply carried with the air from one side of the wheel to the other side of the wheel.

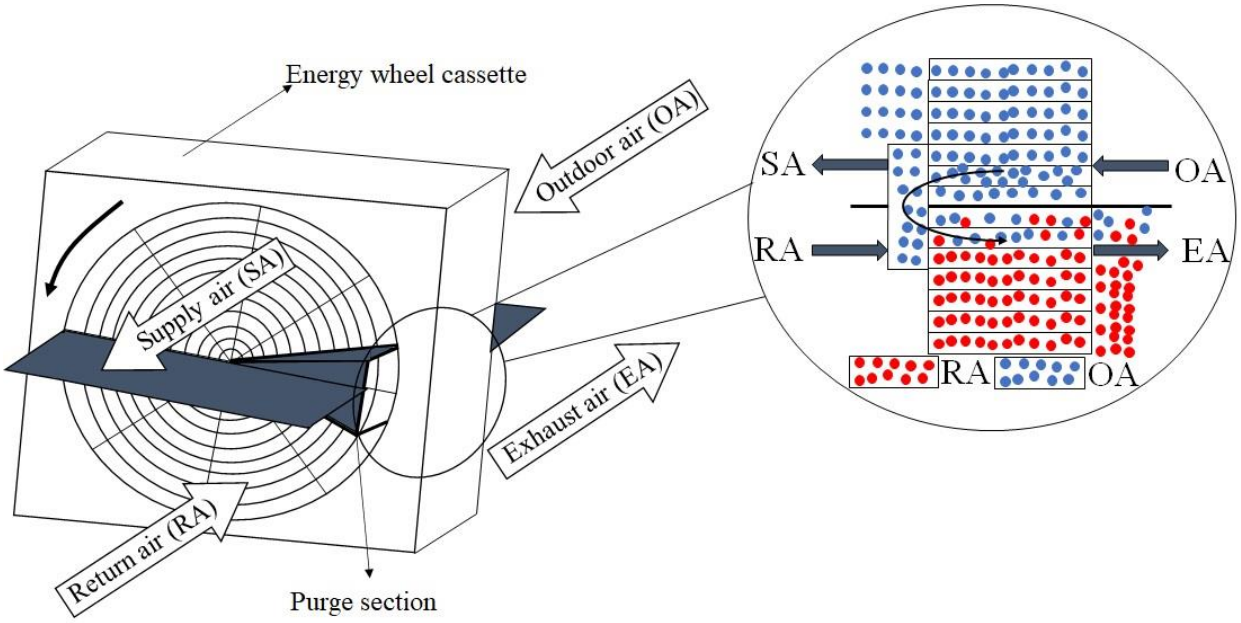

Figure 1.4. Schematic showing a purge section in an energy wheel that transfers outdoor air to exhaust airstream and prevent carryover from return airstream to supply airstream.

1.3.2 Air leakage

The contaminant transfer by air leakage occurs due to pressure difference between the supply and return airstreams. In this case, air leaks through the interface (seals) between the return and supply

airstreams as shown in Figure 1.5. The leakage can occur either from the supply to the return airstream or vice versa, depending on the pressure of the airstreams.

Contaminant transfer due to leakage of contaminated air on the exhaust side to the fresh air on the supply side can be eliminated by maintaining a higher pressure on the supply side than on the exhaust side ($P_{supply} > P_{return}$). The locations of the fans in outdoor, supply, return, and exhaust airstreams play an important role in the air leakage direction [13]. Figure 1.5 shows a schematic of the air leakage mechanism in an energy wheel, where the supply air has a higher pressure than return air.

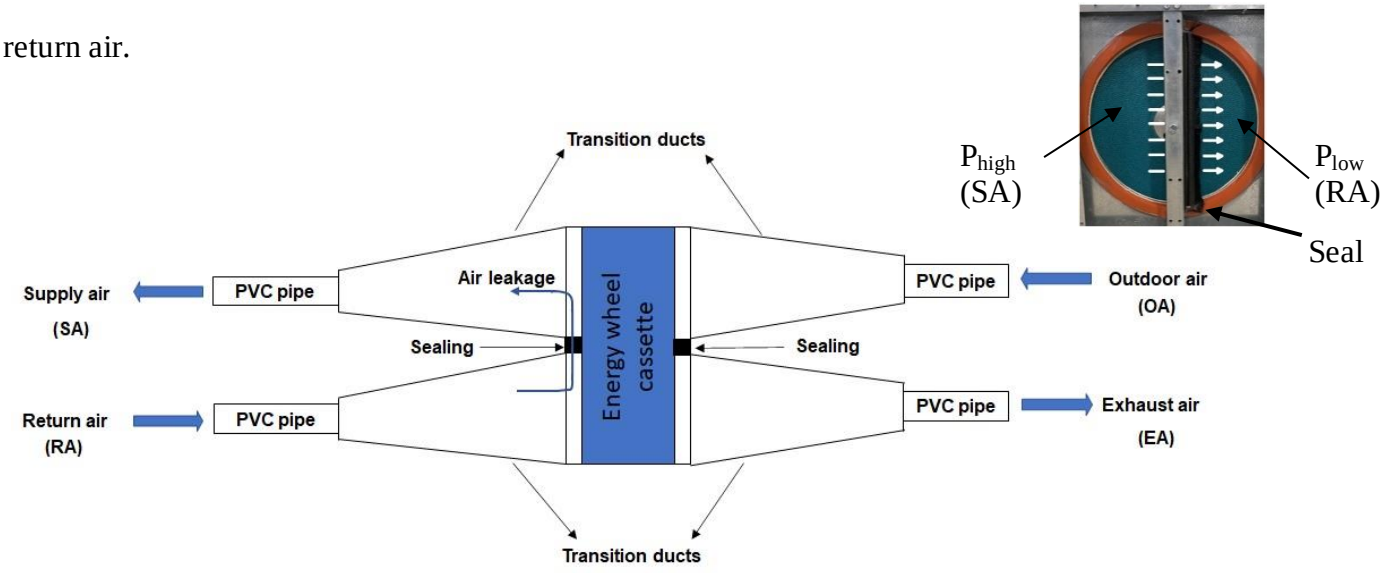

Figure 1.5. Schematic showing gaseous contaminant transfer by air leakage in an energy wheel.

1.3.3 Adsorption/desorption

Contaminant transfer due to adsorption/desorption occurs when the desiccant-coated energy wheel has the capacity to adsorb the gaseous contaminant in one airstream, store the contaminant in the desiccant and then release the gaseous contaminant by desorption in the other airstream (similar to transfer of water vapor). Figure 1.6 presents a schematic of the adsorption/desorption mechanism for a desiccant-coated aluminum sheet, which is a typical construction of many energy wheels.

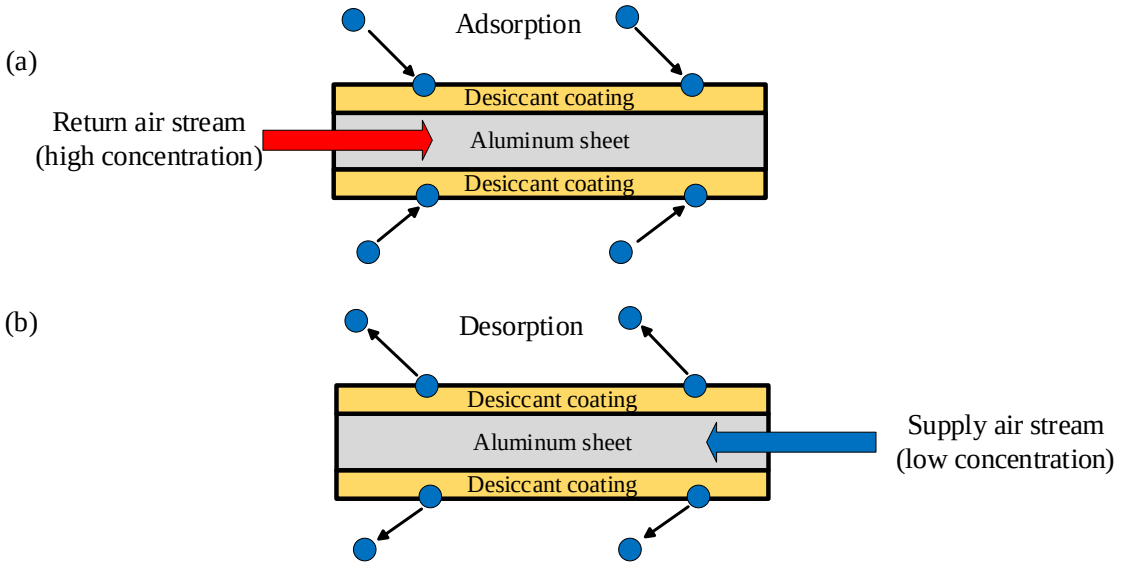

Figure 1.6. Schematic showing gaseous contaminant transfer by adsorption/desorption, where (a) depicts adsorption from the return airstream and (b) depicts desorption into the supply airstream.

The sorption capacity of desiccants will vary for different contaminants. Contaminant transfer between the airstream and the desiccant occurs because of the difference in the vapor pressure of the contaminant between the airstream and the desiccant [14]. Adsorption occurs when the vapor pressure is higher in the air than on the desiccant surface and desorption occurs when the vapor pressure is higher on the desiccant surface than in the air.

Contaminant transfer in energy wheels through adsorption/desorption mechanism is expected to depend on many parameters such as the air conditions (temperature and humidity), the properties of the contaminants, the desiccant [6], and the design of the wheels (i.e., air face velocity, Number of Transfer Unit (NTU), capacity rate ratio (Cr*), and effectiveness).

1.3.4 Absorption/evaporation

In addition to the main mechanisms mentioned above, some gaseous contaminants in the return airstream may be absorbed by the desiccant and evaporate on the supply side. For example, when

water vapor in the return airstream condenses to from a layer of liquid water (or frost) within the energy wheel channels, water soluble gaseous contaminants such as formaldehyde and methanol may absorb in the liquid (or frozen) water. Gaseous contaminant absorption occurs because of attractive forces between the gaseous contaminants and the liquid (frozen) water. When the liquid water evaporates into the supply airstream, the absorbed contaminants may evaporate and transfer to the supply air.

1.3.5 Condensation/evaporation

The condensation of gaseous contaminants will occur if the concentration of the contaminant reaches saturation. Although such high concentrations are expected to be very rare for AAEE applications in building HVAC systems, it may be possible for a contaminant to condense on the exhaust side of the wheel and evaporate on the supply side of the wheel. Contaminant transfer by condensation/evaporation in AAEEs is expected to be small.

1.4 Objectives

As mentioned earlier, this MSc research is part of the ASHRAE RP-1780 research project. One objective of this research project is to conduct a detailed literature review on test methodologies for measuring gaseous contaminant transfer in energy wheels. This objective will be fulfilled in this MSc thesis. Further, a test facility has been set-up by a research engineer (Easwaran Krishnan) in the Thermal Laboratory at the University of Saskatchewan in order to measure gaseous contaminant transfer in energy wheels. The test facility, instrumentation and some experimental data will be presented in this thesis. This MSc research has the following two objectives.

1. Conduct a literature review on test methodologies for measuring gaseous contaminant transfer in energy wheels.

2. Apply and verify a test methodology for measuring gaseous contaminant transfer in energy wheels.

1.5 Thesis structure

This thesis is prepared in a manuscript style and contains two research papers (Chapters 2 and 3) that address the two abovementioned objectives. Chapter 2 addresses the first objective and presents a literature review on test methodologies for measuring gaseous contaminant transfer in energy wheels. Chapter 3 addresses the second objective and describes the test methodology and experimental results for gaseous contaminant transfer in energy wheels. The test facility, test performance data and energy wheel effectiveness values are discussed. It will be shown that the test facility conserves energy and mass during the experiments, provides steady state flow parameters as required in ASHRAE Standard 84 (2020) [15], and results in effectiveness values similar to the manufacturer's data. Finally, Chapter 4 provides a summary and conclusions of thesis and suggestions for further work. Appendix A provides the request for proposal for ASHRAE RP-1780. Appendix B explains details of working principles of gas measurement techniques and their uncertainty analysis.

1.6 List of publications

The two papers that form the core of this thesis are under preparation. Both papers will be prepared and published according to the ASHRAE RP-1780 contract.

Chapter 2: M. Torabi, E. N. Krishnan, J. Soltan, and C. J. Simonson, "A Literature Review on Test Methodologies for Measuring Gaseous Contaminant Transfer in Energy Exchangers," under preparation.

Chapter 3: E.N. Krishnan, H. Reitenbach, M. Torabi, J. Soltan, and C. J. Simonson, "A Test Methodology for Measuring Gaseous Contaminant Transfer in Energy Wheels," under preparation.

CHAPTER 2
LITERATURE REVIEW

2.1 Overview

This chapter presents a literature review on experimental studies for measuring gaseous contaminant transfer in different energy exchangers, which is the first objective of this MSc thesis. In this chapter, 15 papers/reports have been reviewed in detail. These papers/reports describe the different instrumentation and methodologies used and the data measured to quantify the transfer of various gases in various energy exchangers. The measured transfer rates and uncertainties (where available) for the different gases are summarized. The measured transfer rates vary between 0% and 75% with uncertainties between 1% and 30%.

The literature review shows that there are three major mechanisms for gaseous contaminant transfer in energy exchangers: (1) air leakage, (2) carryover, and (3) adsorption/desorption. The published articles reviewed in this chapter will be organized based on the transfer mechanisms. The literature review shows that there are established test methodologies to quantify the gaseous contaminant transfer in energy wheels due to air leakage and carryover. However, there is no established method to measure gaseous contaminant transfer due to the adsorption/desorption mechanism. Furthermore, many studies do not undertake a rigorous uncertainty analysis.

This chapter contains a draft review paper based on the literature review of gaseous contaminant transfer in energy exchangers. The author of the thesis, Mr. Mehrdad Torabi (MSc student), wrote the manuscript and performed the literature data analysis. Mr. Easwaran Krishnan (research engineer) reviewed and commented on the manuscript. Professors Carey Simonson and Jafar Soltan supervised the work.

2.2 Introduction

A search of the literature revealed relatively few (15) studies on gaseous contaminant transfer in energy exchangers over the last thirty-five years. This chapter will first present the standard methods for measuring energy wheel performance and contaminant transfer due to carryover and leakage, followed by research on contaminant transfer in energy wheels, and finally a method to quantify contaminant transfer due to adsorption/desorption in energy wheels. The major findings and contributions of the published articles, comparison of gaseous contaminant transfer results, and effects of operating conditions on gaseous contaminant transfer results, will be discussed.

2.3 Test standards and performance parameters

ASHRAE 84 [15] and CSA C 439-18 [16] Standards provide guidelines to conduct performance tests. The performance of an energy exchanger depends on the design parameters and operating conditions. The direction of airflow and the nomenclature of the inlet and outlet airstreams as given in ASHRAE Standard 84 (2020) [15] are shown in Figure 2.1. The major parameters used to quantify the energy and contaminant transfer performance are presented in separate sections below.

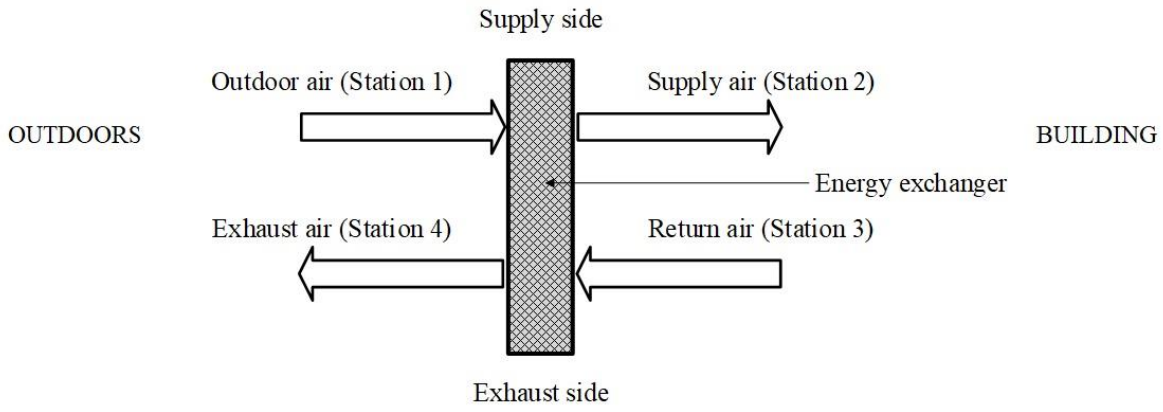

Figure 2.1. Schematic of an air-to-air energy exchanger showing the airflow and measurement stations.

2.3.1 Effectiveness (ε)

Effectiveness is defined as the ratio of actual energy transfer rate at a specific test condition to the maximum energy transfer at the same test condition [17]. The sensible, latent, and total effectiveness can be determined using Eqs. (2.1) to (2.3) according to ASHRAE Standard 84 (2020) [15],

$$\varepsilon_s = \frac{\dot{m}_2 (C_{p,1} T_1 - C_{p,2} T_2)}{\dot{m}_{min\,(2,3)} (C_{p,1} T_1 - C_{p,3} T_3)} \tag{2.1}$$

$$\varepsilon_l = \frac{\dot{m}_2 (W_1 - W_2)}{\dot{m}_{min\,(2,3)} (W_1 - W_3)} \tag{2.2}$$

$$\varepsilon_{tot} = \frac{\dot{m}_2 (h_1 - h_2)}{\dot{m}_{min\,(2,3)} (h_1 - h_3)}, \tag{2.3}$$

where $\dot{m}, T, W, C_p$ and h represent the mass flow rate, temperature, humidity ratio, specific heat capacity, and specific enthalpy at stations 1, 2, and 3 according to the subscripts. Subscripts s, l, and tot stand for sensible, latent, and total, respectively.

2.3.2 Outdoor air correction factor (OACF)

ASHRAE Standard 84 (2020) [15] defines the outdoor air correction factor as the ratio of outdoor air mass flow rate ($\dot{m}_1$) to the supply air mass flow rate ($\dot{m}_2$).

$$OACF = \frac{\dot{m}_1}{\dot{m}_2}. \tag{2.4}$$

2.3.3 Exhaust air transfer ratio (EATR)

Exhaust air transfer ratio (EATR) is used to express the amount of an inert tracer gas (i.e., a gas that does not significantly react with the desiccant coated on the surface of flute channels of the energy exchanger such as sulfur hexafluoride) that is transferred from the exhaust side (station 3)

to the supply side (station 2). EATR is defined as the ratio of tracer gas concentration difference between the supply and the outdoor airstreams relative to the tracer gas concentration difference between the return and the outdoor airstreams [15],

$$\mathrm{EATR} = \frac{C_2 - C_1}{C_3 - C_1}, \tag{2.5}$$

where C_1, C_2, and C_3 are the tracer gas concentration measured at stations 1, 2 and 3, respectively. It should be noted that EATR is a measure of transfer of air through carryover and air leakage mechanisms from exhaust side to supply side of the energy exchanger and is not directly applicable to the measurement of other gaseous contaminants in the device as described in ASHRAE Standard 84 (2020) [15].

The uncertainty in EATR can be calculated using uncertainty propagation methods as [18]

$$U_{\mathrm{EATR}} = \sqrt{\left(U_{C_2}\frac{1}{(C_3 - C_1)}\right)^2 + \left(U_{C_1}\frac{C_2 - C_3}{(C_3 - C_1)^2}\right)^2 + \left(U_{C_3}\frac{C_1 - C_2}{(C_3 - C_1)^2}\right)^2}, \tag{2.6}$$

where U_{C_1}, U_{C_2} and U_{C_3} are uncertainty in the tracer gas concentration measurements at stations 1, 2 and 3, respectively.

Tracer gas measurement procedure: To measure EATR, an inert tracer gas is injected into the return airstream. Then, air samples are drawn from each station, and the concentration of tracer gas is measured using calibrated gas analyzers. The air sampling lines must be short enough to avoid dilution and sample line transients. ASHRAE Standard 84 (2020) [15] requires the uncertainty in EATR to be less than ± 3%. The requirements of the sampling equipment and recommendations on the sampling grid are also provided in the test standards [15], [16].

2.3.4 Energy and mass inequalities

During every performance test, in addition to the performance parameters, the test data should satisfy the energy and mass inequalities [16]. The inequality equations for (i) dry air mass flow rate, (ii) energy transfer, (iii) water vapor mass transfer, (iv) enthalpy transfer, and (v) contaminants mass transfer are provided in Eqs. (2.7) - (2.11) [15].

For sensible energy transfer:

$$\frac{|\dot{m}_1 - \dot{m}_2 + \dot{m}_3 - \dot{m}_4|}{\dot{m}_{\min\,(1,3)}} < 0.05 \tag{2.7}$$

$$\frac{|\dot{m}_1 C_p T_1 - \dot{m}_2 C_p T_2 + \dot{m}_3 C_p T_3 - \dot{m}_4 C_p T_4|}{\dot{m}_{\min\,(1,3)}\, C_p\, |T_1 - T_3|} < 0.20\,. \tag{2.8}$$

For water vapor transfer:

$$\frac{|\dot{m}_1 W_1 - \dot{m}_2 W_2 + \dot{m}_3 W_3 - \dot{m}_4 W_4|}{\dot{m}_{\min\,(1,3)}\, C_p\, |W_1 - W_3|} < 0.20\,. \tag{2.9}$$

For enthalpy transfer:

$$\frac{|\dot{m}_1 h_1 - \dot{m}_2 h_2 + \dot{m}_3 h_3 - \dot{m}_4 h_4|}{\dot{m}_{\min\,(1,3)}\, C_p\, |h_1 - h_3|} < 0.20\,. \tag{2.10}$$

For tracer gas mass inequality:

$$\frac{|\dot{m}_1 C_1 - \dot{m}_2 C_2 + \dot{m}_3 C_3 - \dot{m}_4 C_4|}{\dot{m}_{\min\,(1,3)}\, |C_1 - C_3|} < 0.15\,. \tag{2.11}$$

2.3.5 Energy wheel design parameters

Some important non-dimensional parameters that are used to define energy wheels are the number of transfer units (NTU) and matrix heat capacity rate ratio (Cr*) which can be evaluated using Eqs. (2.12) and (2.13) [17].

$$NTU = \frac{UA}{C_{min.}} \tag{2.12}$$

$$Cr^{*} = \frac{\left(\dot{m}C_p\right)_{matrix}\omega}{\left(C_{min}\right)_{air}}. \tag{2.13}$$

Here, U, A, ṁ, C, and ω are overall heat transfer coefficient, heat transfer surface area, air mass flow rate, heat capacity rate, and rotational speed, respectively.

2.4 Summary of research on contaminant transfer in energy exchangers

The following section summarizes the research on contaminant transfer in energy exchangers and the effect of operating conditions on the transfer rate for various contaminants. Most of the studies have applied the concept of EATR for gaseous contaminants, even for gases that are not inert gases as specified in the test standards [15], [16]. The measurements of non-inert gases, therefore, include all the contaminant transfer mechanisms (carryover, leakage, and adsorption/desorption). The studies will be sorted into two sections based on the main transfer mechanisms and will be presented in chronological order within each section.

2.4.1 Carryover and air leakage of inert gases

2.4.1.1 Fisk *et al.* (1985) [4]

Fisk *et al.* (1985) [4] studied gaseous contaminant transfer from the return airstream to the supply airstream in an energy wheel. Propane (C_3H_8) and sulfur hexafluoride (SF_6) were used to determine the air leakage in the energy wheel. Propane and sulfur hexafluoride were injected upstream of the energy wheel in exhaust side. To improve the mixing of the tracer gases in the airstream, tracer gases were injected through a manifold upstream of an orifice plate and mixing vanes. The concentrations of contaminants were monitored using infrared analyzers. The results showed that

sulfur hexafluoride and propane transfer rates were between 6-7% and 5-7%, respectively, indicating that propane could be a possible inert tracer gas for this application.

2.4.1.2 Khoury *et al.* (1988) [13]

Khoury *et al.* (1988) [13] studied sulfur hexafluoride transfer in a heat wheel. Sulfur hexafluoride was stored in a gas chamber and injected into the return airstream with a rotameter. In the experiments, three-meter-long sampling tubes were used to collect air samples from the center of the air ducts. Air samples were collected into 15 L Tedlar sampling bags. Tedlar Sampling bags were made of polyvinyl fluoride (PVF) film and were used for collection of air samples in different air temperatures. The concentration of sulfur hexafluoride in the collected air samples was measured using infrared spectroscopy with a calibrated MIRAN 1A gas analyzer. The results showed that an average of 1% of sulfur hexafluoride was transferred by the heat wheel from the return air to the fresh supply air. A mass balance showed that 30% of the injected sulfur hexafluoride was lost during the experiment. The authors suggested that the sulfur hexafluoride could have been adsorbed by the wheel cassette. Their experimental data did not include an uncertainty analysis.

2.4.1.3 Andersson *et al.* (1999) [19]

Andersson *et al.* (1999) [19] studied formaldehyde transfer in six energy wheels with and without a purge section. They measured carryover and air leakage using nitrous oxide (N_2O). A vacuum pump and metal tubes were used to draw air samples from the outdoor, supply, return, and exhaust airstreams. An infrared spectrophotometer was used to determine the nitrous oxide concentration in the air samples. Test results showed that 3% of injected nitrous oxide was transferred from the return airstream to the supply airstream for the energy wheels without a purge section (i.e.,

carryover and air leakage) and 1% of injected nitrous oxide was transferred for the wheel with a purge section (i.e., air leakage assuming a well-designed purge section). Results showed that the standard deviations were 1-12% for nitrous oxide concentration. Andersson *et al.* (1999) [19] also conducted experiments with formaldehyde and these tests are described in Section 2.4.2.2.

2.4.1.4 Shang *et al.* (2001) [5]

Shang *et al.* (2001) [5] studied the transfer of nitrous oxide in an energy wheel with and without a purge section. Five pressure differences were applied between the exhaust airstream and outdoor airstream ranging from -254 Pa to +254 Pa. The schematic of their test facility is provided in Figure 2.2.

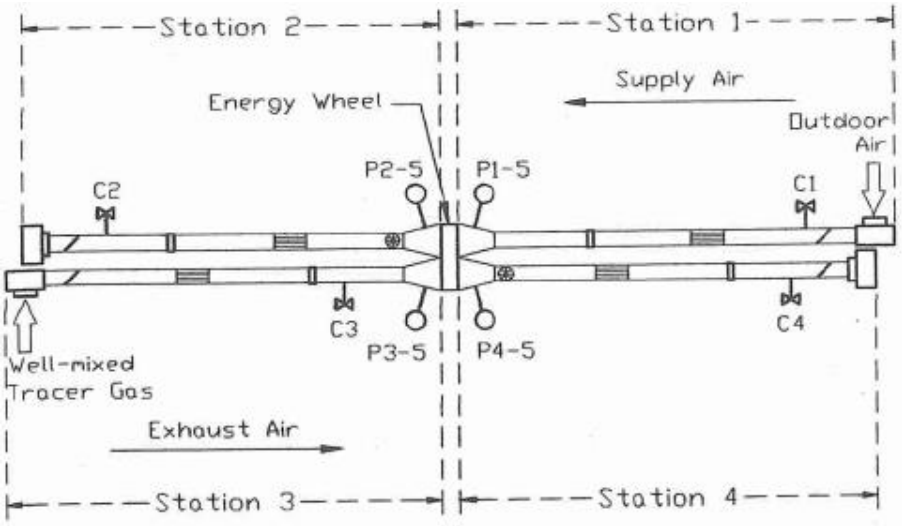

Figure 2.2. Schematic of the test facility used by Shang *et al.* (2001) to measure nitrous oxide contaminant transfer [5].

Experiments were started by injecting nitrous oxide into the return airstream until a concentration of 150 ppm was reached. Air samples were collected in 100 L sampling bags and analyzed with a gas analyzer. Details of the gas measurement techniques such as the type of gas analyzer were not provided.

The results for the experiments on the energy wheel without a purge section showed that EATR was 33% when the pressure difference (P_{supply}-$P_{exhaust}$) was -254 Pa and reduced to 1% when the pressure difference was +254 Pa. Results for experiments on the energy wheel with a purge section showed that EATR was 54% for a pressure difference of -246 Pa and reduced to 1.1% for a pressure difference of +250 Pa. The highest EATR uncertainty was ± 3% at a pressure difference of +250 Pa. They suggested that a purge section increased EATR and uncertainty in measurement when the exhaust side pressure is higher than supply side pressure and therefore, the purge section may not always be beneficial.

2.4.1.5 Sparrow *et al.* (2001) [20]

Sparrow *et al.* (2001) [20] studied carbon dioxide transfer in a flat plate enthalpy exchanger using a novel semi-permeable membrane. The membrane was coated with polymer material which allowed water vapor transfer but prevented the transfer of other gases. This was due to polymer coatings that were synthesized to create pores similar in size to the water vapor molecule (2.6 Å). A pressurized cylinder of carbon dioxide was connected to four distribution tubes to ensure a uniform concentration of carbon dioxide in the return airstream. An infrared spectroscopy technique was used with a resolution of 1 ppm for measuring carbon dioxide concentration in the return, outdoor and supply airstreams. The authors did not measure carbon dioxide concentration in the exhaust airstream to reduce costs; rather they assumed a mass balance for carbon dioxide.

Mass transfer effectiveness for water vapor (i.e., latent effectiveness) was found to be 50% at face velocities between 0.25-0.5 m/s (50-100 fpm) and transfer of carbon dioxide was found to be 1% at a face velocity of 1.5 m/s (300 fpm). A selectivity parameter was introduced for quantifying gas transfer through the applied polymer membrane. This parameter was the ratio of water vapor transfer rate to carbon dioxide transfer rate and ranged between 21 and 61. The study showed that

the membrane transferred water vapor while allowing very little carbon dioxide transfer through the membrane. This study did not provide an uncertainty analysis of the results.

2.4.1.6 Roulet *et al.* (2002) [10]

Roulet *et al.* (2002) [10] studied volatile organic compounds (VOCs) transfer in energy wheels in an auditorium, a laboratory, and a building. Tracer gas experiments with sulfur hexafluoride showed that the transfer rate through air leakage and carryover mechanisms were 7 ± 4% in the auditorium, 5 ± 11% in the laboratory and 26 ± 16% in the building. The higher transfer rate in the building might have been due to higher air flow rates on the exhaust side than on the supply side of the wheel. Roulet *et al.* (2002) [10] reported experimental data for other VOCs, which will be provided in Section 2.4.2.4 as the adsorption/desorption mechanism is dominant for those VOCs.

2.4.1.7 Wolfrum *et al.* (2008) [21]

Wolfrum *et al.* (2008) [21] studied sulfur hexafluoride, toluene and n-hexane transfer in a desiccant wheel coated with a silicate-based desiccant. Tracer gas experiments with sulfur hexafluoride showed a 1% air leakage and carryover from the return airstream to the supply airstream. The pressure differences between the return and supply airstream were set to zero. Experimental data for other VOCs will be presented in Section 2.4.2.5.

2.4.1.8 Patel *et al.* (2014) [22]

Patel *et al.* (2014) [22] performed experiments to measure sulfur hexafluoride, formaldehyde and toluene transfer in a run-around membrane energy exchanger (RAMEE). A RAMEE consists of two energy exchangers, a liquid desiccant running loop and a pump to run liquid desiccant between energy exchangers. These energy exchangers are called liquid-to-air membrane energy exchangers (LAMEEs). Figure 2.3 shows a schematic of a RAMEE.

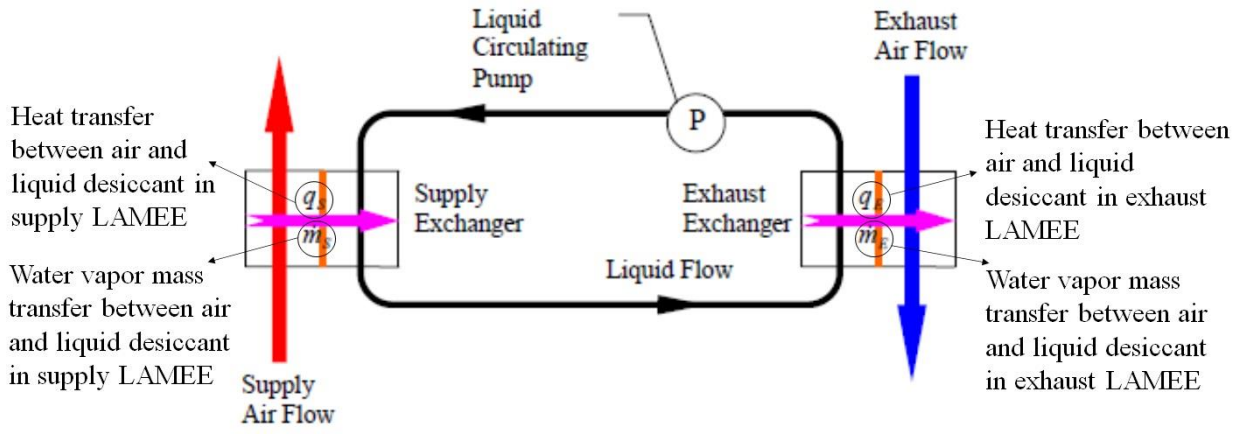

Figure 2.3. Schematic of a run-around membrane energy exchanger (RAMEE) [23].

Experiments with sulfur hexafluoride showed that EATR was almost zero, which was due to its very low solubility in water. EATR results for the formaldehyde and toluene were higher and will be provided in Section 2.4.2.8.

2.4.1.9 Hult *et al.* (2014) [24]

Hult *et al.* (2014) [24] studied sulfur hexafluoride and VOC (carbon dioxide and formaldehyde) transfer in energy wheels using field and laboratory experiments. The carbon dioxide concentration in the outdoor, supply and return airstreams were measured to determine the contributions of air leakage and carryover mechanisms on cross-contamination in an energy wheel. Air samples were collected in silica gel cartridges coated with 2,4-dinitrophenylhydrazine. Sampling cartridges were extracted into 2 mL of high purity acetonitrile. Sample extracts were analyzed using the high performance liquid chromatography (HPLC) technique. Appendix B provides more details about the working principles of the gas measurement techniques such as HPLC, gas chromatography, and infrared spectroscopy.

Laboratory experiments were done in order to validate field experiments at air flow rates between 120-340 m^3/h. Laboratory experiments started with injecting sulfur hexafluoride into the retum

airstream. Air samples were collected using sampling bags and analyzed using a gas chromatography technique. The measured sulfur hexafluoride concentrations were between 20-1200 µg/m^3 and the EATR was between 12% to 19%.

2.4.1.10 Kassai (2018) [25]

Kassai (2018) [25] studied carbon dioxide transfer in an energy wheel coated with a 3Å molecular sieve desiccant. carbon dioxide was injected into return airstream from a 50 L volume cylinder. A TESTO multifunctioning metering instrument was used to measure the carbon dioxide concentration in different airstreams. Results showed that the carbon dioxide transfer from the return airstream to the supply airstream increased with wheel rotational speed. carbon dioxide transfer also increased as air flow rate increased in the return and outdoor airstreams. For example, at a volume flow rate of 400 m^3/h and a wheel rotational speed of 2 rpm the carbon dioxide transfer was 2%, and at a volume flow rate of 800 m^3/h and a wheel rotational speed of 10 rpm the carbon dioxide transfer was 4%.

Their results showed that carbon dioxide transfer was between 2-5% depending on wheel speed and flow rate. It was assumed that the two major mechanisms for carbon dioxide transfer were air leakage and carryover. This study did not present an uncertainty analysis of results and contaminant mass conservation in the experiments.

2.4.2 Adsorption/desorption of non-inert gases

In this section, the experimental studies on contaminant transfer due to adsorption/desorption are summarized. It should be noted that the results of the contaminant transfer experiments reported in this section also include all the possible transfer mechanisms (carryover, leakage, and adsorption/desorption).

2.4.2.1 Fisk *et al.* (1985) [4]

Fisk *et al.* (1985) [4] studied formaldehyde transfer in an energy wheel. Gaseous formaldehyde was produced by evaporating a methanol-free aqueous formaldehyde solution into a secondary airflow. This secondary airflow, containing the gaseous formaldehyde, was injected into the return airstream upstream of the energy wheel. The secondary airflow passed through a manifold upstream the orifice plate and mixers similar to the injection procedure for sulfur hexafluoride and propane. The details of the formaldehyde concentration measurement technique were not provided. Results showed that formaldehyde transfer was between 9-15% depending on the outside air temperature and humidity ratio. Higher outside temperatures and humidity ratios resulted in higher formaldehyde transfer rates. The difference between the formaldehyde transfer rate and the tracer gas transfer rate showed that there were mechanisms other than carryover and leakage that contributed to formaldehyde transfer in the energy wheel.

Fisk *et al.* (1985) [4] concluded that the higher transfer rates of formaldehyde may be due to adsorption of formaldehyde by the desiccant coated wheel on the exhaust side, followed by transfer through wheel rotation to the supply side, and desorption on the supply airstream. They reported an uncertainty of ± 12% in the formaldehyde transfer rate.

2.4.2.2 Andersson *et al.* (1999) [19]

Andersson *et al.* (1999) [19] conducted experiments with formaldehyde in energy wheels. The concentration of formaldehyde in different airstreams was measured using a chemisorption technique employing 2,4-dinitrophenylhydrazine-impregnated glass fiber filters. Six filters were used for air sampling. In addition, where air flow was not homogenous, air sampling was done using grids of metal tubes (1 mm in diameter) located perpendicular to the airstream. These metal

tubes were used for collecting air samples in a bottle. The bottle contained filters for adsorbing formaldehyde, and the filters were analyzed using high performance liquid chromatography (HPLC). It was found that in the worst-case scenario 9% of the formaldehyde transferred from the return airstream to the supply airstream with a standard deviation between 15% and 29%. Results agreed with results reported by Fisk *et al.* (1985) [4] (who measured a formaldehyde transfer rate of 9-15%).

Andersson *et al.* (1999) [19] estimated the effects of formaldehyde transfer in energy wheels on the concentration of formaldehyde in a building. It was assumed that indoor formaldehyde concentration was 20 µg/m^3 in building, the ventilation rate was one air change per hour, and the formaldehyde transfer from the return airstream to the supply airstream was 10%. Figure 2.4 shows that formaldehyde concentration in the indoor air increased to 22 µg/m^3 during the first 2 hours of operation of the ventilation system. After the first 2 hours, the formaldehyde concentration remained constant in the building.

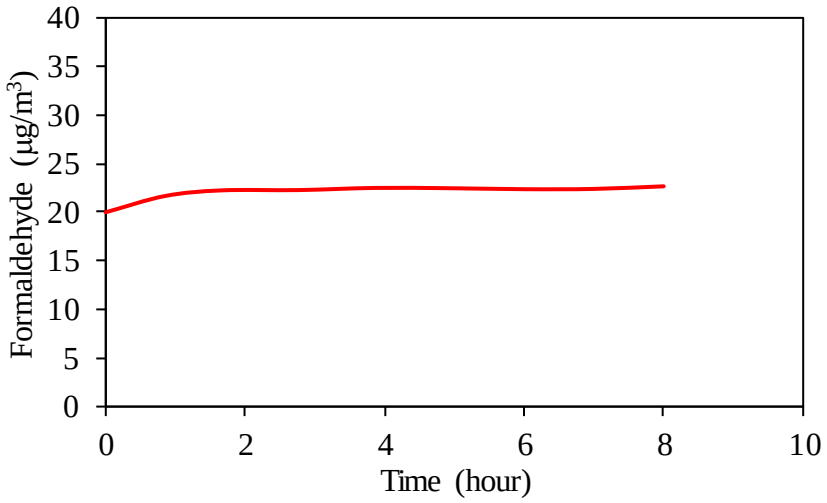

Figure 2.4. Formaldehyde concentration in a building during 8 hours with a 10% EATR in an energy wheel when the initial concentration is 20 µg/m^3 and the ventilation rate is one air change per hour [19].

2.4.2.3 Okano *et al.* (2001) [14]

Okano *et al.* (2001) [14] studied contaminant transfer in energy wheels coated with two different desiccants: ion exchange resin (IER) and silica gel (SG). The ion exchange resin was selected because it is nonporous and little contaminant transfer by adsorption/desorption is expected, while the silica gel was selected since it is a common desiccant material. Experiments were started by generating gaseous contaminants in a box and injecting them into the return airstream. The contaminants tested were ammonia, isopropyl alcohol, toluene, acetic acid, formaldehyde, styrene, acetone, xylene, ethyl methyl ketone, ethyl acetate, butyl acetate, ethyl alcohol, and methanol.

A sorption test was conducted to determine the sorption capacity of the desiccants. The sorption test showed that the ion exchange resin adsorbed 3% by mass of isopropyl alcohol and the different silica gel desiccants adsorbed 17-19% by mass of isopropyl alcohol. The concentration of isopropyl alcohol was not reported in these tests.

The concentration of ammonia, formaldehyde and acetic acid was measured using gas detector tubes, whereas the gas chromatography technique was used for the remaining contaminants. Details of the contaminant injection system and the instruments used to measure the contaminant concentration were not described in the paper.

Experiments with the energy wheel that was coated with the ion exchange resin (IER) showed that ammonia, acetic acid, and formaldehyde transfers were 10%, 7% and 5%, respectively. Other contaminants showed no transfer in the IER energy wheel. Measured results for ammonia from [14] are presented in Figure 2.5. The results show that as the face velocity increases, EATR decreases. In order to determine if this trend is mainly due to a decrease in actual contaminant transfer rate or due to an increase in dilution at higher face velocities (i.e., higher air flow rates), a dashed line is added to Figure 2.5 which represents the change in EATR that would result due to

dilution only (i.e., a constant contaminant transfer rate that is diluted by a higher air flow rate), and is calculated as

$$EATR_b = \frac{EATR_a \cdot V_a}{V_b}, \tag{2.14}$$

where V is the face velocity (i.e., air velocity that hits energy wheel surface). Subscripts a and b represent measured contaminant transfer results and calculated contaminant transfer only due to dilution, respectively. Since the measured results follow a trend similar to the dashed line in Figure 2.5, it can be concluded that the measured decreases in EATR with increasing face velocity are mainly due to dilution and not due to a decrease in the actual contaminant transfer rate.

Figure 2.5 also shows that EATR increases with increasing outdoor air relative humidity in an energy wheel coated with silica gel (SG) and remains constant with increasing outdoor air relative humidity in an energy wheel coated with ion exchange resin (IER).

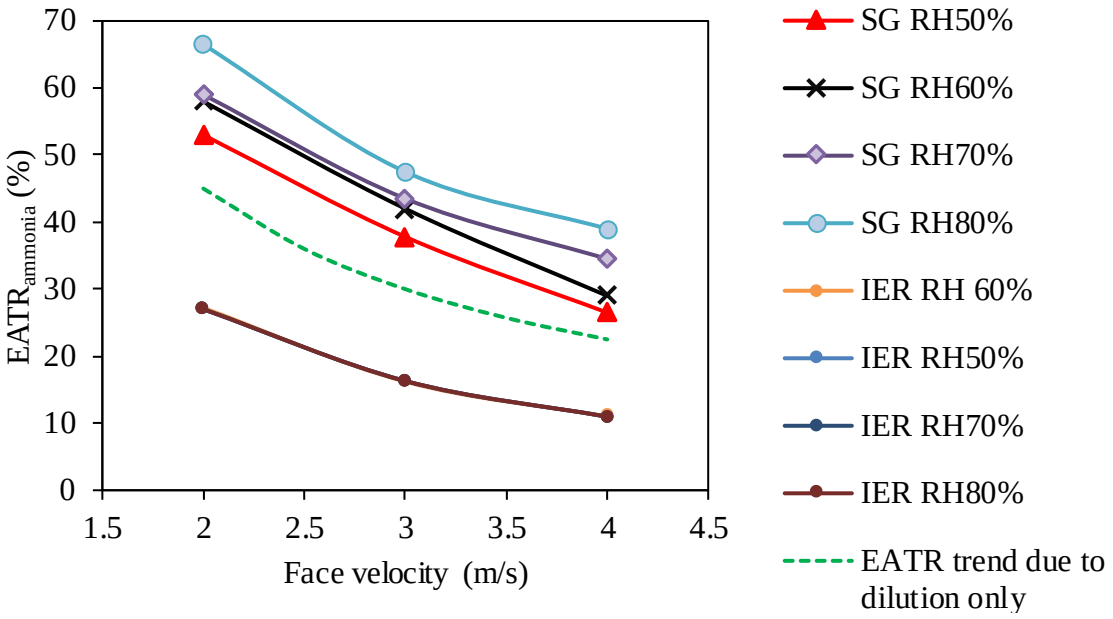

Figure 2.5. EATR as a function of face velocity at different outdoor air relative humidities and with wheels coated with silica gel (SG) and ion exchange resin (IER) desiccants (OA conditions: T = 30°C, RH = 50-80%, rotational speed = 16 rpm) [14]. An additional dashed line is included which represents the change in EATR that would occur at a constant contaminant transfer rate as the face velocity increases.

Further experiments on different desiccants showed that the ion exchange resin, synthesized zeolite, silica gel, and lithium chloride showed 17%, 36%, 43%, and 60% ammonia transfer rate, respectively. The authors noted that the desiccants with smaller pore sizes had higher desiccating capacity (i.e., transfer of water vapor between supply side of the wheel and the exhaust side of the wheel) and had lower contaminant transfer rates.

2.4.2.4 Roulet *et al.* (2002) [10]

Roulet *et al.* (2002) [10] performed contaminant transfer experiments using VOCs with different physical and chemical properties (e.g., saturation degree, boiling point, and polarity). The contaminants selected for the study included n-decane, n-butanol, 1-hexanol, phenol, 1,6-dicholorhexane, hexanal, benzaldehyde, limonene, m-xylene, mesitylene, and dipropyl ether. A liquid mixture of VOCs was used such that one milliliter of the mixture containing equal masses

of all VOCs was injected into a 200 °C airstream for 30 s. The hot air evaporated the contaminants, and the hot and contaminated airstream was delivered to the return airstream of the test facility. Pumps were used to collect air samples from the outdoor, supply, return, and exhaust airstreams. The air samples passed through tubes coated with adsorbing agents. The tubes were then heated, so the adsorbed VOCs would be released and stored in a cold trap. The VOCs in the cold trap were analyzed using gas chromatography. A mass spectrometer was used to identify each contaminant and a flame ionization detector was used to measure the contaminant concentration.

Experimental results showed that the contaminant transfer rate is related to the VOCs boiling point. Chemical compounds with higher boiling points showed higher transfer rates. For example, phenol with a boiling point of 182 °C showed a transfer rate of 48% and limonene with a boiling point of 177 °C showed a transfer rate of 4%. A physical reason for this result was not provided. This research did not examine the effects of operating conditions on VOC transfer by adsorption/desorption in energy wheels.

2.4.2.5 Wolfrum *et al.* (2008) [21]

Wolfrum *et al.* (2008) [21] studied toluene and n-hexane transfer in a desiccant wheel. A syringe pump with 10 mL volume was used to inject a liquid mixture of toluene and n-hexane into the return airstream. The syringe pump injected the VOCs with a flow rate of 1-10 µL/min to a transfer airstream with a flow rate of 28 L/min. The transfer airstream was used to evaporate and mix the VOCs before they were injected into the return airstream. The transfer airstream entered the return airstream 6 m upstream the desiccant wheel. A 50:50 mixture by mass of toluene and n-hexane was injected at 18 µL/min into a transfer airstream with a flow rate of 16990 L/min resulted in concentration of 100 ppb for gaseous toluene and concentration of 125 ppb for gaseous n-hexane.

Air samples were collected using a vacuum pump and passed through a manifold with 10 sorbent tubes. Adsorbed contaminants by the tubes were desorbed and concentrated using a thermo-desorption technique. Gas chromatography was used to identify the concentration of VOC. After determining the VOCs concentration in the sorbent tubes, each tube was heated to 325 °C for 10 minutes to ensure no contaminant remained in the tube for the next experiment. The desiccant wheel transferred 50-80% of the toluene and 10-30% of the n-hexane from the return airstream to supply airstream. A total uncertainty of 5% was included in the results. Results showed that contaminant mass conservation was satisfied.

2.4.2.6 Kodama (2010) [6]

Kodama (2010) [6] studied the transfer of VOCs in energy wheels coated with two types of desiccants: ion-exchange resin (IER) and 3 Å zeolite molecular sieve. These desiccants were selected due to the selectivity feature on water vapor adsorption/desorption and preventing gaseous contaminants from adsorption/desorption. Tests were conducted for pressure difference between the supply and return airstreams of 0 and 250 Pa. The supply airstream had a higher flow rate than that of the return airstream. Carbon dioxide, propane, ammonia, and formaldehyde were tested. Carbon dioxide and propane were injected at constant flow rates using a mass flow controller. Ammonia and formaldehyde were injected by an aeration mechanism where an airstream was supplied through water solutions of the contaminants at a controlled flow rate. Then the ammonia and formaldehyde rich air was injected into the return airstream.

Air samples were collected in sampling bags and analyzed by gas detector tubes and gas chromatography. Carbon dioxide and propane concentrations were measured using gas chromatography technique. Formaldehyde and ammonia concentrations were determined by gas

detector tubes. Gas detector tubes with a measuring range of 0.2-20 ppm for ammonia and 0.05-4 ppm for formaldehyde were applied.

The results showed that ammonia transfer was between 20-46%, carbon dioxide transfer was between 1-3%, formaldehyde transfer was between 6-35%, and propane transfer was between 1-4%. Ammonia showed the highest transfer rate, which was attributed to its higher water-solubility and smaller molecular size. The ion-exchange resin desiccant showed 2-6 times lower contaminant transfer than the 3Å zeolite desiccant. It was concluded that desiccants which adsorb water and water-soluble substances are more likely to transfer VOCs in energy wheels. The results did not include contaminant mass conservation or an uncertainty analysis.

2.4.2.7 Bayer (2011) [7]

Bayer (2011) [7] studied the transfer of VOCs in energy wheels coated with 3 Å molecular sieve desiccants. The studied VOCs included propane, carbon dioxide, methyl isobutyl ketone (MIBK), isopropyl alcohol, xylene, acetaldehyde, methanol, and acetic acid. The wheel rotated at 20 rpm and the pressure of the supply airstream was 109 Pa higher than that of the return airstream.

Air samples were collected in Tedlar sampling bags and analyzed with a photoacoustic spectroscopy technique. The air samples were taken 10 times and the average VOC concentration was reported. The published report did not describe the contaminant injection method nor details of the contaminant concentration measurement technique. Experiments on an energy wheel coated with a 3 Å molecular sieve desiccant showed that contaminant transfer was zero for all contaminants. This work did not contain an uncertainty analysis. It should also be noted that these results were published as a report and were not peer-reviewed.

2.4.2.8 Patel *et al.* (2014) [22]

Patel *et al.* (2014) [22] performed experiments with toluene and formaldehyde in a run-around membrane energy exchanger (RAMEE). Contaminants were injected using a calibrated gas mixture injection technique and a contaminant evaporation technique. In the calibrated gas mixture injection technique, gaseous toluene with a concentration of 150 ppm and gaseous formaldehyde with a concentration of 30 ppm were injected into the exhaust airstream. In the contaminant evaporation technique, liquid contaminants were injected into an evaporation chamber using a syringe pump with flow rates from 0.73 μL/h to 1500 mL/h. Liquid contaminants were evaporated and contaminated air flowed to the exhaust airstream. Air samples were drawn from the supply and exhaust ducts to 100 L Teflon sampling bags. Air samples were analyzed using the Fourier Transform Infrared (FTIR) spectroscopy technique.

The contaminant transfer in the RAMEE occurred due to the concentration difference between the contaminants in the airstream and the contaminants in the liquid desiccant in the LAMEEs. The contaminant transfer mechanisms were described as (1) convection from the exhaust airstream to the membrane surface, (2) diffusion through the membrane to the liquid desiccant, (3) advection of contaminants dissolved in the liquid desiccant to the supply LAMEE, (4) diffusion through the membrane, and (5) convection to the supply airstream.

EATR values were found to be 4-6% for formaldehyde and 2-3% for toluene. The uncertainty in the formaldehyde and toluene transfer rates were 4% and 3%, respectively. The higher EATR for formaldehyde was attributed to a higher diffusivity and water solubility compared to toluene. These values are smaller than the 71% toluene transfer in a desiccant wheel [21] and 8-15% formaldehyde transfer in energy wheels [4], [19]. Moreover, changes in the air flow rate, test

conditions and liquid desiccant flow rate showed no significant effect on the transfer rate of contaminants in the RAMEE.

2.4.2.9 Hult *et al.* (2014) [24]

Hult *et al.* (2014) [24] investigated formaldehyde transfer rate in energy wheels using laboratory and field experiments. Experiments started with injecting liquid formaldehyde into an evaporation chamber using a glass syringe pump. Gaseous formaldehyde with a concentration range of 60-75 $\mu g/m^3$ was delivered to the return airstream. Air samples were collected with 2,4-dinitrophenylhydrazine silica samplers from the outdoor, supply, return, and exhaust airstreams.

Results from the field experiments showed a formaldehyde transfer rate between 28% and 29%. carbon dioxide concentration measurement showed that 92-100% of formaldehyde transfer occurred due to air leakage and carryover mechanisms, and only 0-8% of formaldehyde transfer occurred due to adsorption/desorption mechanism. Laboratory experiments at different air flow rates showed that the formaldehyde transfer rate decreased as the air flow rate increased. Similarly, the researchers found that formaldehyde adsorption/desorption decreased as the air flow rate increased. For example, the contribution of adsorption/desorption on the formaldehyde transfer was 30% at an air flow rate of 85 m^3/h and 10% at an air flow rate of 340 m^3/h. This might have occurred due to the inverse relationship between air flow rate and residence time of formaldehyde in the wheel. In other words, as the air flow rate decreased, the air velocity through the wheel flutes decreased and thus there was more time for formaldehyde molecules to be adsorbed by the desiccants. Formaldehyde transfer results were shown with a total uncertainty of ± 3% for field and laboratory experiments.

2.4.2.10 Nie *et al.* (2015) [26]

Nie *et al.* (2015) [26] studied gaseous contaminant transfer in a flat plate enthalpy exchanger. Toluene, acetone, and ammonia were used. These contaminants were continuously injected into the return airstream with a washing bottle connected to the injection port. The washing bottle was used to control contaminant concentration at the injection port. Details of the contaminant injection technique such as the mass of injected contaminants were not provided. Air samples were taken from the outdoor, supply, return, and exhaust airstreams. Plastic tubes were used to deliver air samples to a photoacoustic multi-gas analyzer.

Results showed that the toluene transfer from the return airstream to the supply airstream was between 7-8%, the acetone transfer was between 5-6%, and the ammonia transfer was between 8-9%. Experiments at different outdoor conditions showed that the toluene transfer in the flat plate enthalpy exchanger was nearly unaffected by outdoor temperature and humidity ratio. For example, when the outdoor air temperature was 35 °C and the humidity ratio was 22 g/kg (63% RH), the toluene transfer was 7%. When the outdoor air temperature decreased to 11 °C and the humidity ratio decreased to 6 g/kg (74% RH), the toluene transfer increased to 8%. Similar results were found for acetone and ammonia. This study did not include an uncertainty analysis nor report whether the mass of contaminants was conserved in the experiments.

2.5 Summary of the literature review

Table 2.1 provides a summary of the measured EATR values and uncertainties for various energy exchangers from the literature. An established test methodology for measuring contaminant transfer due to air leakage and carryover (i.e., due to bulk airflow) in energy wheels is available in ASHRAE Standard 84 (2020) [15]. However, based on the literature review, a similar test

methodology for determining the contribution of adsorption/desorption mechanism in gaseous contaminant transfer in energy wheels is missing.

Table 2.1. Summary of the gaseous contaminant transfer rates and uncertainties measured on various energy exchangers. Studies that reported 3% uncertainty of EATR satisfied ASHRAE Standard 84 requirement.

Gas	Energy exchanger	EATR	Uncertainty	Reference
1. Acetaldehyde	Energy wheel	17%	NR	Bayer (2011) [7]
2. Ammonia	Energy wheel	10-46%	NR	Okano *et al.* (2001) [14], Kodama (2010) [6]
	Flat plate enthalpy exchanger	8-9%		Nie *et al.* (2015) [26]
3. Acetic acid	Energy wheel	7-36%	NR	Okano *et al.* (2001) [14], Bayer (2011) [7]
4. Methanol	Energy wheel	0-11%	NR	Okano *et al.* (2001) [14], Bayer (2011) [7]
5. Isopropyl alcohol	Energy wheel	0-4%	NR	Okano *et al.* (2001) [14], Bayer (2011) [7]
6. Methyl isobutyl ketone	Energy wheel	0-3%	NR	Okano *et al.* (2001) [14], Bayer (2011) [7]
7. Xylene	Energy wheel	0-30%	NR	Okano *et al.* (2001) [14], Bayer (2011) [7], Roulet *et al.* (2002) [10]
8. Carbon dioxide	Energy wheel	0.6-5%	NR	Kodama (2010) [6], Bayer (2011) [7], Kassai (2018) [25]
	Flat plate type mass exchanger	1%		Sparrow *et al.* (2001) [20]
9. Propane or hexane	Energy wheel	0.2-7%	5%	Kodama (2010) [6], Bayer (2011) [7], Fisk *et al.* (1985) [4]
	Flat plate enthalpy exchanger	6-8%		Fisk *et al.* (1985) [4]
	Desiccant wheel	20%		Wolfrum *et al.* (2008) [21]
10. Phenol	Energy wheel	30-75%	NR	Roulet *et al.* (2002) [10]
11. Sulfur hexafluoride	Energy wheel	5-26%	1%	Bayer (2011) [7], Khoury *et al.* (1988) [13], Fisk *et al.* (1985) [4], Roulet *et al.* (2002) [10]
	Flat plate enthalpy exchanger	5-8%		Fisk *et al.* (1985) [4]
12. Formaldehyde	Energy wheel	6-35%	3-29%	Okano *et al.* (2001) [14], Kodama (2010) [6], Andersson *et al.* (1999) [19], Bayer (2011) [7],

				Hult *et al.* (2014) [24], Fisk *et al.* (1985) [4]
	Flat plate enthalpy exchanger	7-12%		Fisk *et al.* (1985) [4]
	RAMEE	5-6%		Patel *et al.* (2014) [22]
13. Nitrous oxide	Energy wheel	1-54%	3%	Shang *et al.* (2001) [5]
14. Acetone	Energy wheel	0	NR	Okano *et al.* (2001) [14]
	Flat plate enthalpy exchanger	5-6		Nie *et al.* (2015) [26]
15. Toluene	RAMEE	2-3%	3-5%	Patel *et al.*(2014) [22]
	Desiccant wheel	70%		Wolfrum *et al.* (2008) [21]
	Flat plate enthalpy exchanger	7-8%		Nie *et al.* (2015) [26]
	Energy wheel	0-30%		Okano *et al.* (2001) [14]
16. Inert tracer gas (for measuring air leakage and carryover)	Air-to-air heat/energy exchanger	----	3%	ASHRAE Standard 84 (2020) [15], CSA Standard C 439-18 (2018) [16]

RAMEE = Run-around membrane energy exchanger, NR = uncertainty not reported

2.6 Analysis of literature data

In the following sections, the literature data will be presented to show the effect of different operating and design parameters on EATR.

2.6.1 Effect of temperature on EATR

Figure 2.6 presents EATR versus outdoor air temperature for different VOCs. EATR for acetaldehyde, ammonia, acetic acid, methanol, and isopropyl alcohol are shown in Figure 2.6 (a), EATR for methyl isobutyl ketone (MIBK), xylene, carbon dioxide, and propane are shown in Figure 2.6 (b), and EATR for sulfur hexafluoride is shown in Figure 2.6 (c). There is no clear relationship between EATR and outdoor air temperature because the design and operating parameters are different in each test (e.g., different exchangers, desiccants, face velocities, pressure conditions, and purge sections). Figure 2.6 tends to indicate that these other parameters play a more important role in contaminant transfer than temperature.

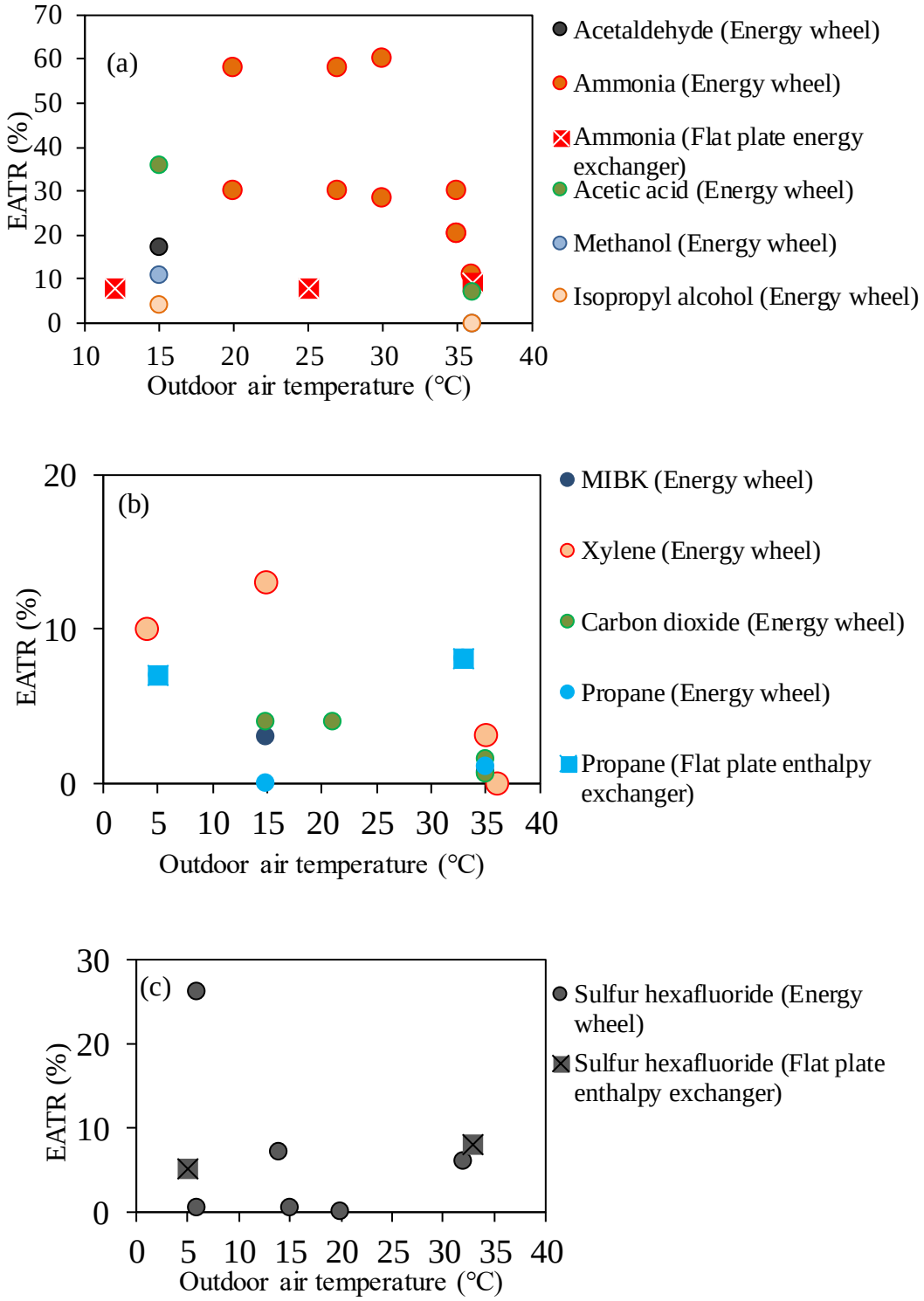

Figure 2.6. EATR for (a) acetaldehyde, ammonia, acetic acid, methanol, and isopropyl alcohol, (b) MIBK, xylene, carbon dioxide, propane, and (c) sulfur hexafluoride versus outdoor air temperatures under varying test conditions.

Okano *et al.* (2001) [14] studied the effect of outdoor air temperature on EATR for ammonia while keeping other parameters constant. They found that changing outdoor air temperature does not change EATR significantly, as can be seen in Figure 2.7. Okano *et al.* (2001) [14] found that energy wheels with different desiccants (silica gel (SG) and ion exchange resin (IER)) show very similar trends for EATR versus outdoor air temperature.

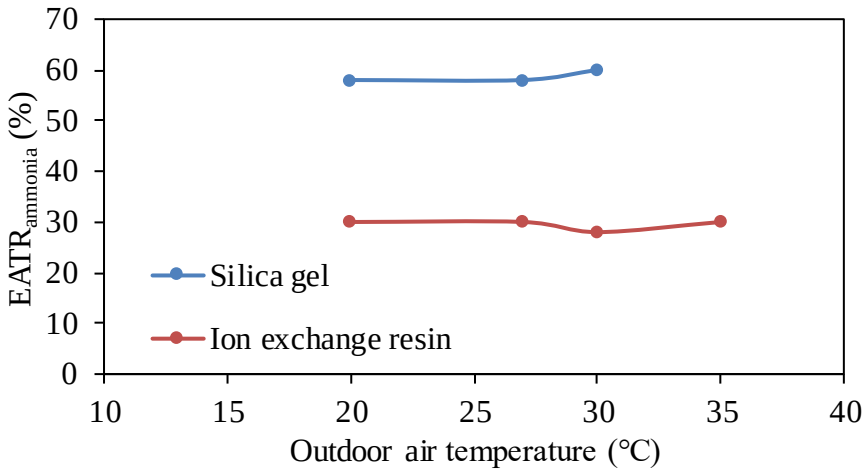

Figure 2.7. EATR for ammonia versus outdoor air temperature at constant test conditions [14].

2.6.2 Effect of humidity on EATR

Figure 2.8 shows that EATR tends to decrease as the outdoor air relative humidity increases for different VOCs. EATR for acetaldehyde, ammonia, acetic acid, methanol, and isopropyl alcohol are shown in Figure 2.6 (a) and EATR for methyl isobutyl ketone (MIBK), xylene, carbon dioxide, and propane are shown in Figure 2.6 (b). However, there is a large scatter in the data because the design and operating parameters are not the same in all tests.

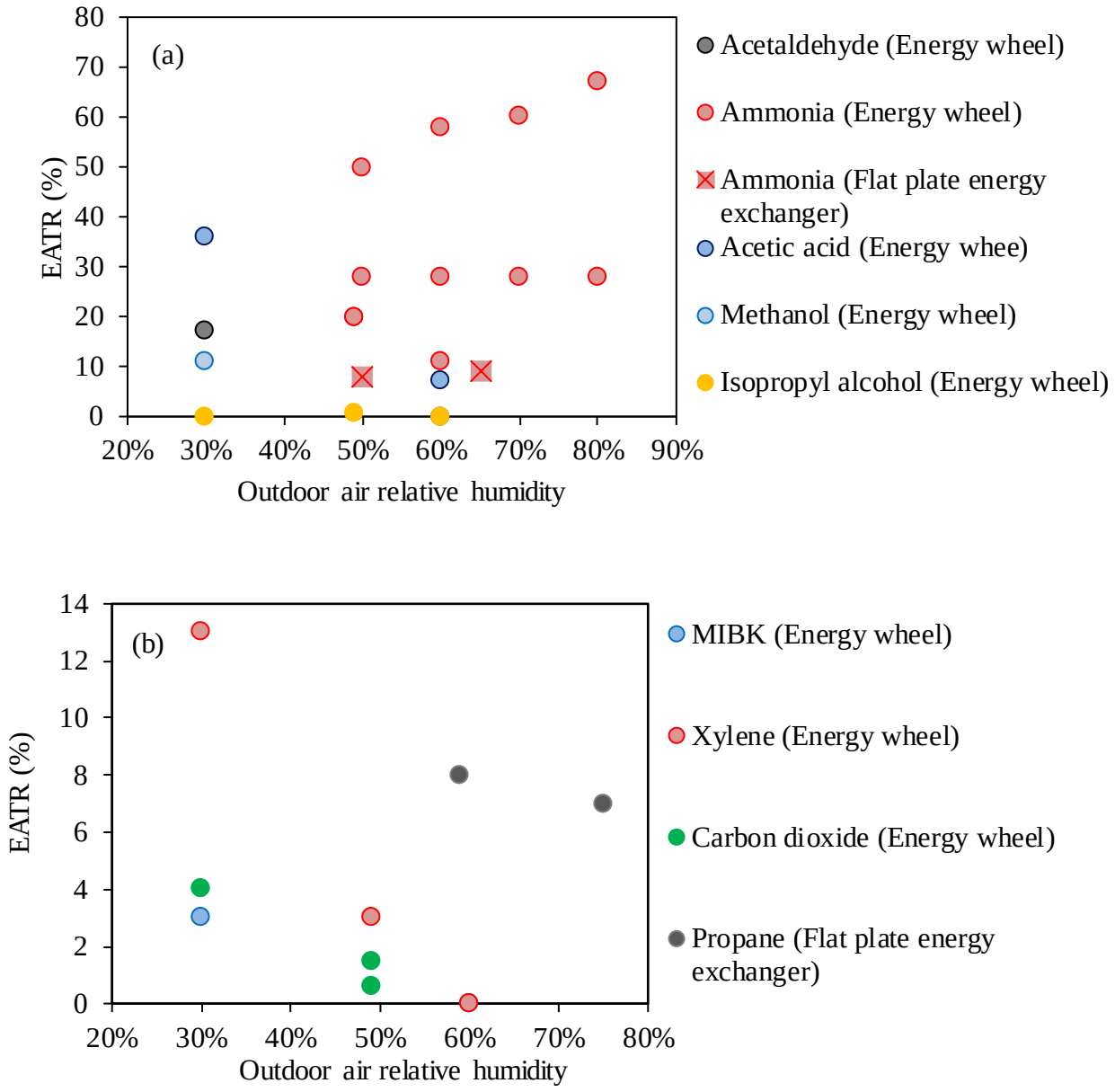

Figure 2.8. EATR for (a) acetaldehyde, ammonia, acetic acid, methanol, and isopropyl alcohol, and (b) MIBK, xylene, carbon dioxide, and propane versus outdoor air relative humidity under varying test conditions.

Figure 2.9 presents the effect of outdoor air relative humidity on EATR for ammonia as measured by Okano *et al.* (2001) for constant design parameters except for the desiccant coating on the wheel [14]. It is seen that EATR increases or remains constant with increasing outdoor air relative humidity depending on the desiccant material coated on energy wheel, which is slightly different

than the apparent trend in Figure 2.9. Okano *et al.* (2001) [14] found that increasing the outdoor air relative humidity increases EATR for ammonia in energy wheels with a silica gel desiccant but does not change EATR in energy wheels with an ion exchange resin desiccant.

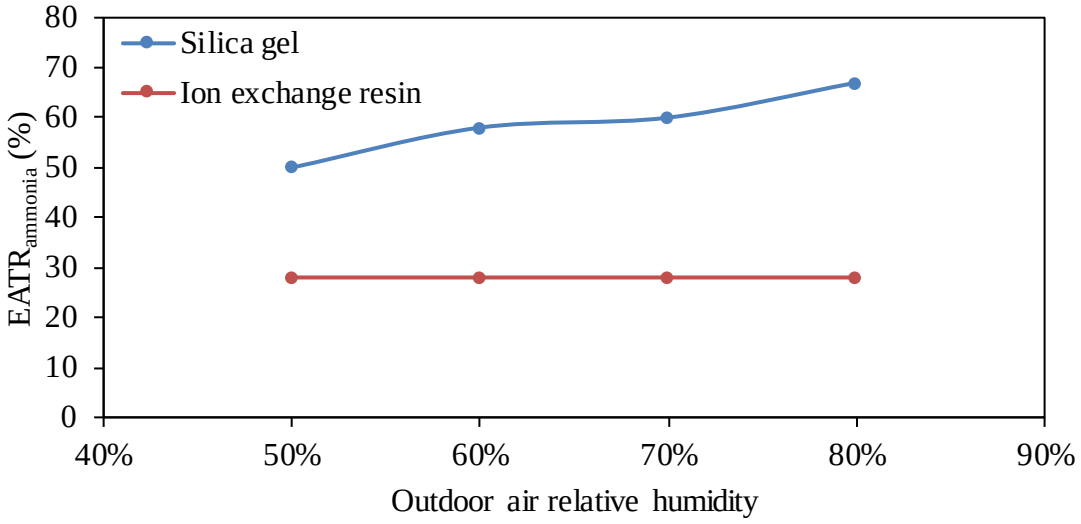

Figure 2.9. EATR for ammonia versus outdoor air relative humidity at constant test conditions [14].

2.6.3 Effect of face velocity on EATR

One may expect the contaminant transfer to depend on the exchanger design (NTU and Cr*). However, since most researchers do not report NTU and Cr* or provide enough information to calculate NTU and Cr*, the effect of face velocity will be presented here. According to Eqs. (2.11) and (2.12), NTU and Cr* are inversely proportional to face velocity [17], [27].

The effect of face velocity on EATR was studied by Okano *et al.* (2001) [14] and is presented in Figure 2.10. Figure 2.10 shows a consistent trend of decreasing EATR with increasing face velocity (decreasing NTU and Cr*) regardless of the desiccant. This trend may be due to the fact that if the contaminant transfer rate is constant, the percent carryover will decrease as the face

velocity (flow rate of air) increases. Figure 2.10 also contains dashed lines to indicate how EATR would change if the contaminant transfer rates were constant at the measured contaminant transfer rate at a face velocity of 2 m/s using Eqn. (2.13) in Section 2.4.2.3. Comparing the solid lines (measured data) and the dashed lines (data based on a constant contaminant transfer rate and dilution) shows that the measured EATR is quite similar (within ± 5%) to EATR calculated assuming a constant contaminant transfer rate. It should also be noted that this study [14] did not report the uncertainty of the EATR results.

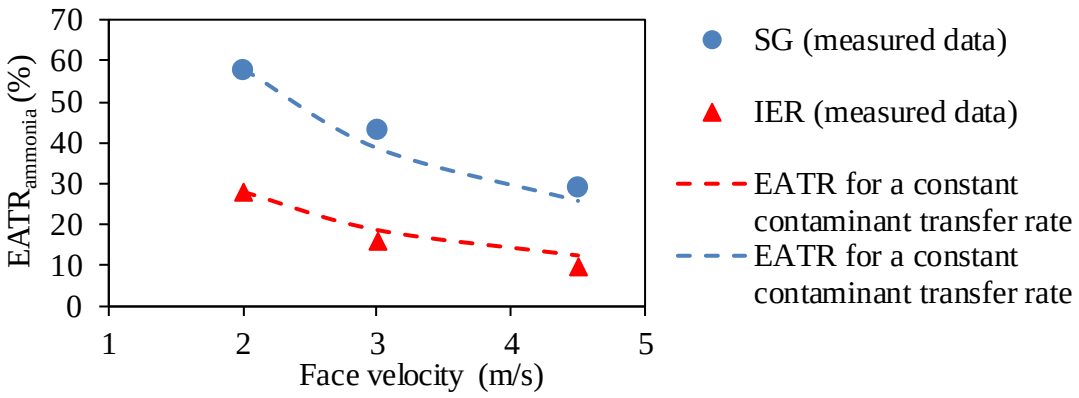

Figure 2.10. EATR for ammonia versus air face velocity at constant test conditions (solid lines) [14] compared to EATR that would exist if the total contaminant transfer rate were constant at a face velocity of 2 m/s (dashed lines).

2.6.4 Effect of effectiveness on EATR

Figure 2.11 presents EATR as a function of total effectiveness for different energy exchangers with different contaminants. In general, EATR increases as the total effectiveness increases. For example, for acetic acid, when the total effectiveness increases from 75% to 90%, EATR increases almost 5 times (from 7% to 36%). This might be due to a decrease in face velocity, which would increase contaminant transfer through carryover as noted in the previous section, or due to an

increase in the adsorption/desorption of the contaminant in the energy wheels (it should be noted that the adsorption/desorption of water vapor also increases as the effectiveness increases). For some VOCs and exchangers (e.g., ammonia in the flat plate energy exchanger [26] and propane in energy wheel [4], [6], [7]), EATR decreases as the total effectiveness increases.

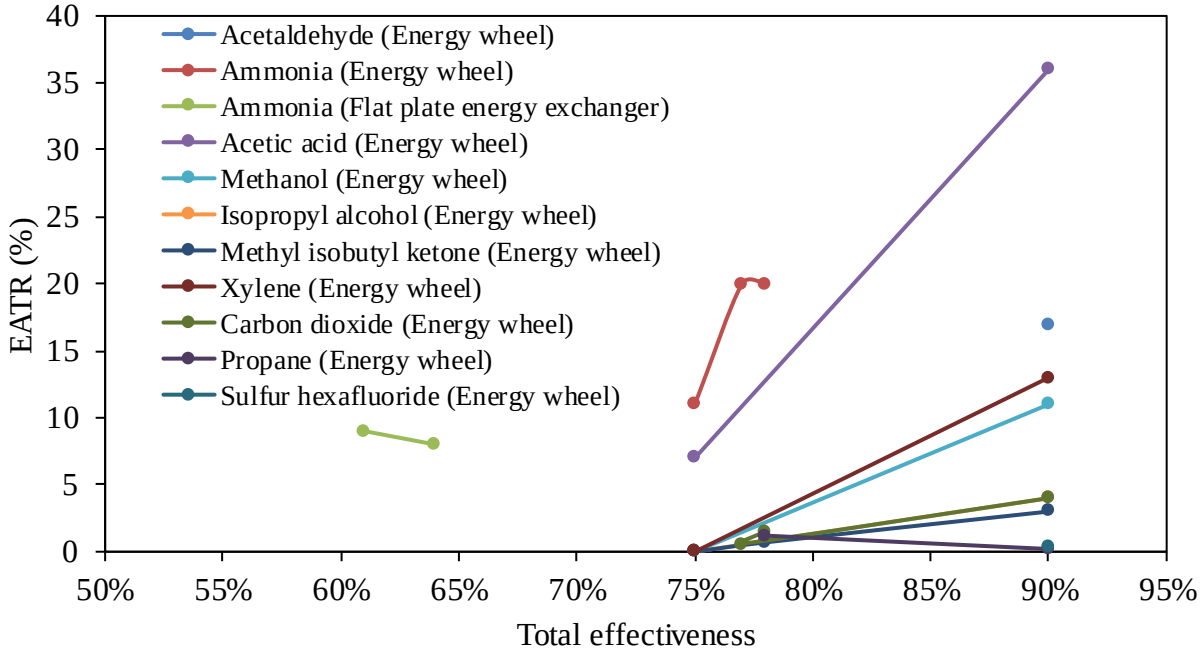

Figure 2.11. EATR as a function of total effectiveness for different energy exchangers.

2.7 New method to determine the contaminant transfer due to adsorption/desorption

ASHRAE 84 (2020) [15] and CSA C 439-18 [16] test standards require an inert tracer gas such as sulfur hexafluoride (SF_6) and the same temperature and humidity conditions in the supply and return airstreams for contaminant transfer experiments. These experiments measure contaminant transfer (i.e., EATR) by bulk airflow only. They do not include the contaminant transfer due to adsorption/desorption and transfer during extreme conditions such as condensation and frosting. Therefore, a methodology needs to be developed to consider these effects.

The literature review revealed that the adsorption/desorption mechanism significantly contributes to gaseous contaminant transfer in energy exchangers. Contaminant transfer due to adsorption/desorption depends on many factors, such as the nature of the contaminant, the type of desiccant, the exchanger design, and the operating conditions. Hence, a new parameter ($EATR_{ad}$) is proposed to quantify the contribution of the adsorption/desorption in gaseous contaminant transfer in energy exchangers. The $EATR_{ad}$ is determined by subtracting the EATR measured with a non-inert gas (e.g. VOCs) from the EATR measured with an inert tracer gas (sulfur hexafluoride – according to ASHRAE Standard 84 (2020) [15]) as given in Eqn. (2.15).

$$EATR_{ad} = EATR_{non-inert} - EATR_{inert} \tag{2.15}$$

The $EATR_{non-inert}$ and $EATR_{inert}$ are the EATR of the gas being tested and the inert gas (i.e., sulfur hexafluoride), respectively. The $EATR_{ad}$ for different gaseous contaminants, which were calculated from data in the literature using Eqn. (2.15), are presented in Figure 2.12. Figure 2.12 shows that $EATR_{ad}$ is highest for acetic acid, phenol, and acetaldehyde. This may be due to the higher water solubility and smaller molecular size of these VOCs. Xylene was studied in two research papers [7], [10] and the $EATR_{ad}$ for xylene was reported to be between 3% and 13%. This difference between the $EATR_{ad}$ values could be due to the different design considerations and test conditions in the different studies. Additional research is required to verify the proposed method of quantifying contaminant transfer due to adsorption/desorption ($EATR_{ad}$) and to determine the uncertainty in $EATR_{ad}$ for various gases and operating conditions.

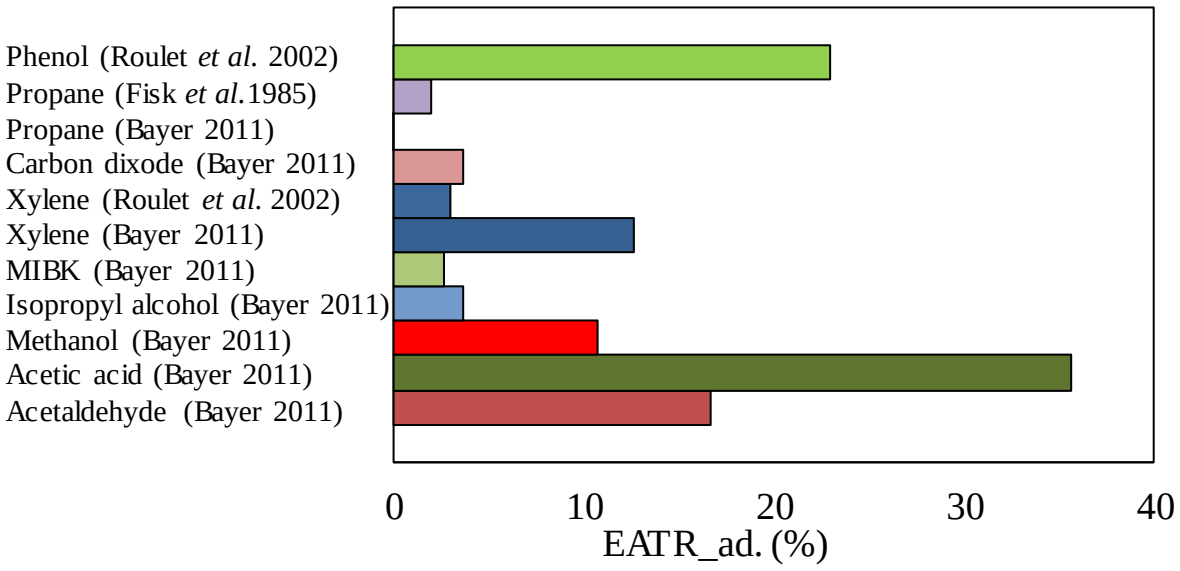

Figure 2.12. $EATR_{ad}$ for different VOCs reported in the literature.

2.8 Conclusions

This chapter reviewed the available experimental studies in the area of contaminant transfer in energy exchangers. Several papers have reported the contaminant transfer rate of various contaminants, and most of them were focused on rotary-type energy exchanges. Based on the available literature on contaminant transfer in energy exchangers, the following conclusions can be made.

- There are three main mechanisms that contribute to gaseous contaminant transfer in energy exchangers: air leakage, carryover, and adsorption/desorption.
- Gaseous contaminant transfer due to air leakage and carryover has been studied and measured extensively in the literature using inert gases. An established test methodology for measuring air leakage and carryover exists and is included in test standards ASHRAE 84-2020 [15] and CSA C439 [16]. Contaminant transfer due to air leakage and carryover

(i.e., bulk air flow from the exhaust side to the supply side of the exchanger) is quantified using the exhaust air transfer ratio (EATR).

- Several researchers have measured contaminant transfer of non-inert gases in energy exchangers. While such measurements inherently include all transfer mechanisms (air leakage, carryover, and adsorption/desorption), no test methods exist in the literature to quantify the adsorption/desorption mechanism. Thus, a method to quantify contaminant transfer due to adsorption/desorption was proposed and applied in this chapter. More research is required to verify the proposed method and its uncertainty.
- The literature review showed that measured gaseous contaminant transfer rates vary between 0% and 75%. The highest transfer rates were measured for phenol, toluene, nitrous oxide, ammonia, acetic acid, and formaldehyde. A common chemical characteristic among these contaminants, except for nitrous oxide (a tracer, and a non-reacting gas), is their high water solubility, which may be a possible reason for high contaminant transfer rates. The high value of EATR for nitrous oxide was due to higher pressure on the exhaust side than the supply side of the energy wheel causing significant contaminant transfer due to air leakage.
- The literature review showed that the uncertainties in measured EATR varied between 1% and 30%, but most studies did not include a detailed uncertainty analysis. Furthermore, most studies did not determine if the experiments conserved mass of gaseous contaminants.
- The literature review showed that the exchanger design parameters (effectiveness and face velocity) have a more significant effect on EATR than the operating conditions (relative humidity and temperature) for the case of energy wheels.

CHAPTER 3
EXPERIMENTAL FACILITY AND RESULTS

3.1 Overview

This chapter addresses the second objective of this MSc thesis, which is to apply and verify a test methodology for measuring gaseous contaminant transfer in energy wheels. The proposed test methodology including the test facility, contaminant injection methods, gas sampling technique, instrumentation, and uncertainty analysis is described. The test facility and methodology are applied to measure the contaminant transfer rates, expressed as a dimensionless ratio known as the exhaust air transfer ratio (EATR), for carbon dioxide (CO_2), sulfur hexafluoride (SF_6), ammonia (NH_3), methanol (CH_3OH), and isopropyl alcohol (C_3H_8O) at different design and operating conditions. The effect of the air face velocity (design parameter) and outdoor air temperature (operating condition) on EATR are investigated. It is shown that outdoor air temperature has a negligible effect on EATR while increasing the air face velocity decreases EATR. The results show that EATR for carbon dioxide and sulfur hexafluoride are nearly equal, which indicates that the transfer of carbon dioxide is mainly due to air leakage and carryover. The proposed method for determining the contaminant transfer due to adsorption/desorption in energy wheels, that was presented in Chapter 2 of the thesis, is applied and verified. The EATR test data show that the contribution of adsorption/desorption is significant for ammonia, methanol, and isopropyl alcohol. A common characteristic of ammonia, isopropyl alcohol, and methanol is that they are all polar chemicals.

This chapter is part of a research paper that is under preparation. The authors of the paper will be Easwaran Krishnan, Hayden Reitenbach, Mehrdad Torabi, Jafar Soltan, and Carey Simonson. Mehrdad Torabi wrote this chapter with input from Easwaran Krishnan and Carey Simonson.

Easwaran Krishnan and Mehrdad Torabi jointly conducted the experiments and analyzed the experimental data. Easwaran Krishnan provided Figures 3.13 to 3.16 in this chapter. Hayden Reitenbach and Easwaran Krishnan developed the test methodology and the test facility. Professors Carey Simonson and Jafar Soltan provided oversight for the research.

3.2 Test facility

The contaminant transfer experiments presented in this chapter were conducted using an existing energy wheel test facility at the University of Saskatchewan. The test facility has been used by previous graduate students and researchers [8], [28], [29] to test various air-to-air energy exchangers in accordance with ASHRAE Standard 84 (2020) [15].

The test facility is shown in Figures 3.1 and 3.2 and consists of an air handling system, a test section (containing the energy wheel), a gas injection system, and a gas sampling system. The function of the air handling system is to transport air to/from the test section and allow the measurement of the air properties at different measurement stations. The air handling system contains four air lines including outdoor air (OA), supply air (SA), return air (RA), and exhaust air (EA). The gas injection system was used to control the injection of contaminants to RA. The gas sampling system consisted of a vacuum pump, Teflon sampling tubes with solenoid valves to draw air samples and a gas analyzer to measure the concentration of the gas samples.

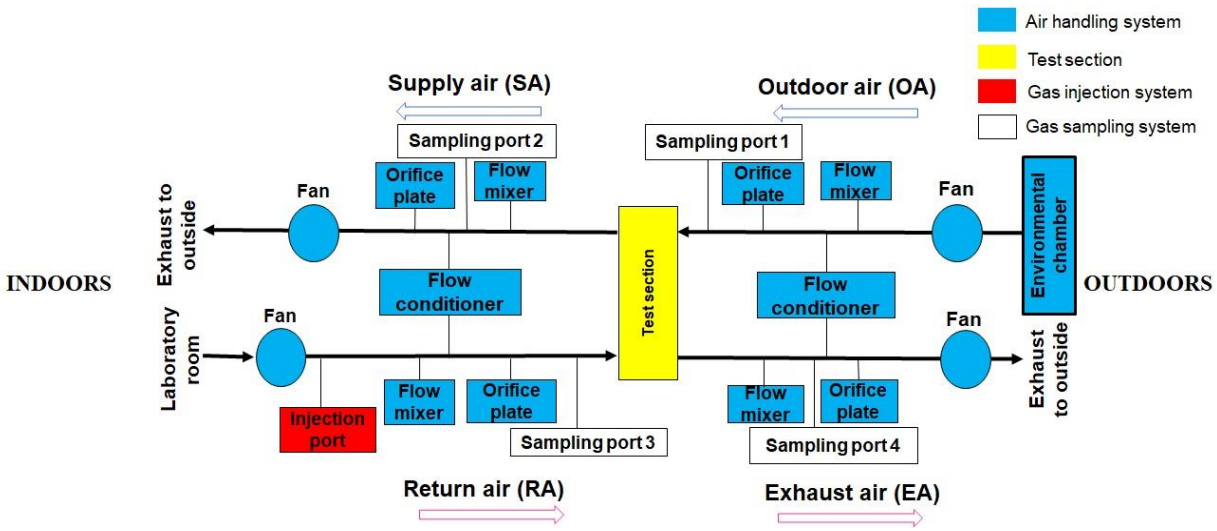

Figure 3.1. Schematic of the energy wheel test facility showing the air handling system, test section, gas injection system, and gas sampling system.

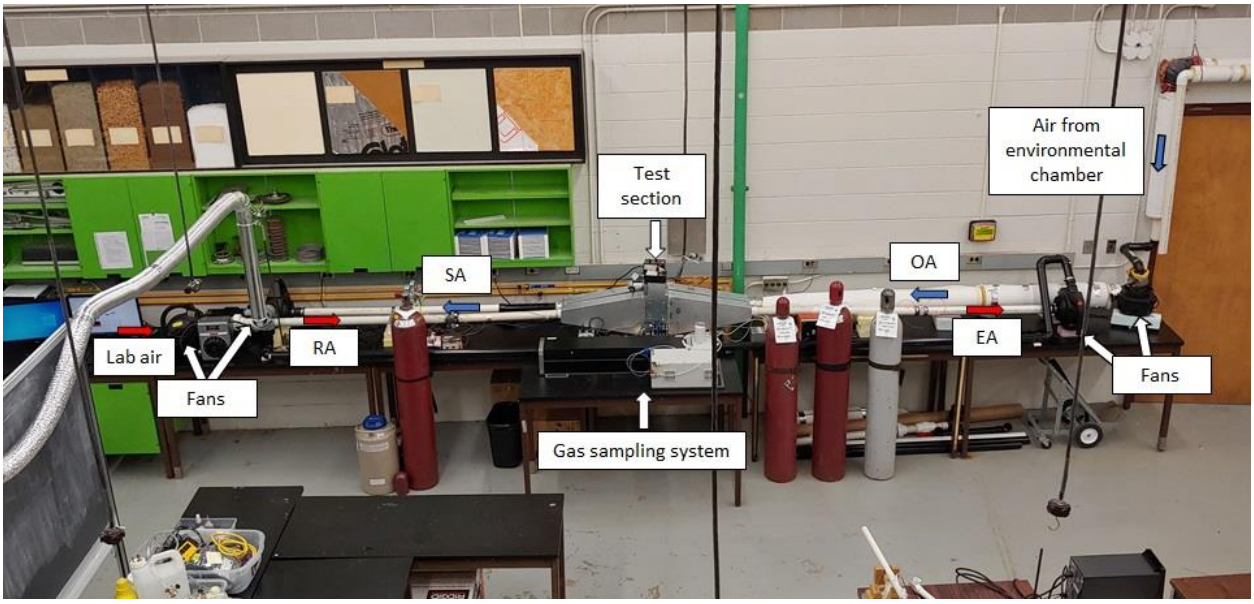

Figure 3.2. Photograph of the energy wheel test facility used in the contaminant transfer experiments.

3.2.1 Air handling system

Four centrifugal blowers (5 hp (3.73 kW) vacuum fans) were used to provide the required airflow to the test section and maintain the desired pressures in the supply and exhaust air lines. The supply and exhaust air lines were made of 5 cm (2 inch) circular PVC pipes and the flow rates were

controlled by varying the rotational speed of the blowers using variable voltage transformers. Flow mixers were used to provide uniform temperature, relative humidity, and contaminant concentration in the airflow at the measurement stations. Air temperatures and relative humidities were measured using T-type thermocouples and capacitive humidity sensors, respectively (more details of the instrumentation, calibration and uncertainty are provided in Section 3.2.5). The airflow rate was measured with an orifice plate and a differential pressure transducer. Honeycomb-shaped flow conditioners were installed upstream of the orifice plates to reduce flow disturbances and achieve an accurate measurement of the airflow rate (i.e., providing fully developed flow before the orifice plate). The construction and installation of the orifice plates were based on ISO 5167 Standard [30].

An environmental chamber provided conditioned air from -40°C to +40°C and 20% RH to 90% RH at airflow rates in a range of 10 L/s to 50 L/s (20 CFM to 100 CFM). PID-controlled tubular heaters were used to control temperature in the test section with a maximum deviation of ± 0.3°C at the test section inlet in outdoor airstream.

3.2.2 Test section

The energy wheel under test was located inside the test section. Figure 3.3 shows a picture of the test section and diffusers. The test section contained a molecular sieve coated energy wheel having a diameter of 250 mm and a thickness of 100 mm. A belt-driven gear motor was used to rotate the energy wheel, and the rpm was controlled with the help of a Dayton DC speed controller. The wheel speed was 18 rpm in all the tests. The leakage of air between the test section and the surroundings was reduced by applying a silicone sealant to all mating surfaces between the wheel cassette and the diffusers. In addition, air leakage was reduced by keeping the pressure in the test section near atmospheric pressure.

Figure 3.4 shows a picture of the energy wheel face and the seal between the supply and exhaust sides of the wheel. As discussed in Section 1.3.2, to prevent air leakage from the RA to the SA, the SA pressure should be higher than RA pressure. This higher pressure in the SA side was maintained in the experiments to prevent air leakage from the RA to the SA (i.e., air leakage occurred from the SA to the RA as shown in Figure 3.4).

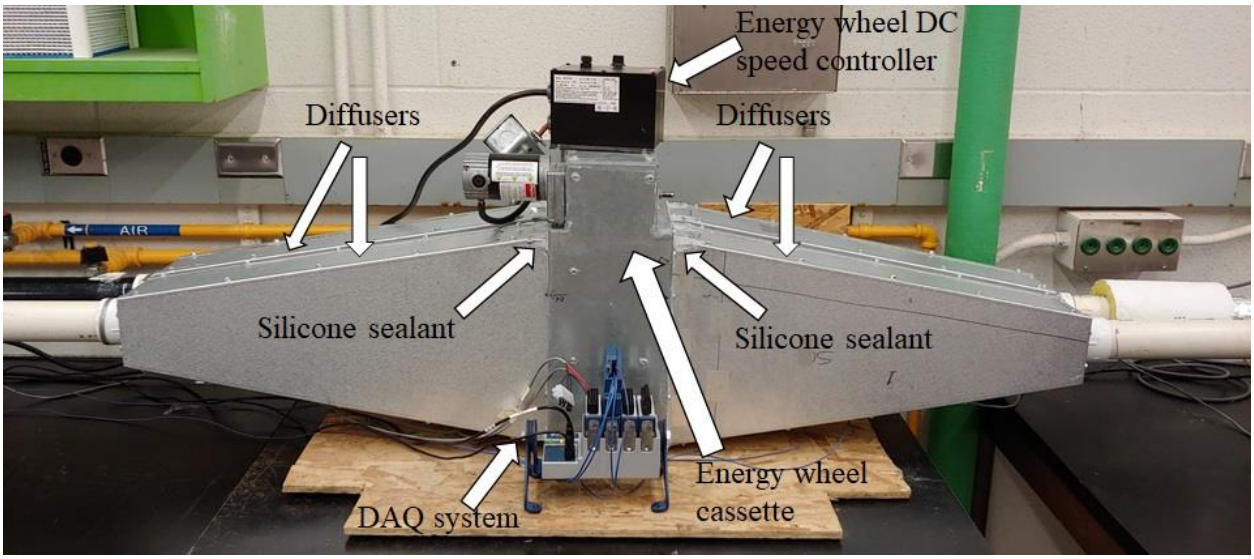

Figure 3.3. Photograph of the test facility showing the energy wheel cassette and diffusers.

Figure 3.4. The energy wheel face and seals showing the direction of air leakage from the high-pressure side (P_{high}) or SA to the low-pressure side (P_{low}) or RA.

3.2.3 Gas injection system

As shown in Figure 3.1, the contaminants were injected into the RA to represent contaminated air from a building. A flow mixer was located downstream of the injection port to ensure adequate mixing of the contaminant and a uniform contaminant concentration at the measurement station and wheel inlet. Both gases and liquids were used as a contaminant source. The contaminant injection technique was chosen based on the availability of contaminants in gaseous or liquid states at room temperature (i.e., boiling point of contaminants). Since carbon dioxide and sulfur hexafluoride are gaseous at room temperature (i.e., carbon dioxide and sulfur hexafluoride have very low boiling points), they were injected using a gas injection technique. Also, since ammonia, methanol, and isopropyl alcohol are available in a liquid state at room temperature (they have higher boing points than carbon dioxide and sulfur hexafluoride), a liquid evaporation technique was used for injecting these contaminants. More details on the gas injection techniques are provided in following sections.

3.2.3.1 Gas injection technique

Figure 3.5 contains a schematic and a photograph of the gas injection system. This method was used to inject carbon dioxide and sulfur hexafluoride. A commercially available pressurized cylinder containing the gaseous contaminant was used as an external source to inject the contaminant. The flow rate of the contaminant was controlled using a rotameter to achieve the desired concentration in the RA. The advantage of the gas injection technique is that it is simple to implement and control and produces a steady concentration of contaminants in the RA as shown in Figure 3.6. The main drawback of this technique is that the costs are generally higher per mass of contaminant than the liquid injection technique, and the cylinders can hold less mass of

contaminant than liquid containers and thus the cylinders may need to be replaced after only a few experiments.

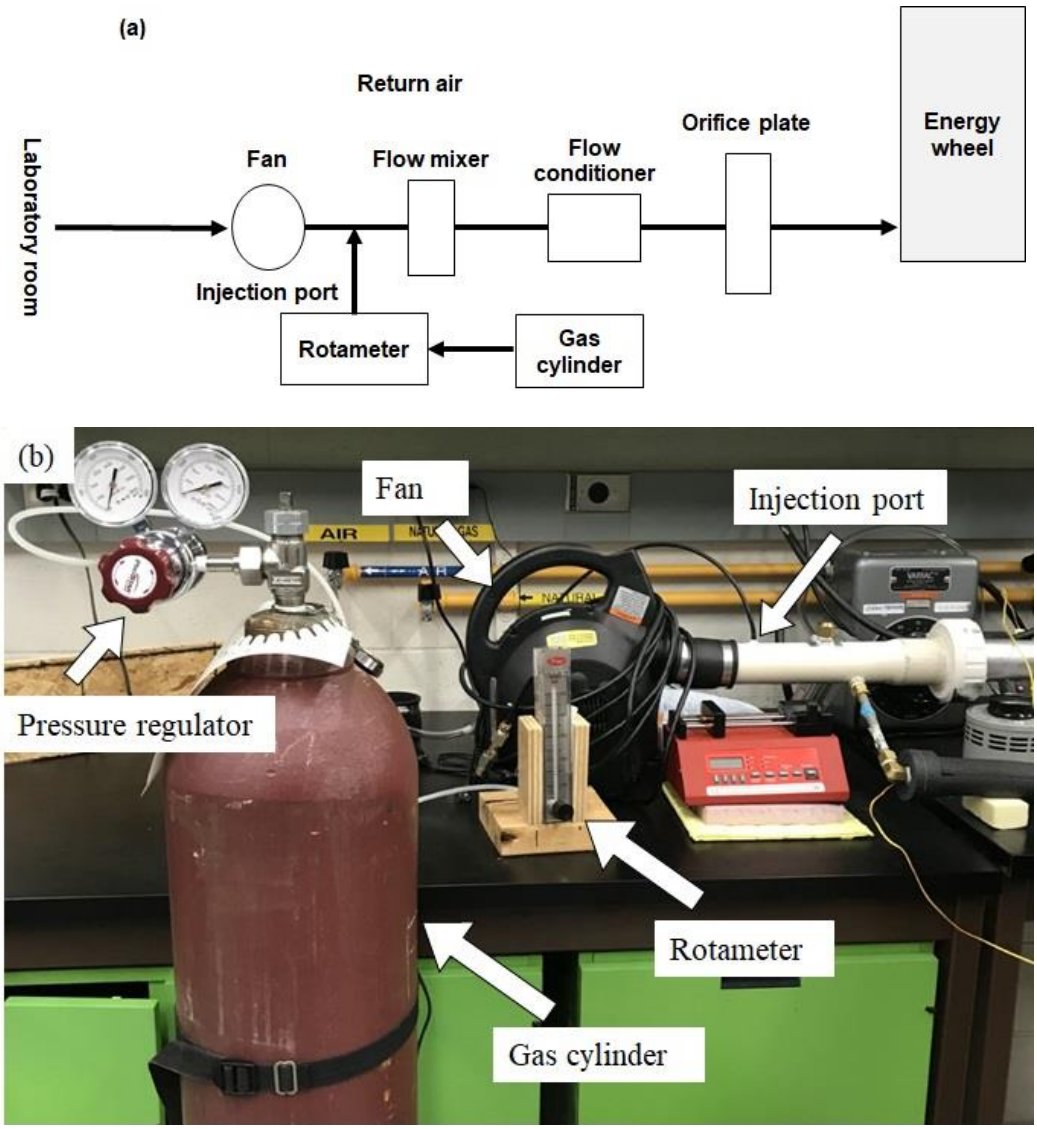

Figure 3.5. (a) Schematic diagram and (b) photograph of the gas injection system showing the rotameter, gas cylinder, and injection port.

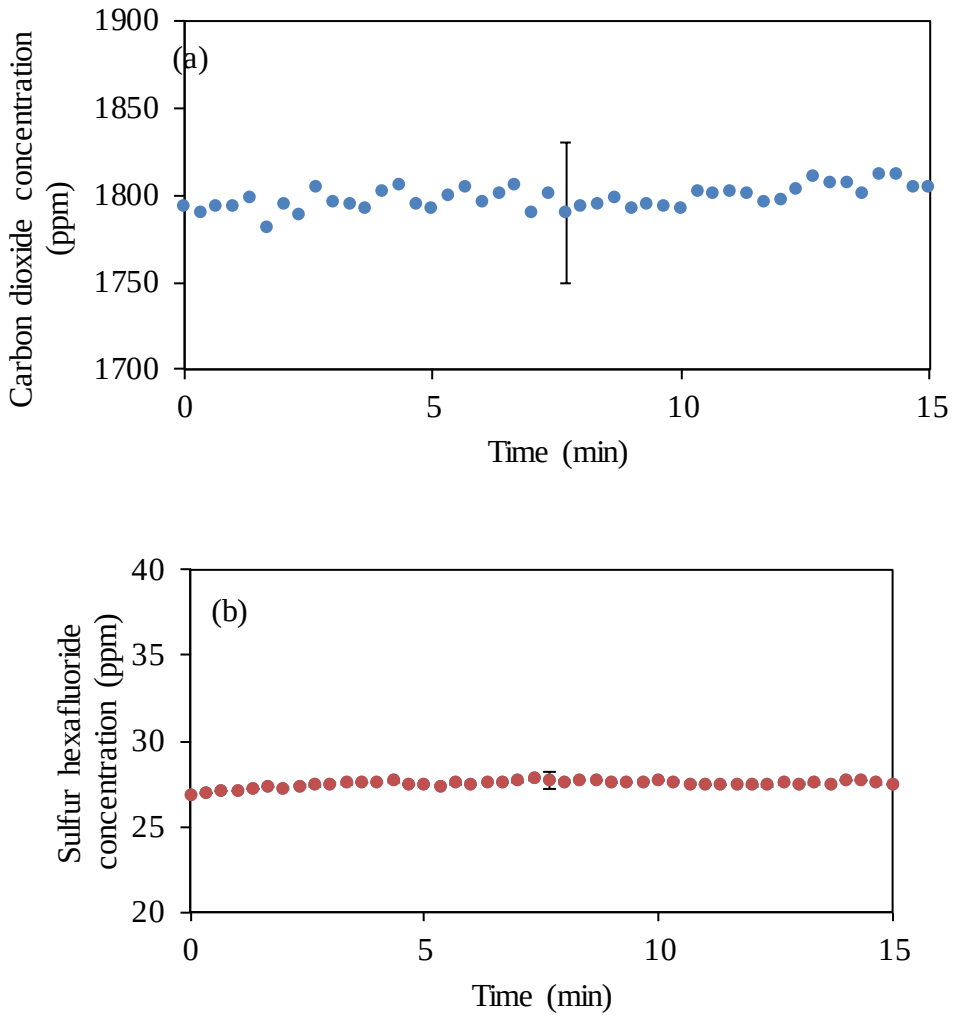

Figure 3.6. Concentration of (a) carbon dioxide and (b) sulfur hexafluoride as a function of time in the RA when the gases are injected using the gas injection technique. The error bars indicate the uncertainty in the measured concentration.

3.2.3.2 Liquid evaporation technique

Figure 3.7 contains a schematic and a photograph of the liquid evaporation technique used for injecting ammonia, methanol, and isopropyl alcohol. Ammonia was mixed with water (30% ammonia and 70% water by mass), and methanol and isopropyl alcohol were used in pure liquid forms. In this method, a syringe pump (LongerPump model NE 300) was used to inject the liquid contaminants into a warm airstream (60 ± 2 °C with a flow rate of 12 ± 1 L/min) that flowed

through a metal tube. A tubular heater was used to heat a compressed airflow which was controlled using a rotameter, as shown in Figure 3.7(a). As the syringe pump injected the liquid contaminants into the warm airstream, contaminants were evaporated and carried with the airflow to the RA. The liquid evaporation technique is less expensive and safer compared to the gas injection technique but is more complicated to set up and control. The contaminant concentration is not as steady with the liquid injection technique (as shown in Figure 3.8) compared to the gas injection technique (Figure 3.6). The period behavior of contaminant concentration in Figure 3.8 (a) and (c) is mainly due to periodic injection of contaminants by syringe pump, in which the pump pushed the syringe into the metal tube, liquid contaminants were injected, and pump withdrew the syringe. This process was repeated and resulted in a periodic contaminant concentration in Figure 3.8 (a) and (c). The temperature and flow rate of airstream in the metal tube increased for injection of methanol, which resulted in less periodic concentration of methanol in RA.

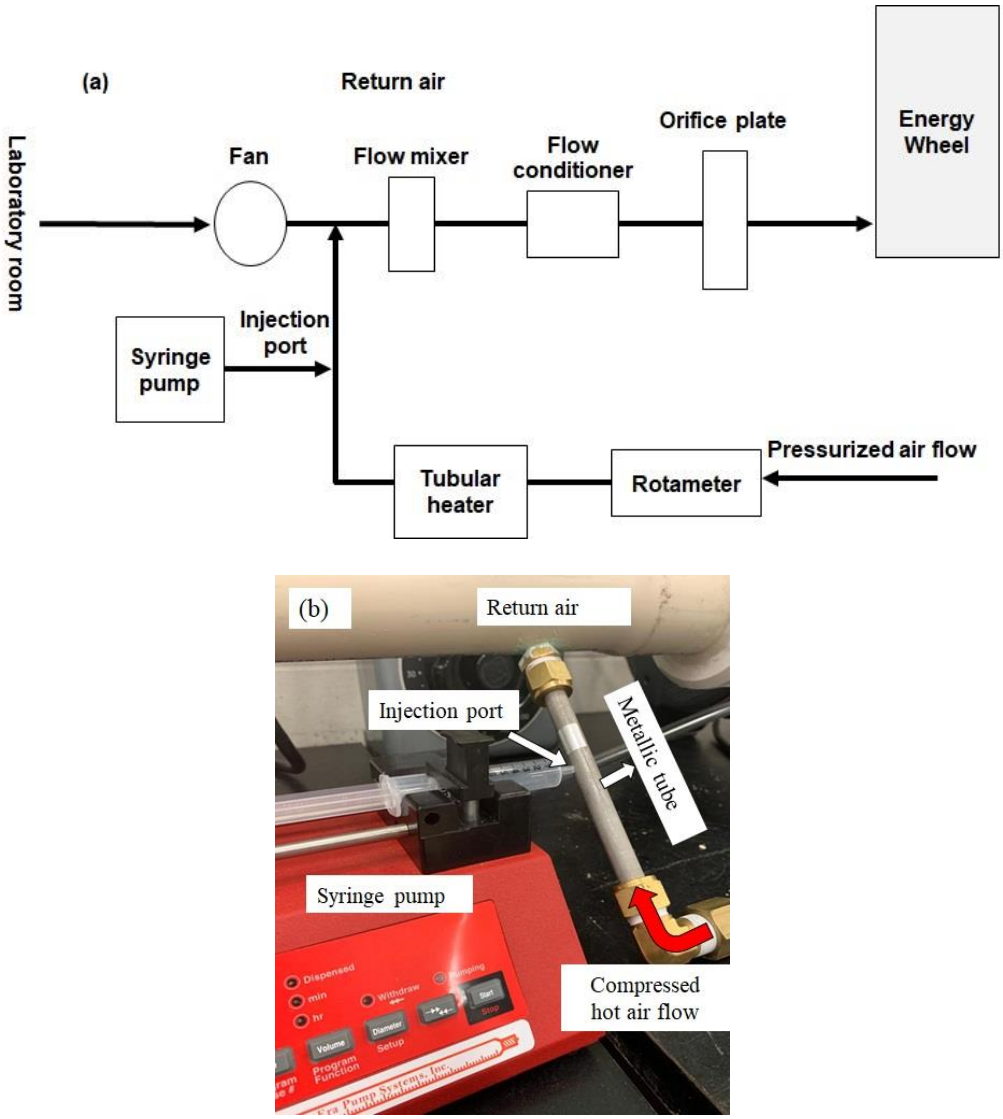

Figure 3.7. (a) Schematic diagram and (b) photograph of the liquid evaporation system showing the syringe pump and injection port for liquid injection.

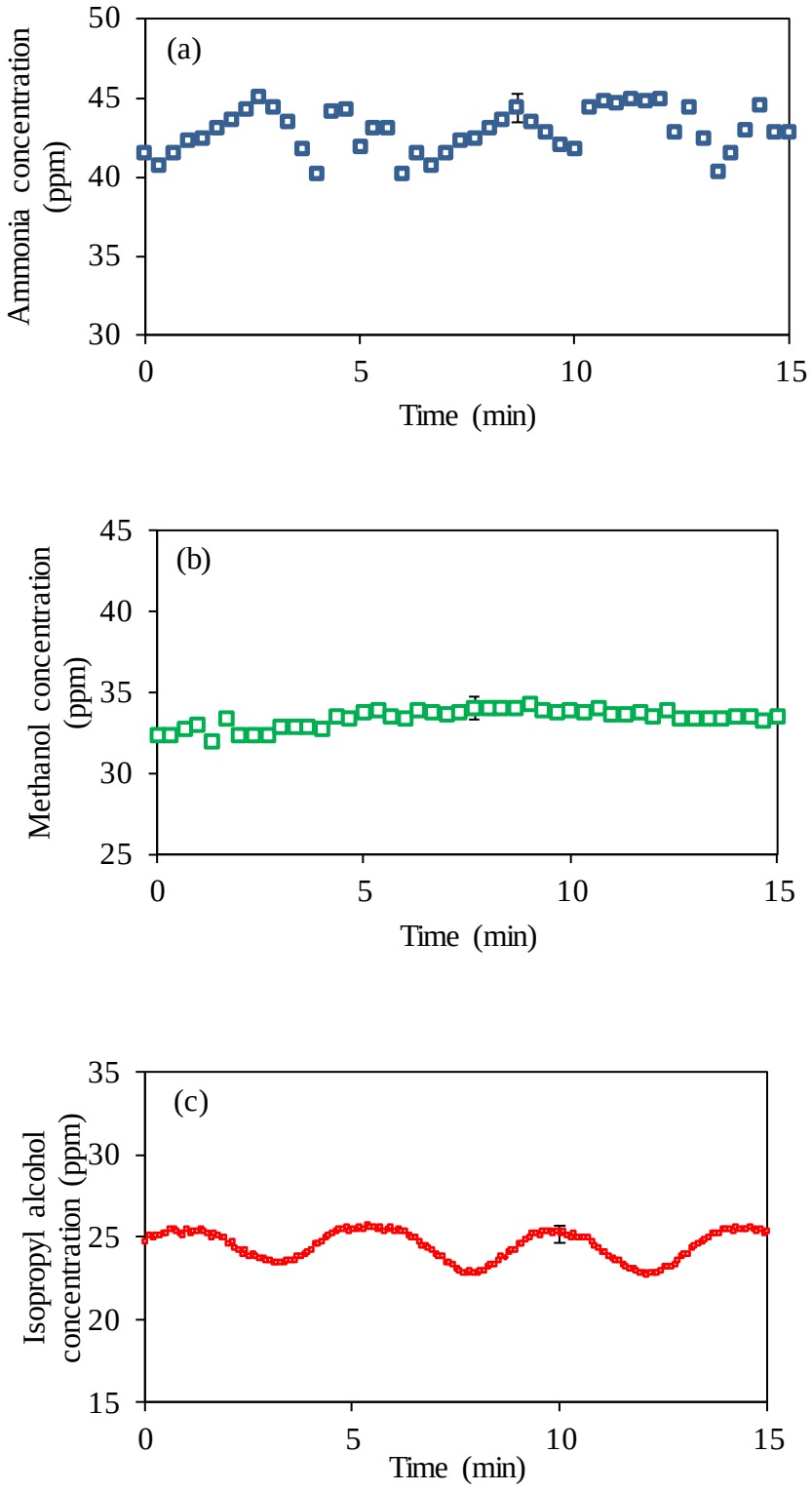

Figure 3.8. Concentration of (a) ammonia, (b) methanol, and (c) isopropyl alcohol as a function of time in the RA when the gases are injected using the liquid injection technique. The error bars indicate the uncertainty in the measured concentration.

3.2.3.3 Gaseous contaminants

More than 300 volatile organic compounds (VOCs) have been identified in air [11]. In ASHRAE RP-1780, 11 VOCs (i.e., xylene, acetaldehyde, ammonia (NH_3), sulfur hexafluoride (SF_6), acetic acid, methyl isobutyl ketone (MIBK), isopropyl alcohol (C_3H_8O), phenol, carbon dioxide (CO_2), methanol (CH_3OH), propane/hexane) were specified for contaminant transfer experiments. In this MSc research, carbon dioxide, sulfur hexafluoride, ammonia, methanol, and isopropyl alcohol were selected for contaminant transfer experiments. These contaminants were chosen based on (i) concentration of the VOCs in indoors, (ii) ability to measure the concentrations, and (iii) chemical and physical characteristics (i.e., operational safety).

In this MSc research, the effects of operating conditions (outdoor air temperature) and design parameters (air face velocity that is velocity of air hitting energy wheel surface) on EATR were investigated. Furthermore, the proposed test method for measuring the contribution of adsorption/desorption in contaminant transfer in energy wheels presented in Chapter 2 was applied and verified. The proposed test method is applied for carbon dioxide, ammonia, methanol, and isopropyl alcohol. Table 3.1 contains the properties of water and the selected contaminants for this MSc research [8], [31], [32].

Table 3.1. Properties of water and selected VOCs in this MSc research [8], [31], [32].

Chemicals	Molecular weight (g/mol)	Molecular diameter (Å)	Boiling point (°C)
sulfur hexafluoride	146.06	5.5	-64
carbon dioxide	44.01	3.3	-79
ammonia	17.03	2.6	-33
isopropyl alcohol	60.1	16	83
methanol	32.04	3.8	65
water	18.01	2.6	100

3.2.4 Gas sampling technique

Figure 3.9 shows a schematic of the gas sampling technique used to draw air samples from the different measurement stations. The gas samples were collected from all the airlines via Teflon sampling tubes connected to sampling ports and a vacuum pump (model: 1LAA-10M-1000X, GAST, USA). The sampling ports were designed following the guidelines provided in ASHRAE Standard 84 (2020) [15]. Computer-controlled solenoid valves were used to select which measurement station (OA, SA, RA, and EA) was sampled at any time. The sampling order applied was: OA, SA, EA, and RA to reduce the effect of drawing samples on the airflow rate through the energy wheel which may affect the contaminant transfer rate.

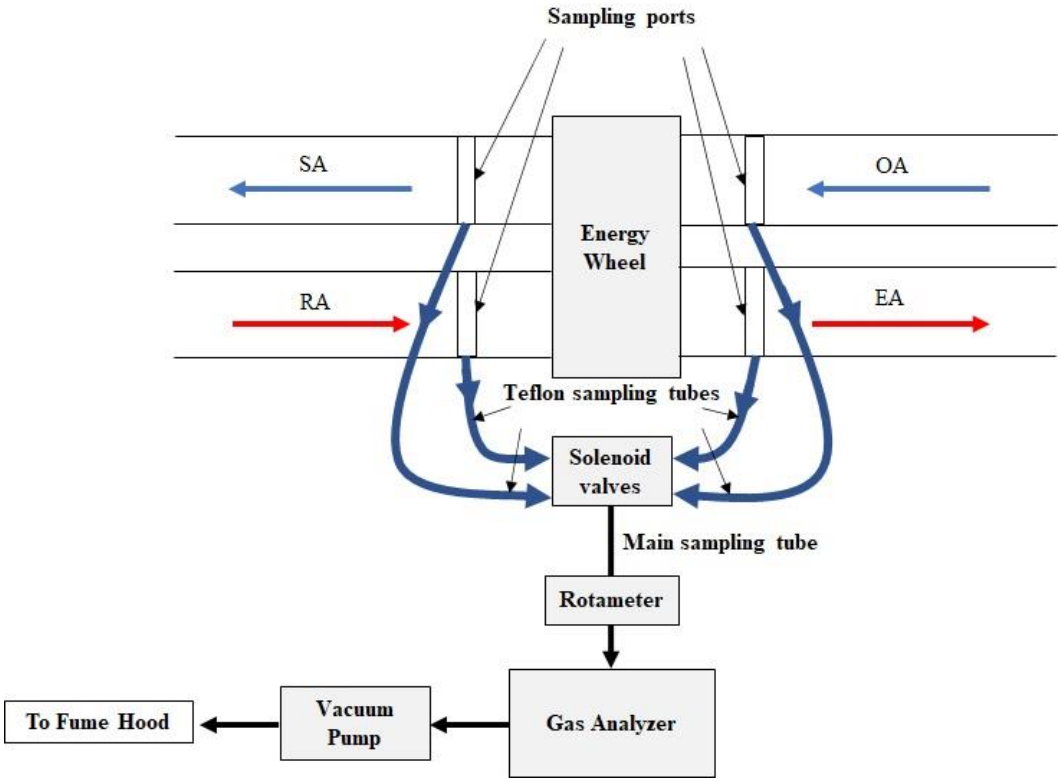

Figure 3.9. Schematic diagram of the gas sampling technique showing the sampling ports, sampling tubes, solenoid valves, and gas analyzer for measuring the gas concentration at different measurement stations.

Figure 3.9 shows that the Teflon sampling tubes were connected to a main sampling tube after the solenoid valves. The gas samples from the main sampling tube were directed to a Fourier transform infrared (FTIR) gas analyzer for concentration measurements. A rotameter set to 0.5 L/s (2% of the main flow at 22 L/s (50 CFM)) was used to control the flow rate of the gas sample to the FTIR gas analyzer. After measuring the concentration of one station, the cell of the FTIR gas analyzer was flushed with nitrogen (N_2). It was found that a nitrogen flow rate of 40 L/min for 3 minutes (i.e., 120 L of nitrogen for the 100 L gas analyzer cell) was adequate to flush the gas analyzer as shown in Figure 3.10. The gas samples from the FTIR gas analyzer were exhausted to a fume hood through a separate exhaust duct.

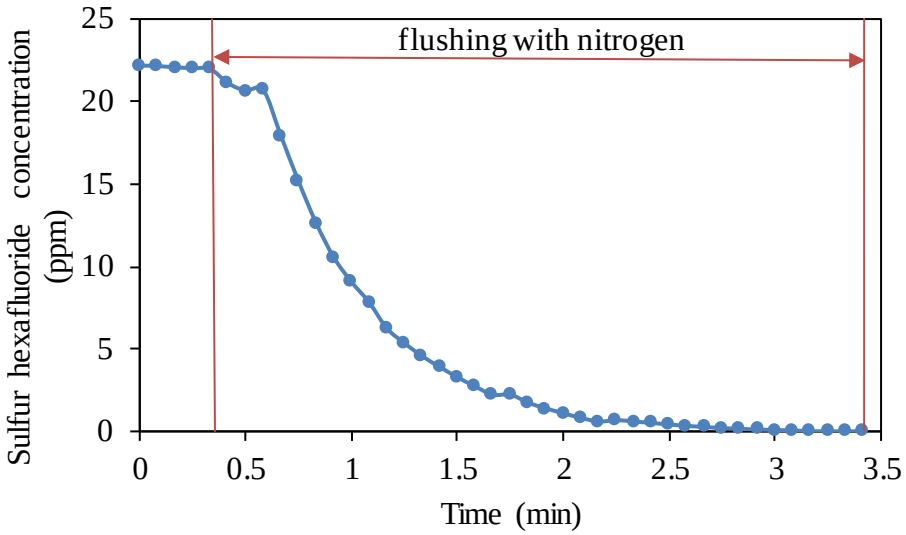

Figure 3.10. Sulfur hexafluoride concentration versus time when the FTIR cell is flushed with 40 L/min flow of nitrogen for three minutes.

With the gas sampling method, the real time monitoring of concentration at each measurement station was done separately, since simultaneous measurement of gas samples from different stations was not possible. More details about real time measurement of gas concentration in different stations are provided in Section 3.4.1.

3.2.5 Instrumentation and uncertainty analysis

Calibrated Copper-Constantan (T-type) thermocouples, capacitive humidity sensors, and pressure transducers were used to measure the air temperature, humidity, and pressure, respectively. Thermocouples, humidity sensors and pressure transducers were calibrated using a Hart Scientific dry-well temperature calibrator [33] (± 0.1 °C), Thunder Scientific humidity generator [34] (± 0.5% RH), and a Druck precision portable pressure calibrator DPI 605 [35] (± 1 Pa), respectively. During the calibrations, a sampling time of 10 seconds was used to determine the transients in the temperature and humidity measurements. Five thermocouples and one humidity sensor were used

at each measurement station. A Gasmet™ FTIR gas analyzer (model: CR-100M) was used to measure the concentration of contaminants (see Section 3.2.5.1).

A National Instruments (NI) data acquisition system was used to acquire and store the data in a computer during the experiments. A LabVIEW (v. 16) program was used to monitor temperature, humidity, pressure, and concentration data in experiments. The instrumentation and calibration details are reported in Table 3.2.

Table 3.2. Instrument specifications and calibration details.

Measurement parameter	Instrument	Calibration range	Total Uncertainty
Temperature	Omega T-type thermocouples	-30 to +40°C	± 0.2°C
Relative humidity	Honeywell Capacitive humidity sensors	0-95% RH at 24°C	± 2%
Differential pressure (across orifice plate)	Validyne differential pressure transducer	0-3.5 kPa	20 Pa
Differential pressure (across the wheel)		0-860 Pa	8 Pa
Mass flow rate	Orifice plates	-	1-2.5%
Concentration of gaseous contaminants	Gasmet FTIR spectroscopy	-	2%

3.2.5.1 Gasmet gas analyzer

The Gasmet gas analyzer measures gas concentration using FTIR spectroscopy [36]. In FTIR spectroscopy, a gaseous sample concentration is related to the absorbance of infrared (IR) light as the IR light passes through the sample, i.e., the more absorbing gas molecules that are present in the sample, the more IR radiation will be absorbed. The linear relationship between gas concentration and IR radiation absorbance is known as Beer's law, as shown in Eq. (3.1) [36]:

$$\log\left(\frac{I_0}{I}\right) = \log\left(\frac{1}{TR}\right) = A = a \cdot b \cdot c \tag{3.1}$$

Here, I and I_0 are intensity of the IR radiation that has passed through the sample gas and the intensity of the IR radiation for background measurement (i.e., the intensity of the IR radiation that passed through zero gas, i.e., nitrogen gas which is non-absorbing), respectively [37]. TR, A, a, b, and c are transmittance, absorbance, absorptivity (m^2/mol), optical path length (m), and concentration (mol/m^3), respectively. In Eq. (3.1) the concentration is unknown and can be calculated since absorbance is measured by the FTIR gas analyzer, absorptivity is known through the background measurement, and the optical path length is a known quantity of the FTIR gas analyzer, which is 100 m (the light passes 100 times through the 1 m long cell in the gas analyzer) [37].

A sample output data set for IR spectroscopy gas analyzer is showed in Figure 3.11. The concentration of the gases in a sample is determined by comparing the reference spectrum and sample spectrum with the help of Calcmet software (V.12) developed by Gasmet™ [38]. The FTIR gas analyzer has a length of 1 meter and IR light passes through the sampling cell 100 times in order to maintain 100 meters of path length for the IR light. The intensity and frequency of the IR light that passes through the gas and are received by the Gasmet sensor is compared with the intensity and frequency of the radiated IR light. The difference between the frequency of radiated and received IR lights allows the Calcmet software to determine the chemical compounds in the sample gas [37]. The concentration of these chemical compounds (gases) is determined based on calibration tests conducted by Gasmet over a range of gases and concentrations.

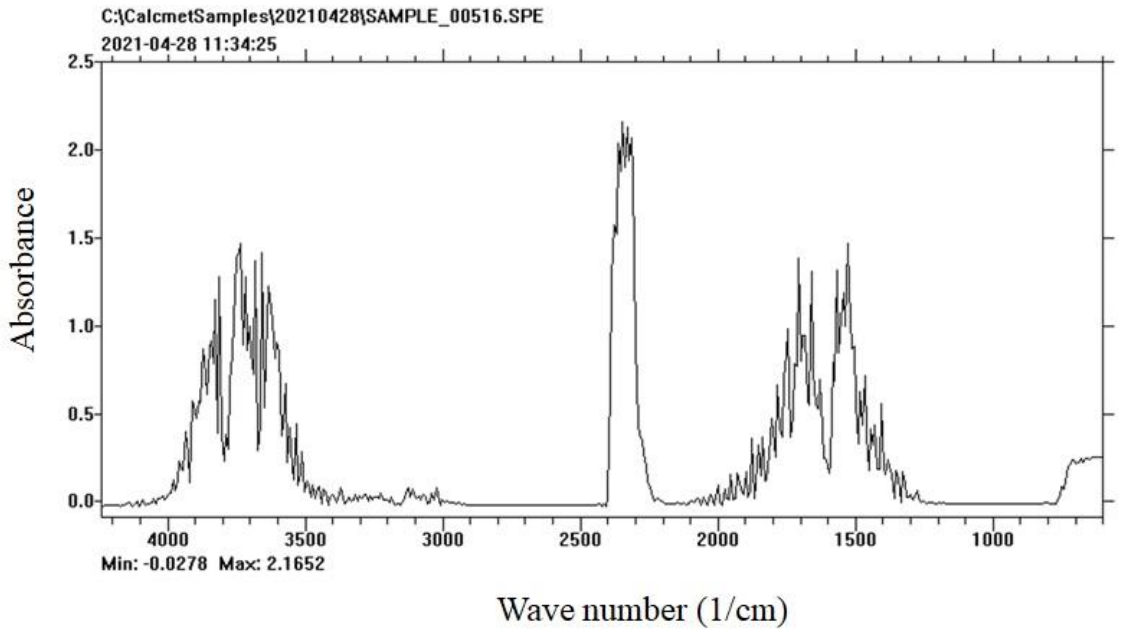

Figure 3.11. Sample gas measurement data with FTIR spectroscopy technique [38].

3.2.6 Energy wheel performance test results and verification of the test facility

ASHRAE Standard 84 (2020) [15] provides the normative criteria for the acceptance of test data during energy wheel performance testing. These criteria ensure steady state operating conditions and acceptable mass and energy balances. Effectiveness and EATR are the two performance parameters to quantify the energy recovery performance and the transfer of contaminants when the wheel operates under balanced flow conditions. The effectiveness and EATR equations were introduced in Chapter 2 (Eqs. (2.1) - (2.3) and (2.5)). The EATR test data needs to satisfy the operating condition inequality checks (i.e., Eqs. (2.7) - (2.11)) according to ASHRAE Standard 84 (2020) [15]. In addition, it is important to verify the performance of the energy wheel with manufacturer's data to assure that the facility is functional. The detailed operating conditions for the test used to verify the test facility are given in Figure 3.12 and Table 3.3.

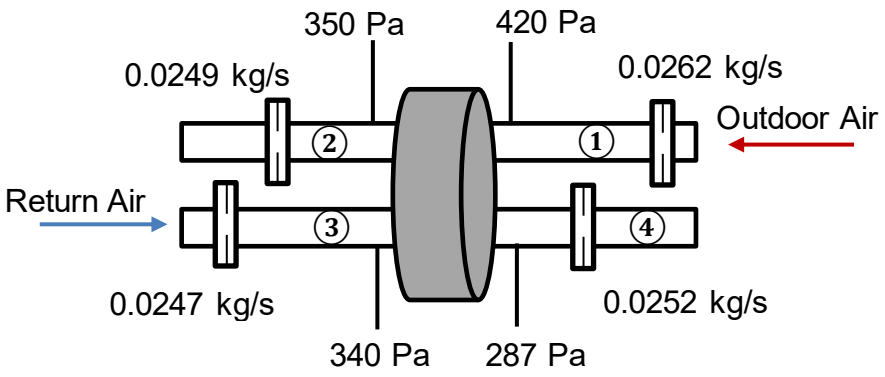

Figure 3.12. Schematic diagram showing the energy wheel test conditions at an air flow rate of 24 L/s (50 CFM) and a face velocity of 1 m/s.

Table 3.3. Operating conditions during the test on the energy wheel at a nominal air flow rate of 24 L/s (50 CFM).

	Parameter	Values
Outdoor air	Temperature	35.5 °C
	Flow rate	0.026 kg/s
	Humidity ratio	10.2 g_w/kg_a
	Relative humidity	29%
Return air	Temperature	27 °C
	Flow rate	0.024 kg/s
	Humidity ratio	16.1 g_w/kg_a
	Relative humidity	73%
Wheel rotational speed		18 rpm
Face velocity		1 m/s
Outdoor air correction factor (OACF)		1.05

3.2.6.1 Operating condition inequalities

Figure 3.13 shows the inequality checks to ensure tests are conducted at steady state for temperature (T) and humidity ratio (W) in the RA and OA where dT (dW) is the maximum deviation of any temperature (humidity ratio) reading from time-averaged mean value of T (W).

Indices 1 and 3 represent the OA and RA stations, respectively [15]. The temperature and humidity inequalities from ASHRAE Standard 84 (2020) [15] are given in Eqs. (3.2) - (3.5).

$$\frac{|dT_1|}{|T_1 - T_3|} < 0.02 \tag{3.2}$$

$$\frac{|dT_3|}{|T_1 - T_3|} < 0.02 \tag{3.3}$$

$$\frac{|dW_1|}{|W_1 - W_3|} < \begin{cases} 0.05 \text{ for } (W_1 > W_3) \\ 0.1 \text{ for } (W_1 < W_3) \end{cases} \tag{3.4}$$

$$\frac{|dW_3|}{|W_1 - W_3|} < \begin{cases} 0.05 \text{ for } (W_1 > W_3) \\ 0.1 \text{ for } (W_1 < W_3) \end{cases} \tag{3.5}$$

The inequality results are evaluated after 90 min of energy wheel operation to confirm the steady-state conditions. While ASHRAE Standard 84 (2020) [15] requires 60 min of wheel operation to reach steady-state conditions, experiments were continued for 30 more min to ensure the inequality checks were satisfied. The maximum measured temperature and humidity inequalities are 0.5% and 2.5%, respectively, and are lower than the ASHRAE Standard 84 (2020) [15] allowed inequality limits of 2% for temperature and 5% for humidity.

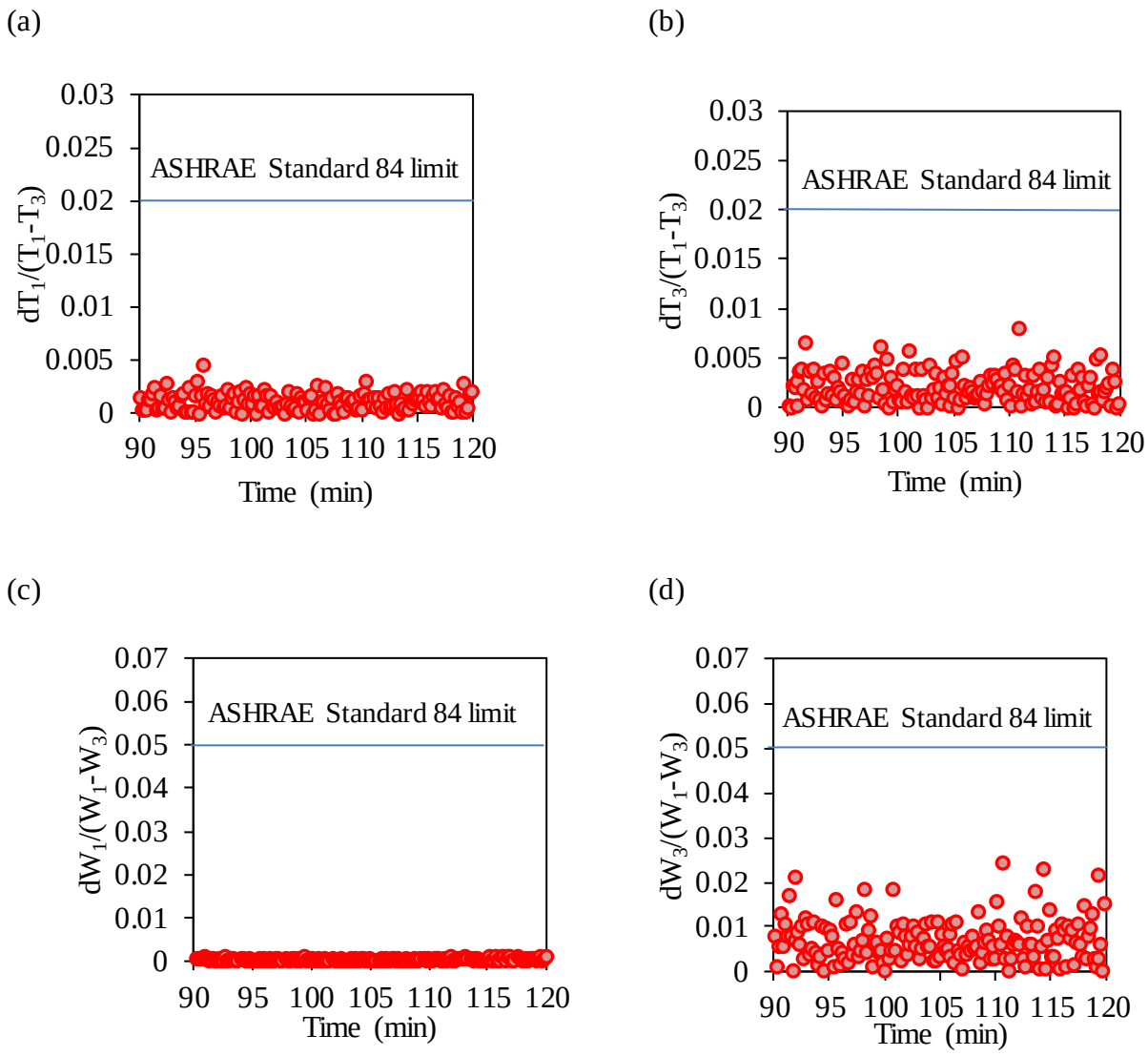

Figure 3.13. Results of the temperature and humidity inequality check according to ASHRAE Standard 84 (2020) [15] for OA (a and c) and RA (b and d).

3.2.6.2 Mass and energy inequalities

Figure 3.14 shows inequality checks for dry air mass flow rate, water vapor and enthalpy transfer based on Eqs. (2.7), (2.9), and (2.10), respectively. It is seen that the dry air flow rate inequality is about 2%, and the water vapor and energy inequalities are about 8%. The maximum allowed inequalities for these parameters are 5% for dry air mass flow rate and 20% for water vapor and enthalpy transfer [15]. From the inequality check results, the following conclusions are made: (i)

the test facility conserves mass and energy, (ii) the facility can provide steady-state (time-invariant) airflow properties at the energy wheel inlet, and (iii) the facility meets the requirements of ASHRAE Standard 84 (2020) [15].

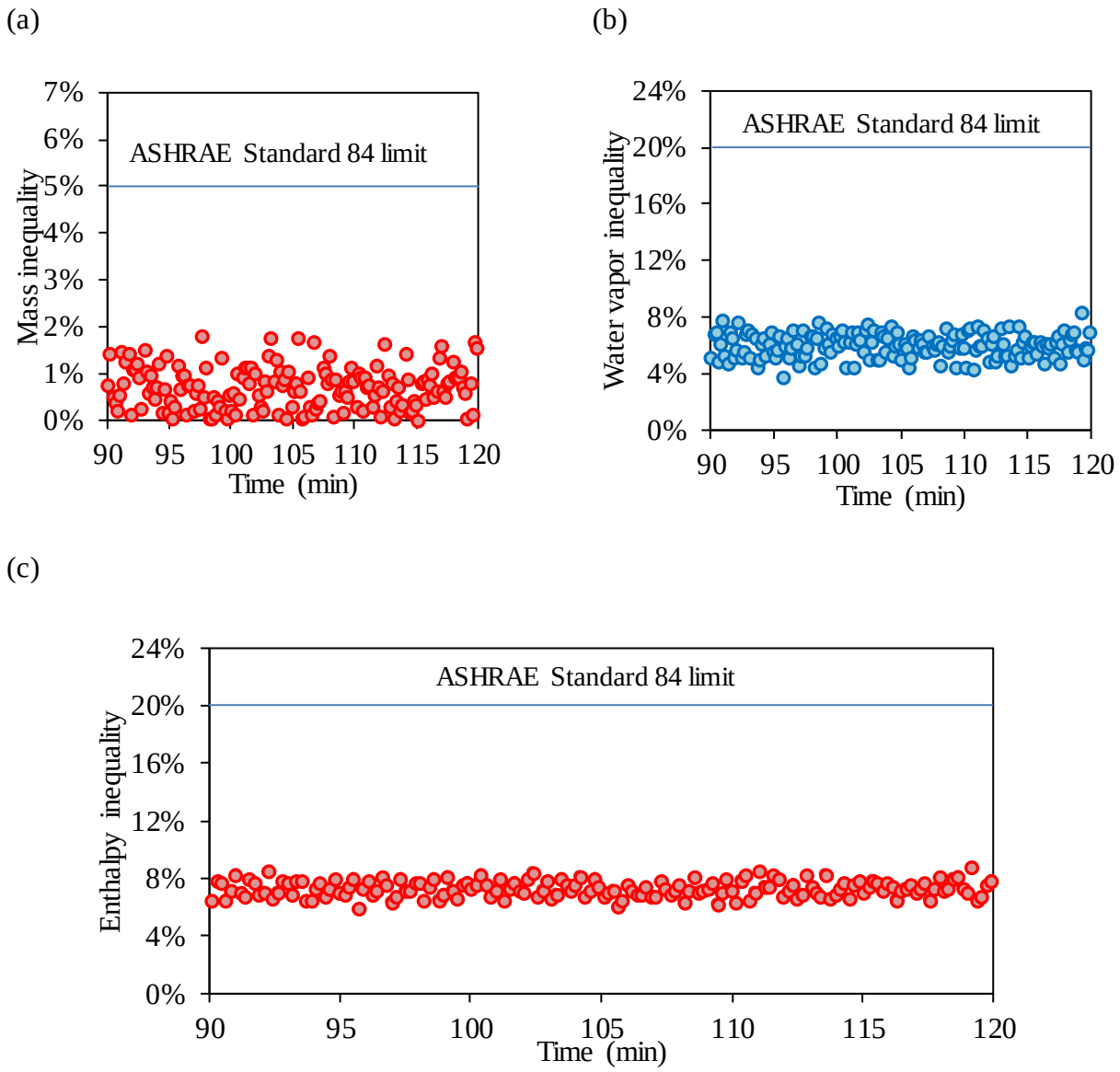

Figure 3.14. Results of the inequality check for (a) dry air mass flow rate, (b) water vapor, and (c) energy transfer.

3.2.6.3 Effectiveness

The sensible, latent, and total effectiveness of the energy wheel are determined using the temperature, humidity, and flow rate measurements. The instantaneous effectiveness values for the duration between 90-120 min are presented in Figure 3.15. The effectiveness of the wheel is determined by averaging these instantaneous effectiveness values.

The calculated sensible effectiveness is 83 ± 5%, latent effectiveness is 73 ± 7%, and total effectiveness is 79 ± 6%. The uncertainties in effectiveness values are acceptable as the maximum allowed uncertainties in ASHRAE Standard 84 (2020) [15] are ± 5% for sensible, ± 7% for latent, and ± 5-7% for total effectiveness.

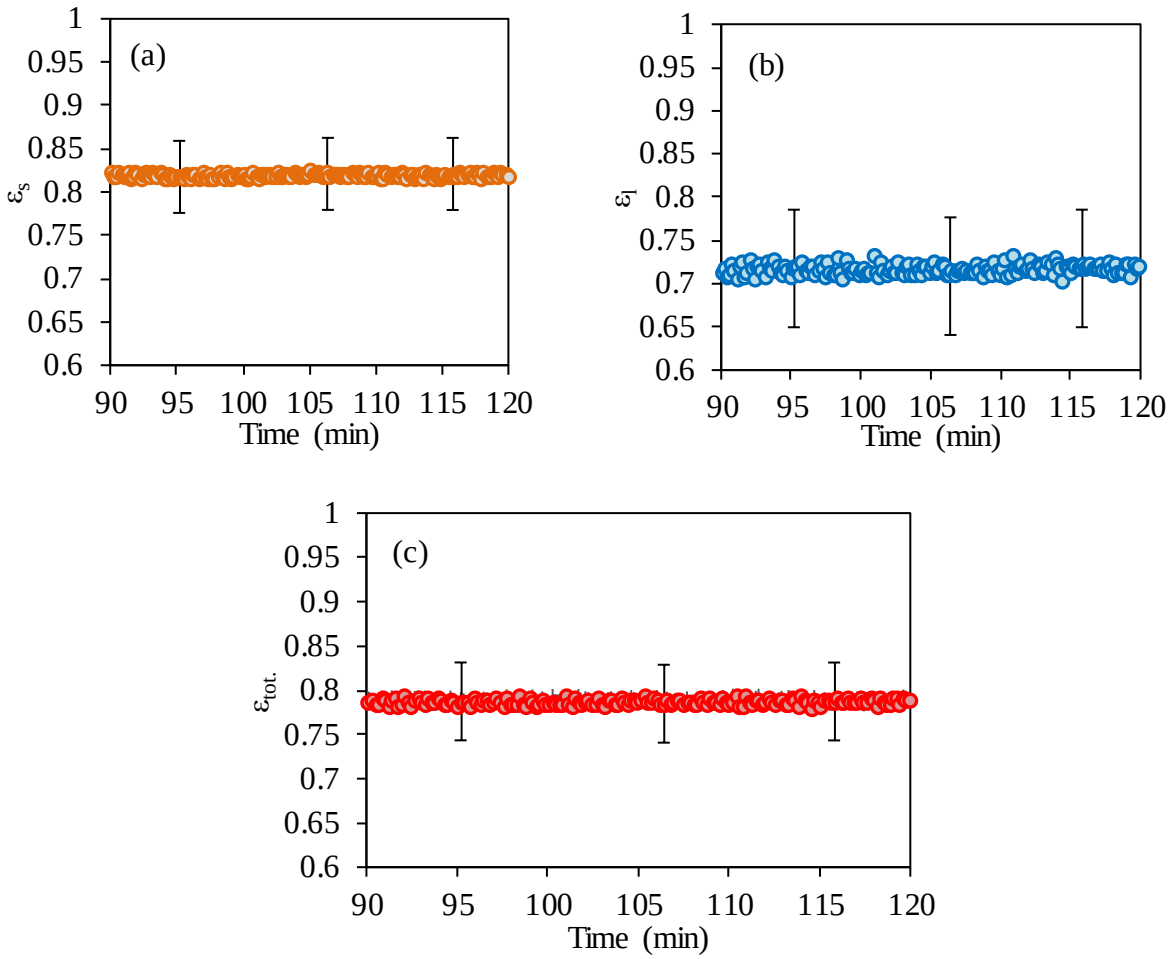

Figure 3.15. Instantaneous (a) sensible, (b) latent, and (c) total effectiveness values after the test has reached steady state conditions according to ASHRAE Standard 84 [15].

Figure 3.16 compares the average effectiveness obtained from the experiments with the manufacturer's data. The manufacturer's data are based on a simulation software, not actual experimental data, and no uncertainty limits are reported. However, the uncertainties can be assumed to be in the same order as experimental data from ASHRAE Standard 84 (2020) [15]. The experimental and manufacturer's sensible effectiveness data agree within ± 5%, whereas differences of 9% and 7% are observed in the latent and total effectivenesses, which is higher than the measured uncertainty in these parameters. Slight leakages in the test facility and interaction of

the wheels/airstreams with the surroundings could result in effectiveness variations. Considering these possibilities, it is reasonable to claim that the test facility provides reliable results.

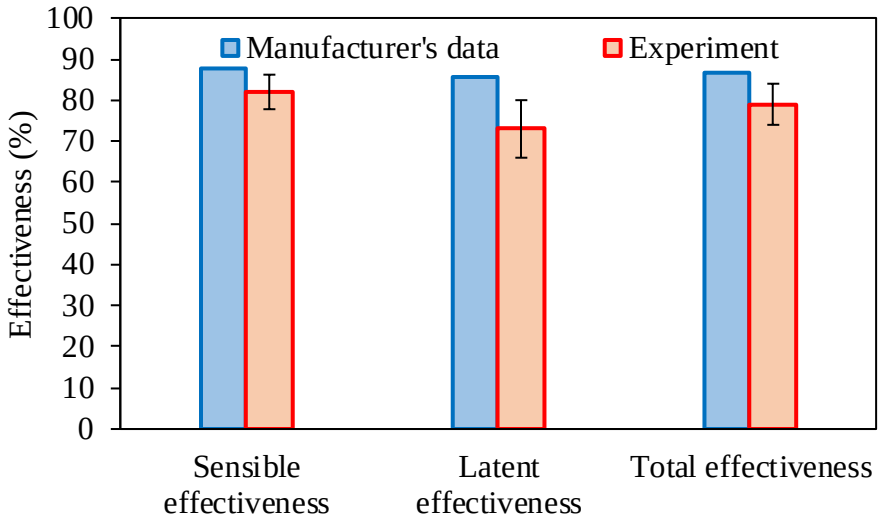

Figure 3.16. Comparison of the average effectiveness values obtained from the experiments and the manufacturer.

3.3 Results and discussions

In this section, the real-time concentration measurement data and EATR results for the selected contaminants are presented. The effect of the outdoor air temperature, air flow rate (face velocity) and various gaseous contaminants on EATR will be shown for the test conditions in Table 3.4 where tests 1-4 (carbon dioxide) and 5-8 (sulfur hexafluoride) investigate the effect of outdoor air temperature (highlighted in yellow), tests 3 and 9-10 (carbon dioxide) investigate the effect of air flow rate (highlighted in green), and tests 3, 7, and 11-13 (ammonia, methanol, and isopropyl alcohol) investigate the effect of various gases (highlighted in blue). At the end of this section, the experimental results will be compared with data from the literature review presented in Chapter 2.

Table 3.4. Test conditions for different experiments where different sets of experiments are highlighted.

Test number	Contaminant	Temperature (°C)		Relative humidity (%)		Flow rate (L/s [CFM])	
		Return	Outdoor	Return	Outdoor	Return	Outdoor
1	CO_2	27	1	50	45	22 [47]	22 [47]
2	CO_2	28	10	50	50	22 [47]	22 [47]
3	CO_2	25	25	48	47	23.6 [50]	23 [49]
4	CO_2	25	31	45	47	23.6 [50]	23.6 [50]
5	SF_6	25	1.5	48	48	22.7 [48]	22.7 [48]
6	SF_6	25	10	49	50	23 [49]	22.7 [48]
7	SF_6	25	25	48	46	22.7 [48]	22.7 [48]
8	SF_6	28	31	46	47	23 [49]	23.6 [50]
9	CO_2	24	25	48	48	19 [40]	19 [40]
10	CO_2	24	25	48	46	28 [60]	28 [60]
11	NH_3	24	24	50	50	23.6 [50]	23.6 [50]
12	C_3H_8O	24	24	50	50	23.6 [50]	23.6 [50]
13	CH_3OH	24	24	50	50	23.6 [50]	23.6 [50]

3.3.1 Measured concentration data

Figure 3.17 contains the measured sulfur hexafluoride concentration as a function of time at the different measurement stations for test number 7 from Table 3.4. The real time measurement was done in the following order: OA, SA, EA, and RA. The reason the measurements were done in that order was to keep the flow rate of the RA through the wheel constant while the other airstreams were being measured. It should be noted that measuring the gas concentration requires a small flow rate of air (40 L/min, which is 3% of the nominal 23 L/s RA flow) to be drawn from the measurement station, thus the airflow rate through the wheel changes slightly when the RA and

SA concentrations are being measured. The order and timing of the measurement sequence were controlled by LabVIEW and solenoid valves.

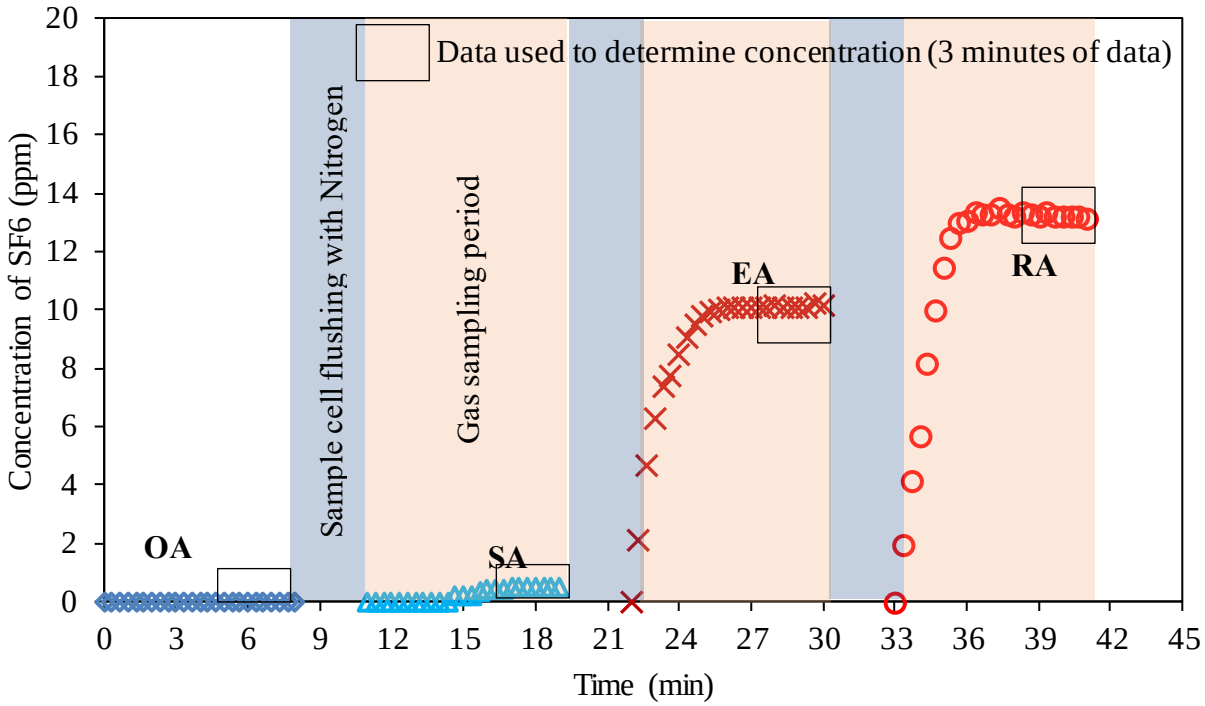

Figure 3.17. Concentration measurements of sulfur hexafluoride at OA, SA, EA, and RA versus time for test number 7.

Figure 3.17 shows that the gas concentration for the different stations was calculated based on the concentrations measured over a period of 3 min at the end of an 8 min measurement period. In the first measurement period, gas samples from the OA were directed to the Gasmet gas analyzer and real time measurements were made for 8 min. The average of the last 3 min was used as the contaminant concentration in the OA. Then, the solenoid valve of the OA station was closed by the LabVIEW program, and the sample cell was flushed with nitrogen with a flow rate of 40 L/min for 3 min in order to flush the OA gas from the Gasmet test cell.

Next, the solenoid valve for the SA station was opened, and 40 L/min of SA were directed to the gas analyzer for 8 min (5 min for filling the sample cell and 3 min for measurement). Again, the

average of last the 3 min of measurements was used as contaminant concentration in the SA. After the gas samples from the SA were measured, the solenoid valve for SA was closed and the gas analyzer test cell was flushed with nitrogen for 3 min. The same procedure was followed for the EA and RA measurement stations.

3.3.2 Effect of outdoor air temperature on EATR

Figure 3.18 shows EATR as a function of outdoor air temperature for carbon dioxide and sulfur hexafluoride. It is noted that sulfur hexafluoride is recommended as a tracer gas for EATR experiments as it is a non-reactive gas and is not adsorbed by desiccant materials (i.e., there is no sulfur hexafluoride transfer through adsorption/desorption) [15]. Furthermore, since the experiments were conducted at a positive pressure difference between the supply and exhaust sides (30 Pa higher on the supply side), air leakage only occurred from the supply side to the exhaust side. Therefore, the contaminant transfer in sulfur hexafluoride experiments occurred mainly due to carryover.

The EATR values for carbon dioxide and sulfur hexafluoride change from 1.1% to 2.5% with an uncertainty of 1.1% to 3%. The average value for EATR is 1.9 ± 1.7% for carbon dioxide and 1.7 ± 1.9% for sulfur hexafluoride. The EATR values and related uncertainties for sulfur hexafluoride and carbon dioxide are very similar at different outdoor air temperatures. This indicates that carbon dioxide is also not adsorbed in the desiccant materials and transferred only by carryover. Figure 3.18 also shows that the outdoor air temperature does not significantly affect EATR. Tables 3.5 and 3.6 provide the contaminant mass inequality and concentrations of carbon dioxide and sulfur hexafluoride for the different tests, respectively. It is seen that contaminant mass inequality satisfies the ASHRAE Standard 84 (2020) [15] requirement of 15% according to inequality checks presented in Eq. (2.10) of Chapter 2.

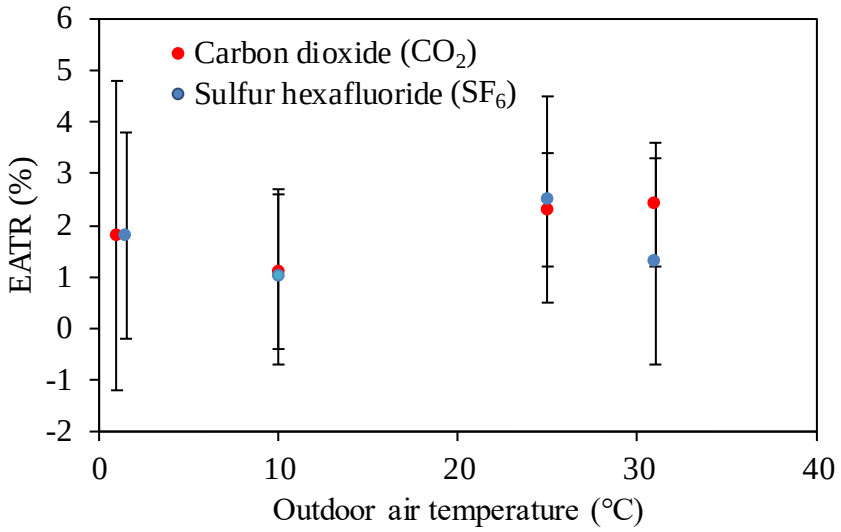

Figure 3.18. Effect of outdoor air temperature on the measured EATR for carbon dioxide and sulfur hexafluoride.

Table 3.5. Mass inequality and concentration of carbon dioxide at different measurement stations in tests with varying outdoor air temperatures.

Test number	OA (ppm)	SA (ppm)	RA (ppm)	EA (ppm)	EATR (%)	Mass inequality (%)
1	487	507	1581	1495	1.8 ± 3	2
2	496	507	1456	1412	1.1 ± 1.5	6
3	491	514	1489	1416	2.3 ± 1.1	6
4	462	490	1630	1385	2.4 ± 1.2	1

Table 3.6. Mass inequality and concentration of sulfur hexafluoride at different measurement stations in tests with varying outdoor air temperatures.

Test number	OA (ppm)	SA (ppm)	RA (ppm)	EA (ppm)	EATR (%)	Mass inequality (%)
5	0	0.45	24.8	20.7	1.8 ± 2	4
6	0	0.3	29.5	21.5	1 ± 1.7	8
7	0	0.6	24.0	25.0	2.5 ± 2	3
8	0	0.35	27.5	21.5	1.3 ± 2	10

3.3.3 Effect of air face velocity on EATR

Figure 3.19 presents the effect of air face velocity on EATR for carbon dioxide using tests 3, 9, and 10. Experiments were done at air face velocities of 0.8, 1, and 1.2 m/s. Figure 3.19 shows a consistent trend of decreasing EATR with increasing air face velocity (EATR decreased from 3.9 ± 0.7% to 1.5 ± 1.2% when the air face velocity increased from 0.8 m/s to 1.2 m/s).

To find out the main reason for decreasing EATR of carbon dioxide with increasing air face velocity, Figure 3.19 shows a dashed line that represents changes in EATR if the contaminant transfer rate would be constant at an air face velocity of 0.8 m/s. The dashed line was calculated using Eq. (2.13) and shows the changes in EATR that would occur if the contaminant transfer rate was constant and EATR would change only because of dilution. It is seen that EATR for a constant contaminant transfer rate (dashed line) is within the uncertainty limits of the measured EATR. Therefore, it can be concluded that the decrease in EATR due to increased air face velocities is mainly due to dilution of contaminants and not because of the reduction in actual contaminant transfer rate. Table 3.7 shows the contaminant mass inequality and concentration of carbon dioxide at different measurement stations for these experiments. The contaminant mass inequality is less than the 15% allowed in ASHRAE Standard 84 (2020) [15] for all experiments.

By comparing Figures 3.18 and 3.19, it can be realized that the air face velocity has a more important impact on EATR than outdoor air temperature. This reveals that air face velocity can be considered as a controlling parameter in EATR experiments, while outdoor air temperature did not show a significant impact on EATR.

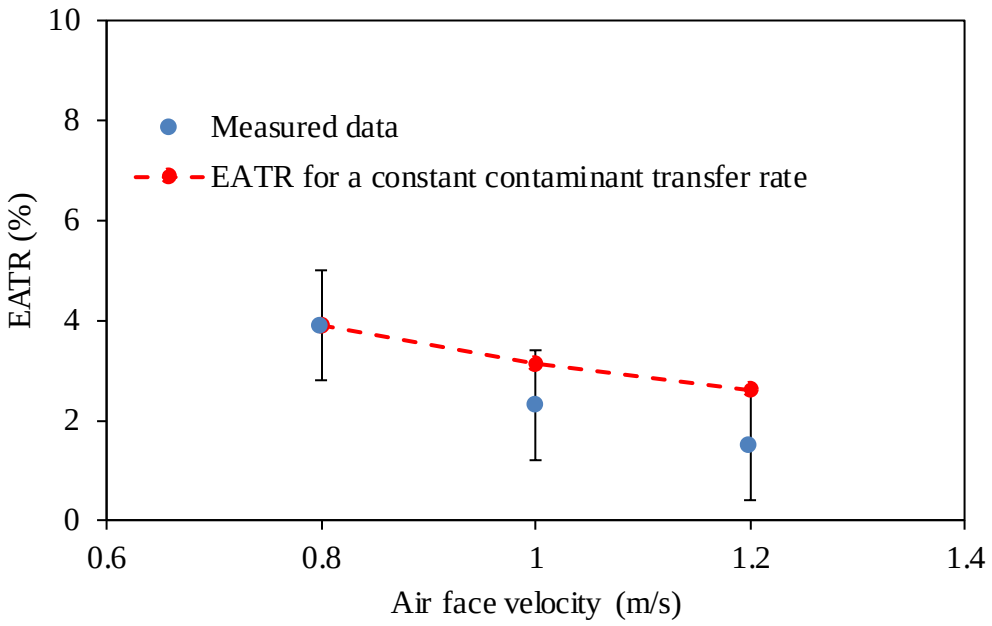

Figure 3.19. Effect of air face velocity on EATR for carbon dioxide.

Table 3.7. Mass inequality and concentration of carbon dioxide at different measurement stations in tests with varying air face velocities.

Test number	Air face velocity (m/s)	OA (ppm)	SA (ppm)	RA (ppm)	EA (ppm)	EATR (%)	Mass inequality (%)
9	0.8	471	528	1932	1790	4 ± 1	2
3	1	491	514	1489	1416	2 ± 1	6
10	1.2	477	495	1660	1476	2 ± 1	1

3.3.4 EATR due to adsorption/desorption

In this section, the proposed method for determining the contaminant transfer due to adsorption/desorption ($EATR_{ad}$) in the energy wheel (as was presented in Section 2.7) is applied and verified. $EATR_{ad}$ is calculated by subtracting $EATR_{non-inert}$ (i.e., EATR for the tested contaminant) from $EATR_{inert}$ (i.e., EATR for the inert tracer gas which is sulfur hexafluoride in these experiments).

$$\mathrm{EATR_{ad}} = \mathrm{EATR_{non-inert}} - \mathrm{EATR_{inert}} \quad (3.6)$$

Equation (3.6) is applied for ammonia, methanol, isopropyl alcohol, and carbon dioxide, and the results are shown in Figure 3.20. The OA and RA temperatures were at 24 ± 1°C, and the OA and RA relative humidities were 50 ± 2% for the tests in Figure 3.20. The OA and RA air face velocities were 1 m/s.

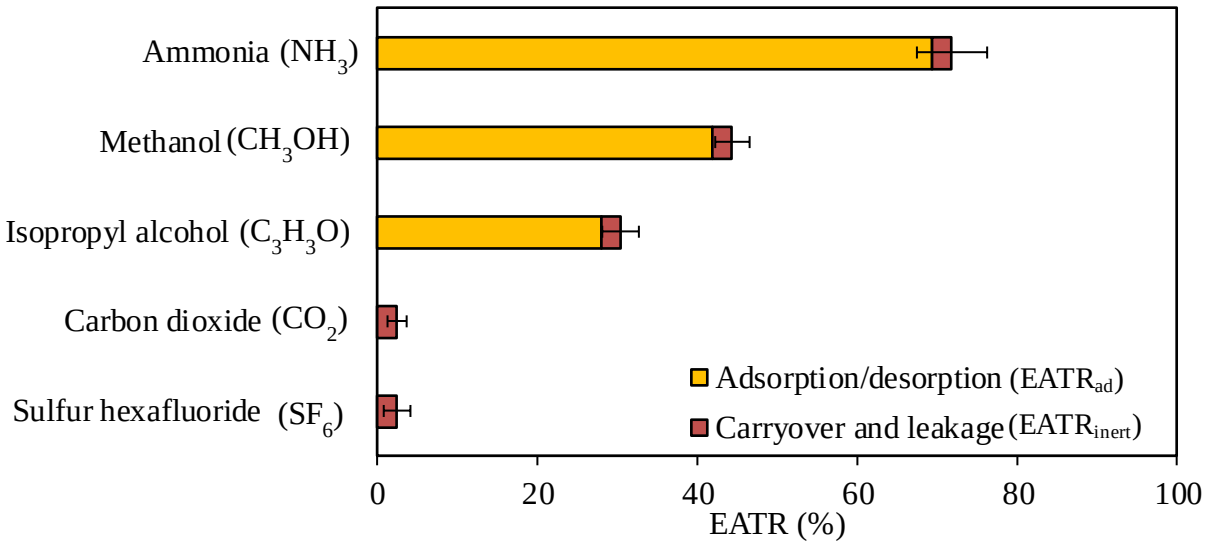

Figure 3.20. Measured EATR of five contaminants showing the contributions of air leakage and carryover (in red) and adsorption/desorption (in yellow).

Figure 3.20 shows the contaminant transfer due to air leakage and carryover (i.e., $\mathrm{EATR_{inert}}$) and adsorption/desorption (i.e., $\mathrm{EATR_{ad}}$), which combine to give the total measured EATR. It is seen that ammonia shows the highest transfer due to adsorption/desorption (70 ± 5%), followed by methanol (42 ± 3%), isopropyl alcohol (28 ± 3%), and carbon dioxide (-0.2 ± 2). The high amount of adsorption/desorption for ammonia might be mainly because ammonia has physical properties (molecular size and weight) very similar to water, as seen in Table 3.1. Also, methanol has a molecular size very similar to water, which indicates the importance of the molecular size of the contaminants for adsorption/desorption on the surface of desiccants.

Furthermore, it is noted that ammonia, methanol, and isopropyl alcohol are polar contaminants similar to water. Since water is a polar molecule and it is adsorbed on desiccants, it may be realized that polar molecules such as ammonia, isopropyl alcohol, and methanol are also adsorbed. In addition, carbon dioxide and sulfur hexafluoride are non-polar molecules which prevents them from adsorbing/desorbing on desiccants (as it is seen in Figure 3.20, where there is no adsorption/desorption for carbon dioxide).

Table 3.8 shows the contribution of the adsorption/desorption ($EATR_{ad}$), air leakage and carryover ($EATR_{inert}$) on the total contaminant transfer rate ($EATR_{non-inert}$), and contaminant mass inequality for the different contaminants. It is seen that contaminant mass inequality for the experiments with sulfur hexafluoride, carbon dioxide, and methanol satisfy ASHRAE Standard 84 (2020) requirement [15], but the experiments with ammonia and isopropyl alcohol do not. It is noted that the uncertainty in $EATR_{ad}$ was calculated according to uncertainty propagation rules

$$U_{EATR_{ad}} = \sqrt{(U_{EATR_{inert}})^2 + (U_{EATR_{non-inert}})^2}. \quad (3.7)$$

[18] as:

Table 3.8. Contribution of adsorption/desorption ($EATR_{ad}$) and air leakage and carryover ($EATR_{inert}$) on the contaminant transfer rate and mass inequality for the various gases.

Test	Contaminant	$EATR_{inert}$ (%)	$EATR_{non-inert}$ (%)	$EATR_{ad}$ (%)	Mass inequality (%)
7	sulfur hexafluoride	2.5 ± 1.6	2.5 ± 1.6	0	3
3	carbon dioxide	2.5 ± 1.6	2.3 ± 1.2	-0.2 ± 2	6
11	Ammonia	2.5 ± 1.6	72.5 ± 4.4	70 ± 5	31
12	Methanol	2.5 ± 1.6	44.5 ± 2.2	42 ± 3	13
13	isopropyl alcohol	2.5 ± 1.6	30.5 ± 2.3	28 ± 3	19

3.3.5 Comparison with literature data

Figure 3.21 shows a comparison between the measured EATR for ammonia, isopropyl alcohol, methanol, carbon dioxide, and sulfur hexafluoride with data from the literature. The literature data with the most similar test conditions (wheel size, wheel rotational speed, air flow rate, desiccant material, duct size, etc.) were selected in order to provide the most comparable test results. It is seen that the order of the EATR values measured in this thesis are similar to the order in the literature (e.g., ammonia has the highest EATR value followed by methanol). However, the EATR values for isopropyl alcohol and sulfur hexafluoride are unexpectedly high in the literature. The measured EATR value in the thesis for sulfur hexafluoride is 2.5 ± 1.6%, while Roulet *et al.* (2002) [10] reported EATR for sulfur hexafluoride as 25%.

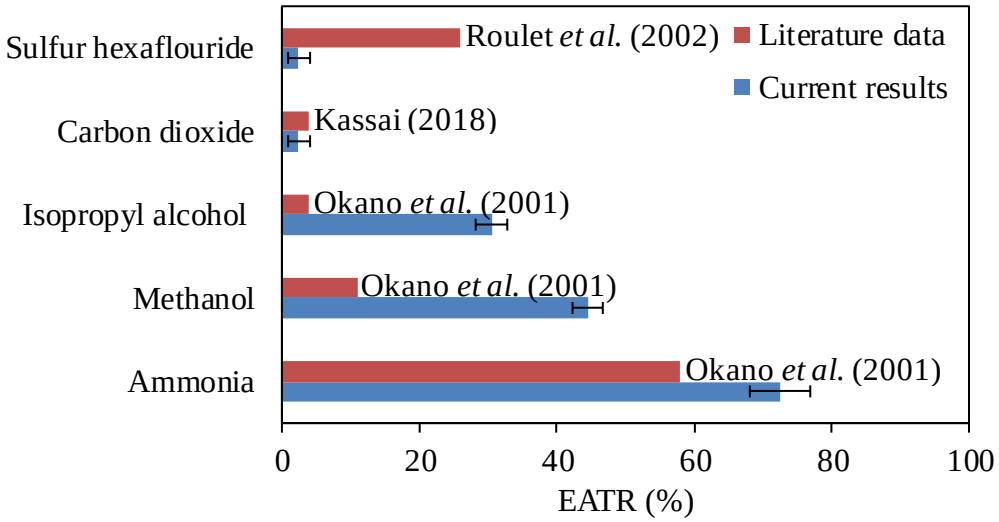

Figure 3.21. Comparison of EATR values measured in this thesis and values from the literature.

The difference between the measured results and literature data is mainly due to different design and operating conditions. It can be concluded that while the literature data can be compared with the EATR results in this thesis, there are different design and operating conditions that prevent a

precise comparison between the measured results and literature data. It should also be noted that the uncertainties in the measured EATR values were not reported for any of literature data in Figure 3.21.

3.4 Conclusions

In this chapter, the second objective of this thesis (i.e., to apply and verify a test methodology for measuring gaseous contaminant transfer in energy wheels) was fulfilled. The test method was applied and verified for carbon dioxide, ammonia, isopropyl alcohol, and methanol. Performance test data were presented which verify the test methodology, and energy wheel effectiveness values were compared with manufacturer's data. A test methodology was introduced and EATR results for different contaminants were presented. The following are the major conclusions from this chapter.

- A test facility for measuring the gaseous contaminant transfer in energy wheels was introduced and measurement results presented.
- The performance test data showed that facility conserves mass and energy during the experiments, provides steady state airflow properties in the test section, and thus satisfies ASHRAE Standard 84 (2020) requirements.
- Sensible, latent, and total effectiveness data were compared with manufacturer's data. It was found that facility produces test data similar to the manufacturer's data. Therefore, it is claimed that the test facility provides reasonable test data.
- A proposed test method for measuring contribution of adsorption/desorption in contaminant transfer in energy wheels was applied and verified. The test method was

verified by testing four gaseous contaminants (methanol, isopropyl alcohol, ammonia, carbon dioxide, and one tracer gas (sulfur hexafluoride)).

- The $EATR_{ad}$ for ammonia, methanol, and isopropyl alcohol was reported as 70 ± 5%, 42 ± 3%, and 28 ± 3%, respectively. The high $EATR_{ad}$ of ammonia might be mainly because ammonia has physical properties very similar to water (molecular size and weight). In addition, ammonia, methanol, and isopropyl alcohol are polar chemicals (same as water), which is expected to allow them to be adsorbed/desorbed by desiccants.
- The experimental data for carbon dioxide and sulfur hexafluoride showed that outdoor air temperature does not have a significant impact on EATR. In fact, EATR did not change significantly when the outdoor air temperature changed from 1°C to 31°C. Furthermore, the average EATR values for carbon dioxide and sulfur hexafluoride were very similar (1.9 ± 1.7% for carbon dioxide and 1.7 ± 1.9% for sulfur hexafluoride), which indicates that the carbon dioxide transfer in energy wheels only occurs due to carryover and leakage.
- Experimental data for carbon dioxide showed that the EATR consistently decreased from 3.9 ± 0.7% to 1.5 ± 1.2% as the air face velocity increased from 0.8 m/s to 1.2 m/s. The EATR decrease was mainly due to dilution of contaminant in higher airflow rates and not due to reduction in the actual contaminant transfer rate. Air face velocity was found to have a more important impact on EATR than outdoor air temperature.
- EATR results for ammonia, methanol, isopropyl alcohol, carbon dioxide, and sulfur hexafluoride were compared with literature data. The EATR results reported in literature are different from the measured EATR values in this thesis. The difference in

EATR values between the measured EATR values and literature data were mainly due to different design and test conditions.

CHAPTER 4
SUMMARY, CONCLUSIONS, AND FUTURE WORK

4.1 Summary

This MSc research was part of ASHRAE Research Project (RP) 1780 titled "Test method to evaluate cross-contamination of gaseous contaminants within total energy recovery wheels", and there were two main objectives for this MSc research. The first objective was to conduct a literature review on test methodologies for measuring gaseous contaminant transfer in energy wheels, and the second objective was to apply and verify a test methodology for measuring gaseous contaminant transfer in energy wheels. Since the literature review showed that there is no established test methodology to determine the contribution of adsorption/desorption in contaminant transfer in energy wheels, a test methodology was applied and verified for measuring contaminant transfer due to adsorption/desorption in energy wheels. The test facility, instrumentation and experimental data were presented in the thesis.

The literature review in Chapter 2 showed that several researchers have measured contaminant transfer in energy exchangers and have reported results in terms of Exhaust Air Transfer Ratio (EATR). The EATR values include all contaminant transfer mechanisms: (1) carryover of gas contained in the flutes of a rotating wheel, (2) leakage of gas past seals separating the airstreams, and (3) adsorption of gas by the desiccant from the airstream with a high contaminant concentration followed by desorption to the other airstream. ASHRAE Standard 84 (2020) provides a test method for determining EATR for inert gases, which accounts for contaminant transfer due to bulk air flow only (i.e., (1) carryover and (2) leakage). Thus, a method to determine contaminant transfer due to (3) adsorption/desorption was presented in Chapter 2 and applied to the literature data. It was found that the contaminant transfer in energy wheels due to

adsorption/desorption was the highest for acetic acid, phenol, and acetaldehyde. The literature review showed that most researchers did not conduct a thorough uncertainty analysis, or consider contaminant mass conservation in their experiments. The literature data show that there are no clear relationships between contaminant transfer (EATR) and operating conditions (temperature and humidity). This could be due to different test conditions and wheel designs (e.g., wheel size, desiccant, duct size, purge section, pressure difference, etc.) used in the experiments. On the other hand, the literature review showed that the design conditions (effectiveness and face velocity) had a noticeable impact on EATR.

An existing test facility was used to conduct EATR experiments on an energy wheel coated with a molecular sieve desiccant, and the contribution of adsorption/desorption to contaminant transfer was determined. The results were presented in Chapter 3 for EATR experiments performed according to ASHRAE Standard 84 (2020) and at different operating (temperature) and design (face velocity) conditions. The experimental results showed that face velocity has a more significant impact on EATR than temperature. The average measured EATR value was 1.9 ± 1.7% for carbon dioxide and 1.7 ± 1.9% for sulfur hexafluoride. Therefore, it was concluded that carbon dioxide behaves very similarly to sulfur hexafluoride and is transferred only through bulk air transfer (i.e., air leakage and carryover). Experiments with different contaminants showed that EATR due to adsorption/desorption is highest for ammonia (70 ± 5%), followed by methanol (42 ± 3%), isopropyl alcohol (28 ± 3%), and carbon dioxide (-0.2 ± 2). The smaller molecular size and higher water solubility could be the reasons for the high EATR of ammonia compared to the other tested contaminants.

4.2 Conclusions

The main conclusions of this thesis are given below.

1. A test methodology for measuring the contribution of adsorption/desorption in gaseous contaminant transfer in energy wheels is not available in the literature.
2. Energy wheel design parameters (face velocity and effectiveness) affect EATR more than operating conditions (temperature and humidity).
3. The literature shows that EATR for acetic acid, phenol, and acetaldehyde is higher than for other contaminants, which is likely due to the transfer of these gases by adsorption/desorption since these gases have a high water solubility and are small molecules.
4. The proposed test methodology meets the requirements of ASHRAE Standard 84 (2020) and provides EATR due to adsorption/desorption with an uncertainty of less than ± 5% at the 95% confidence interval.
5. The measured EATR values are very similar for carbon dioxide and sulfur hexafluoride indicating that carbon dioxide is transferred only by carryover and leakage (for the case of energy wheels with molecular sieve desiccants) and by carryover only when the pressure is higher on the supply side than on the exhaust side of the wheel.
6. EATR decreases with increasing face velocity and does not change significantly with increasing temperature.
7. EATR due to adsorption/desorption is highest for ammonia, followed by methanol, isopropyl alcohol, and carbon dioxide. The reasons for the higher adsorption/desorption of ammonia on desiccants might be its smaller molecular size and higher water solubility.

4.3 Future work

The following activities are recommended for future research.

- Apply the proposed test methodology for different contaminants such as xylene, acetic acid, phenol, and acetaldehyde as required in ASHRAE RP-1780.
- Verify the test methodology proposed in this thesis for energy wheels with different desiccants such as silica gel or ion-exchange resin.
- Perform numerical modelling of gaseous contaminant transfer in energy wheels and develop numerical models to predict EATR for different energy wheel design and operating conditions.
- Determine EATR for different energy exchangers such as liquid-to-air membrane energy exchangers and flat-plate membrane energy exchangers. These experimental data can help determine the energy exchangers that minimize the return of gaseous contaminants into a building via the supply air.
- Perform a comprehensive literature review on gaseous contaminant measurement techniques. The advantages and disadvantages of these techniques can be meticulously reviewed and reported, which would assist researchers and engineers in the HVAC industry to select the best gas measurement techniques for contaminant transfer experiments. Furthermore, the literature review could contain an uncertainty analysis for the various gas measurement instruments.
- Conduct a literature review on modelling of contaminant transfer in energy exchangers.
- Perform sorption studies of various gaseous contaminants on solid desiccants and identify the best candidates for energy exchanger applications.

REFERENCES

[1] J. A. Leech, W. C. Nelson, R. T. Burnett, S. Aaron, and M. E. Raizenne, "It's about time: A comparison of Canadian and American time-activity patterns," *Journal of Exposure Analysis and Environmental Epidemiology*, vol. 12, no. 6, pp. 427–432, 2002.

[2] R. Kosonen and F. Tan, "The effect of perceived indoor air quality on productivity loss," *Energy and Buildings*, vol. 36, pp. 981–986, 2004.

[3] Natural Resources Canada, "HVAC & Energy Systems," 2020. [Online]. Available: https://www.nrcan.gc.ca/energy/efficiency/data-research-and-insights-energy-efficiency/housing-innovation/hvac-energy-systems/3937.

[4] W. J. Fisk, B. S. Pedersen, D. Hekmat, R. E. Chant, and H. Kaboli, "Formaldehyde and tracer gas transfer between airstreams in enthalpy-type air-to-air heat exchangers," in *ASHRAE Winter Meeting Conference*, Chicago, Jan. 27-30,1985, pp. 1–30.

[5] W. Shang, M. Wawryk, and R. W. Besant, "Air crossover in rotary wheels used for air-to-air heat and moisture recovery," *ASHRAE Transactions: Research*, vol. 107, pp. 72–83, 2001.

[6] A. Kodama, "Cross-contamination test of an enthalpy wheel loading a strong acidic cation ion-exchange resin or 3A zeolite as a desiccant material," *Journal of Chemical Engineering of Japan*, vol. 43, no. 10, pp. 901–905, 2010.

[7] C. W. Bayer, "Total energy recovery wheel contaminant transfer study report," Columbia, Missouri, Hygieia Sciences LLC, 2011.

[8] H. Patel, "Contaminant transfer in a run-around membrane energy exchanger," MSc Thesis, Department of Mechanical Engineering, University of Saskatchewan, Saskatoon, 2014.

[9] ASHRAE, *ASHRAE HVAC Systems and Equipments Handbook*. Atlanta, 2008.

[10] C. A. Roulet, M. C. Pibiri, R. Knutti, A. Pfeiffer, and A. Weber, "Effect of chemical composition on VOC transfer through rotating heat exchangers," *Energy and Buildings*, vol. 34, no. 8, pp. 799–807, 2002.

[11] ASHRAE, *ASHRAE Fundamentals Handbook*. Atlanta, 2013.

[12] D. Vallero, *Air pollution calculations: Quantifying pollutant formation, transport, transformation, fate and risks*, First edition. Illinois: Elsevier, 2019.

[13] G. A. Khoury, S. N. Chang, D. A. Lessley, A. A. Abdelghani, and A. C. Anderson, "An investigation of reentrainment of chemical fume hood exhaust air in a heat recovery unit," *American Industrial Hygiene Association Journal*, vol. 49, no. 2, pp. 61–65, 1988.

[14] H. Okano, H. Tanaka, T. Hirose, H. Funato, S. Ishihara, and S. Chirarattananon, "A novel total heat exchanger with little odor transfer using ion exchange resin as a desiccant," *ASHRAE Transactions: Research*, vol. 107, no. 2, pp. 66–71, 2001.

[15] ANSI/ASHRAE, *Standard 84, Method of testing air-to-air heat/energy exchangers*. Atlanta, 2020.

[16] Canadian Standards Association, *Standard laboratory methods of test for rating the performance of heat/energy-recovery ventilators*. Canada: CSA Group, 2018.

[17] R. K. Shah and D. P. Sekulic, *Fundamentals of heat exchanger design*. Hoboken: John Wiley & Sons, Inc., 2003.

[18] ASME/ANSI, *Performance test code 19.1. Test uncertainty: Instruments and apparatus*. New York, 1998.

[19] B. Andersson, K. Andersson, J. Sundell, and P. Zingmark, "Mass transfer of contaminants in rotary enthalpy exchangers," *Indoor Air*, vol. 3, no. 2, pp. 143–148, 1993.

[20] E. M. Sparrow, J. P. Abraham, G. P. Martin, and J. C. Y. Tong, "An experimental investigation of a mass exchanger for transferring water vapor and inhibiting the transfer of other gases," *International Journal of Heat and Mass Transfer*, vol. 44, no. 22, pp. 4313–4321, 2001.

[21] E. J. Wolfrum, D. Peterson, and E. Kozubal, "The volatile organic compound (VOC) removal performance of desiccant-based dehumidification systems: Testing at sub-ppm VOC concentrations," *HVAC and R Research*, vol. 14, no. 1, pp. 129–140, 2008.

[22] H. Patel, G. Ge, M. R. H. Abdel-Salam, A. H. Abdel-Salam, R. W. Besant, and C. J. Simonson, "Contaminant transfer in run-around membrane energy exchangers," *Energy*

and Buildings, vol. 70, pp. 94–105, 2014.

[23] H. Fan, C. J. Simonson, R. W. Besant, and W. Shang, "Performance of a run-around system for HVAC heat and moisture transfer applications using cross-flow plate exchangers coupled with aqueous lithium bromide," *HVAC & R Research*, vol. 12, no. 2, pp. 313–336, 2006.

[24] E. L. Hult, H. Willem, and M. H. Sherman, "Formaldehyde transfer in residential energy recovery ventilators," *Building and Environment*, vol. 75, pp. 92–97, 2014.

[25] M. Kassai, "Experimental investigation of carbon dioxide cross-contamination in sorption energy recovery wheel in ventilation system," *Building Services Engineering Research and Technology*, vol. 39, no. 4, pp. 463–474, 2018.

[26] J. Nie, J. Yang, L. Fang, and X. Kong, "Experimental evaluation of enthalpy efficiency and gas-phase contaminant transfer in an enthalpy recovery unit with polymer membrane foils," *Science and Technology for the Built Environment*, vol. 21, no. 2, pp. 150–159, 2015.

[27] W. M. Kays and A. L. London, *Compact heat exchangers*, Third edition. New York: McGraw-Hill, Inc, 1984.

[28] M. Rafati Nasr, F. Fathieh, D. Kadylak, R. Huizing, R. W. Besant, and C. J. Simonson, "Experimental methods for detecting frosting in cross-flow air-to-air energy exchangers," *Experimental Thermal and Fluid Science*, vol. 77, pp. 100–115, 2016.

[29] K. Mahmud, G. I. Mahmood, C. J. Simonson, and R. W. Besant, "Performance testing of a counter-cross-flow run-around membrane energy exchanger (RAMEE) system for HVAC applications," *Energy and Buildings*, vol. 42, no. 7, pp. 1139–1147, 2010.

[30] ISO, *International Standard: ISO 5167-1 Measurement of fluid flow by means of pressure differential devices inserted in circular cross-section conduits running full--Part 1: General principles and requirements*. Geneva, 2003.

[31] B. Bettens, S. Dekeyzer, B. Van Der Bruggen, J. Degrève, and C. Vandecasteele, "Transport of pure components in pervaporation through a microporous silica membrane," *Journal of Physical Chemistry B*, vol. 109, no. 11, pp. 5216–5222, 2005.

[32] H. Hu, J. Zhu, F. Yang, Z. Chen, M. Deng, L. Weng, Y. Ling, and Y. Zhou, "A robust: Etb-type metal-organic framework showing polarity-exclusive adsorption of acetone over methanol for their azeotropic mixture," *Chemical Communications*, vol. 55, no. 46, pp. 6495–6498, 2019.

[33] Hart Scientific, *9105 / 9107 Dry-well Calibrator User's Guide*. Utah, 2002.

[34] Thunder Scientific® Corporation, "Model 1200 Mini 'Two-Pressure' Humidity Generator." https://www.thunderscientific.com/humidity_equipment/model_1200.html.

[35] G. Druck, "DPI 605 Precision Portable Pressure Calibrator." .

[36] S. C.-P. Hsu, "Infrared Spectroscopy," in *Handbook of Instrumental Techniques for Analytical Chemistry*, Prentice Hall PTR, Arlington, 1997, pp. 247–277.

[37] G. T. Oy, "FTIR gas analysis," Helsinki, Finland, 2016. [Online]. Available: http://classtap.pbworks.com/f/SkillSoft+-+Blended+Elearning.pdf.

[38] T. O. Gasmet™, "In-Lab series instruction & operating manual for the Gasmet CR-100M FTIR gas analyzer model," Helsinki, Finland, 2006.

[39] J. R. J. Paré and J. M. R. Bélanger, *Instrumental methods in food analysis*, First edition. Elsevier, 1997.

APPENDIX A
ASHRAE RP-1780 Request-For-Proposal

The following document is provided as the original version of ASHRAE RP-1780 Request-For-Proposal (RFP) published in 2018. The RFP was changed slightly in next version of the ASHRAE RP-1780 RFP published in 2019. The only change between the two versions of RFP is removal of -20 ºF test condition from the original document.

INVITATION TO SUBMIT A RESEARCH PROPOSAL ON AN ASHRAE RESEARCH PROJECT

1780-TRP, "Test method to evaluate cross-contamination of gaseous contaminant within total energy recovery wheels"

Attached is a Request-for-Proposal (RFP) for a project dealing with a subject in which you, or your institution have expressed interest. Should you decide not to submit a proposal, please circulate it to any colleague who might have interest in this subject.

Sponsoring Committee: TC 9.10, Laboratory Ventilation
Co-sponsored by: TC 2.3, Gaseous Air Contaminants and Gas Contaminant Removal Equipment; TC 9.6, Healthcare Facilities; SSPC 62.1, SSPC 62.1, Ventilation for Acceptable Indoor Air Quality

Budget Range: $200,000 may be more or less as determined by value of proposal and competing proposals.

Scheduled Project Start Date: **April 1, 2019** or later.

All proposals must be received at ASHRAE Headquarters by 8:00 AM, EST, December 17, 2018. NO EXCEPTIONS, NO EXTENSIONS. Electronic copies must be sent to rpbids@ashrae.org. Electronic signatures must be scanned and added to the file before submitting. The submission title line should read: 1780-TRP, "Test method to evaluate cross-contamination of gaseous contaminant within total energy recovery wheels", and "*Bidding Institutions Name*" (electronic pdf format, ASHRAE's server will accept up to 10MB)

If you have questions concerning the Project, we suggest you contact one of the individuals listed below:

For Technical Matters
Technical Contact
Roland Charneux
Place Honore-Beaugrand
Montreal, QC H1K 3Y7
CANADA
Phone: 5143825150 (2222)
E-Mail: rcharneux@pageaumorel.com

For Administrative or Procedural Matters:
Manager of Research & Technical Services (MORTS)
Michael R. Vaughn
ASHRAE, Inc.
1791 Tullie Circle, NE
Atlanta, GA 30329
Phone: 404-636-8400
Fax: 678-539-2111
E-Mail: MORTS@ashrae.net

Contractors intending to submit a proposal should so notify, by mail or e-mail, the Manager of Research and Technical Services, (MORTS) by December 3, 2018, in order that any late or additional information on the RFP may be furnished to them prior to the bid due date.

All proposals must be submitted electronically. Electronic submissions require a PDF file containing the complete proposal preceded by signed copies of the two forms listed below in the order listed below. **ALL electronic proposals are to be sent to rpbids@ashrae.org.**

All other correspondence must be sent to ddaniel@ashrae.org and mvaughn@ashrae.org. Hardcopy submissions are not permitted. **In all cases, the proposal must be submitted to ASHRAE by 8:00 AM, EST, December 17, 2018. NO EXCEPTIONS, NO EXTENSIONS.**

The following forms (Application for Grant of Funds and the Additional Information form have been combined) must accompany the proposal:

(1) ASHRAE Application for Grant of Funds (electronic signature required) and
(2) Additional Information for Contractors (electronic signature required) ASHRAE Application for Grant of Funds (signed) and

ASHRAE reserves the right to reject any or all bids.

State of the Art (Background)

Some research has been done by manufacturers, and some in Japan at Kanazawa University. As per the review of the available literature that has been done, there is actually no test procedure to evaluate the gaseous contaminant transfer and at which temperature and humidity conditions that these tests should be conducted.

The basic function of laboratory HVAC systems is the management of contaminant concentrations in the space in order to reduce the risk to the researchers of ingesting or being in contact with these contaminants. Unlike commercial spaces, energy-intensive laboratories use high volumes of filtered outdoor air to dilute airborne contaminants. This requires large amount of outside air that has to be cooled, dehumidified, heated and humidified, resulting in very high energy use. As per DOE (2008) there are about 9000 laboratory buildings in the US totaling about 650 million square feet of work area. According to EPA, US laboratories consumed about 150 million MWHr/yr in 2005. Of this, approximately 60% (or 90 million MWhr/yr) was associated with the HVAC systems.

Historically, the glycol loop, which utilizes a coil to transfer thermal energy between the exhaust and supply air streams, has been considered the safest energy recovery system for laboratory HVAC systems. This technology eliminates the risk of contaminant transfer in the incoming air from the exhausted air stream. However, this technology is only about 40-45% efficient in winter and even lower in the summer, since it does not recover the latent heat of the exhausted air. It also provides no heating season humidification.

ASHRAE Standard 90.1 now mandates the use of total energy recovery devices for most buildings. To determine compliance with ASHRAE Standard 62.1 for most building types, 62.1 provides Classification of Air and acceptable Exhaust Air Transfer Ratios (which are certified by AHRI). However, for laboratory applications, 62.1 directs the user to environmental health and safety experts and these experts needs to establishing the degree of contaminant transfer air exhibited by a given product in a specific ERV installation. This research will provide tools for use by these experts and is essential for all building types, not just laboratories, since transfer contaminated air cannot be considered outdoor air. To determine the proper outdoor air correction factor (OACF) the approximate degree of contaminant transfer air must be known.

As ASHRAE 62.1 now permits the use of total energy recovery wheels under certain conditions for laboratory hood exhaust The ASHRAE community needs qualitative data and tests procedures on the potential cross-contamination of these devices.

Over the past 20 years, some manufacturers have developed specialized desiccant transfer surfaces and advanced purge sections to limit the transfer of airborne particulate and gaseous contaminants contained within the exhaust air stream. Substantial research has been completed by the Georgia Tech Research Institute and a University in Japan for select manufacturers. Field data of cross-contamination levels has been reported at various technical conferences, including ASHRAE. However a standard test procedure does not exist, so the validity of the results is always in question. Therefore, ASHRAE should address the concern of contaminant transfer within total energy devices by developing a standard testing procedure.

Justification and Value to ASHRAE

The Environmental Health and Safety professionals, laboratory designers and other ASHRAE Members need reliable gaseous contaminant transfer data measurements methodologies to complete the necessary risk assessment when evaluating energy recovery systems for their laboratory ventilation projects. Technologies shown to limit contaminant transfer would allow greater energy savings and reduce the carbon footprint.

Compared to commercial buildings, the opportunity for energy savings in laboratories is much greater. ASHRAE should play a leadersdhip role in optimizing the HVAC systems in laboratories while keeping safety a top priority.

Objectives

The objectives of this study are to:

1) Review current testing methodologies and relevant research data available;
2) Develop a draft test methodology and establish minimum specifications for the test facility and instrumentation;

3) Evaluate the draft test methodology with various gaseous chemicals representative of contaminants of concern and operating conditions representative of a laboratory, vivariums and similar facilities. Also consider various incoming outside air temperatures and humidity.
4) Validate the test methodology based on the test results collected under laboratory conditions;
5) Produce a final test method for establishing gaseous cross contamination rate measurement that is reliable and effective for manufacturers/test laboratories to employ.

Scope:

1. Establish a scientific approach to develop a test methodology to evaluate gaseous cross-contamination transfer within total energy wheels recovery devices. Including a review of the available literature and research publications relating to methods for testing cross-contamination and reported data. Note the different environmental conditions under which total energy recovery wheels shall be tested.
2. Based on the literature review and existing research publications, develop a draft test methodology. This should include specifying the most appropriate test facility and instrumentation capabilities in which to conduct the testing, selecting an appropriate number of contaminants of concern to test, and selecting the environmental conditions which should be varied to determine any impact on carry-over rates as part of the energy recovery device evaluation (see list below)
3. Laboratory testing:
    - The contractor will be responsible for building/finding access to a laboratory facility with the capabilities necessary and designed to meet ASHRAE 84 requirements to implement the methodology testing and evaluate the impact of selected design parameters from the list below Select appropriate contaminants; considering molecular properties of the contaminant (i.e., polarity, water solubility, molecular size, etc.). The list shall be comprehensive enough to represent a typical laboratory fume hood exhaust, vivarium or other applications. Chemicals necessary level of accuracy and to represent a worst-case scenario. Chemicals chosen must be easy to measure by instrumentation readily available for precision analysis (i.e. mass spectrometer, gas chromatograph, photo-acoustical multi-gas analyzer, etc.) The listed contaminants below are a minimum.
    - Evaluate the potential impact of design parameters associated with recovery devices that would likely influence gaseous contaminant transfer taking into account current, best design practices
        - Airflow/face velocity,
        - temperature,
        - condensation,
        - relative humidity,
        - freezing,
        - pressure differential between airstreams.
4. Finalize Test Method and :
    - Provide documentation (final report with data) to establish the effectiveness of the test procedure confirming the ability to deliver the necessary precision to document gaseous contaminant transfer as a percentage of the challenge concentration.
    - Provide rational behind the design variables tested and the impact on carry-over established for those variables investigated.
    - Secure industry (non-identified of 2 different manufacturers) samples of at least 2 total energy recovery products employing different desiccant types. Test each of these 2 samples for the full range of gaseous chemicals selected and temperature and humidity conditions listed below and publish the carry-over percentage measured complete with error bars to highlight the precision of the data. Use at least one of these samples to evaluate the impact of design parameters on carry-over (i.e face velocity, humidity level, pressure differential, condensation, freezing, etc.)

- Provide drawings of a test facility layout that can accommodate the Test Method established and which can also be easily constructed by manufacturers of the recovery devices or research laboratories interested in completing such testing. Recommend instrumentation to be used, procedures for introducing the challenge chemicals and collection of the samples to be evaluated.
- Summarize the test method, all data and recommended procedures in a manner to allow for peer review and for eventual implementation into ASHRAE 84 or other standard.

Background Information:

A substantial body of research work has been conducted in this field over the past 25 years by the Georgia Tech Research Institute, Dr. Charlene Bayer (now Director of Hygieia Sciences), Johns Hopkins School of Medicine and The Japanese Fukuoka Institute of Technology.

The selected chemicals should represent a strategic sampling from different chemical groups, water solubility, polarity and kinetic diameter (molecular size) which can be safely used within a test laboratory and be precisely measured. As part of a DOE funded research project, researchers at the Georgia Tech Research Institute evaluated this list of parameters to recommend the following chemical families for testing.

Contaminants chosen with properties

- Acetaldehyde - small aldehyde, water soluble and polar
- Ammonia
- Acetic acid - small acid, water soluble and polar
- Methanol - smallest alcohol, water soluble very polar
- Isopropyl alcohol - small alcohol, water soluble and polar
- Methyl isobutyl ketone - small ketone, somewhat water soluble and polar
- Xylene - Aromatic hydrocarbon, non-polar and water immiscible
- Carbon dioxide - Small oxide, non-polar and water soluble
- Propane or hexane - Alkane (straight chain hydrocarbon), non-polar, water immiscible
- Phenolic gases

The Sulfur Hexafluoride is specifically chosen since it is a gaseous contaminant that will not be transferred by any desiccant surface and can therefore be a reliable challenge gas to quantify purge inefficiency and seal leakage. Any contaminant carry-over for another challenge gas beyond the percentage measured for the SF6 is therefore desiccant carry-over.

Other contaminants that may or may not be considered contaminants of concern since they are not a health risk but could be a nuisance odor for a specific application would also be covered by the test standard for specific labs or non-lab applications, allowing for the same procedure to be used for other chemicals not included in the initial group recommended for testing for laboratory fume hood applications.

The list of chemical should be reviewed by the PI of this research project and confirm this list as a minimum.

Task #1: Do a complete literature review
Task #2: Validate the list of chemicals proposed in the present WS and comment if needs be.
Task #3: Have the test rig plans and characteristics validated by the PMS.
Task #4: After completing the installation, validate the test rig at high and low limit conditions of temperature, pressure, humidity and flow. Define the wheel air leakage/transfer.
Task #5: Prepare a draft method of testing chemicals.
Task #6 : For one chemical, do the complete series of test at specified temperature and humidity. These values should be reviewed by the PMS before continuing testing of other chemicals.
Task #7: Validate the testing methodology, update and document the test methodology.

Task #8: Tests all other chemicals at the various prescribed temperature and humidity conditions and report measured datas.
Task #9: Write the final test procedure.

Deliverables:

Results will include: A complete literature review of existing scientific studies on this topic; provide a comparison of the previously reported measured data; validate that the developed test procedure is acceptable and consistent; establish the limitations of the test procedure including the challenge chemicals to be used; validate via in-situ installations that the test procedure is applicable; and determine the metrics that impact the cross-contamination rates.

There are several required deliverables for this project. These include:

1. A complete literature review of existing scientific studies on this topic. This will initially be presented to the PMS for review and approval as milestone 1. This review will also be included in the final project report for publication by ASHRAE.
2. List the chemicals that has been validated and the reason why they were chosen.
3. Submit the test rig plans and operation characteristics of flow, temperture, humidity, pressure, etc..
4. Validate in-situ the operation characteristics of the rig at all limit conditions and report these datas to the PMS
5. A draft test method in a format that could become the basis for a new ASHRAE test method. This draft, in initial format, will be presented to the PMS for review
6. Submit datas after testing of one chemicals at all temperatures and humidity conditions. Describe procedures and measurement instruments used. Comments also on accuracy and reliability of results.
7. Propose adjustments to the test procedure if needed.
8. Proceed with testing all other chemicals and provide the datas to the PMS.
9. Submit a report on the validation of the developed test procedure showing that it is acceptable and consistent by establishing the limitations of the test procedure including commenting on the challenge chemicals that has been used.
10. Final report documenting all of the information and requirements set forth in sections 1-9 in the Scope/Technical approach/ Tasks section of this document. Final report recommending how to conduct testing, collect, analyze and report datas.
11. Final test method written to serve as the basis of a new ASHRAE test method.
12. ASHRAE Transaction article and/or other publications required by ASHRAE.

Progress, Financial and Final Reports, Technical Paper(s), and Data shall constitute the deliverables ("Deliverables") under this Agreement and shall be provided as follows:

a. Progress and Financial Reports

Progress and Financial Reports, in a form approved by the Society, shall be made to the Society through its Manager of Research and Technical Services at quarterly intervals; specifically on or before each January 1, April 1, June 10, and October 1 of the contract period.

The following deliverables shall be provided to the Project Monitoring Subcommittee (PMS) as described in the Scope/Technical Approach section above, as they are available:

Furthermore, the Institution's Principal Investigator, subject to the Society's approval, shall, during the period of performance and after the Final Report has been submitted, report in person to the sponsoring Technical Committee/Task Group (TC/TG) at the annual and winter meetings, and be available to answer such questions regarding the research as may arise.

b. Final Report

A written report, design guide, or manual, (collectively, "Final Report"), in a form approved by the Society, shall be prepared by the Institution and submitted to the Society's Manager of Research and Technical Services by the end of the Agreement term, containing complete details of all research carried out under this Agreement, including a summary of the control strategy and savings guidelines. Unless otherwise specified, the final draft report shall be furnished, electronically for review by the Society's Project Monitoring Subcommittee (PMS).

Tabulated values for all measurements shall be provided as an appendix to the final report (for measurements which are adjusted by correction factors, also tabulate the corrected results and clearly show the method used for correction).

Following approval by the PMS and the TC/TG, in their sole discretion, final copies of the Final Report will be furnished by the Institution as follows:

-An executive summary in a form suitable for wide distribution to the industry and to the public.
-Two copies; one in PDF format and one in Microsoft Word.

c. *Science & Technology for the Built Environment* or ASHRAE Transactions Technical Papers

One or more papers shall be submitted first to the ASHRAE Manager of Research and Technical Services (MORTS) and then to the "ASHRAE Manuscript Central" website-based manuscript review system in a form and containing such information as designated by the Society suitable for publication. Papers specified as deliverables should be submitted as either Research Papers for HVAC&R Research or Technical Paper(s) for ASHRAE Transactions. Research papers contain generalized results of long-term archival value, whereas technical papers are appropriate for applied research of shorter-term value, ASHRAE Conference papers are not acceptable as deliverables from ASHRAE research projects. The paper(s) shall conform to the instructions posted in "Manuscript Central" for an ASHRAE Transactions Technical or HVAC&R Research papers. The paper title shall contain the research project number (1780-RP) at the end of the title in parentheses, e.g., (1780-RP).

All papers or articles prepared in connection with an ASHRAE research project, which are being submitted for inclusion in any ASHRAE publication, shall be submitted through the Manager of Research and Technical Services first and not to the publication's editor or Program Committee.

d. Data

Data is defined in General Condition VI, "DATA"

e. Project Synopsis

A written synopsis totaling approximately 100 words in length and written for a broad technical audience, which documents 1. Main findings of research project, 2. Why findings are significant, and 3. How the findings benefit ASHRAE membership and/or society in general shall be submitted to the Manager of Research and Technical Services by the end of the Agreement term for publication in ASHRAE Insights

The Society may request the Institution submit a technical article suitable for publication in the Society's ASHRAE JOURNAL. This is considered a voluntary submission and not a Deliverable. Technical articles shall be prepared using dual units; e.g., rational inch-pound with equivalent SI units shown parenthetically. SI usage shall be in accordance with IEEE/ASTM Standard SI-10.

Level of Effort

This project is expected to take 6 person-months of a PI and 10 person-months of technicians. The total duration of the research project is expected to be 15 months. Estimated cost of $200 000

Other Information for Bidders

Potential Test rig required:
Test facility designed in accordance with ASHRAE Standard 84 having a capacity of 500 to 2 000 CFM at 500 fpm incoming face velocity. Balanced airflow to be utilized for testing.

The location of the supply fan upstream of the wheel and the exhaust fan downstream. Establish the wheel purge air volume of the testing rig. The tracer gas testing must be done with established airflows, pressure differentials and temperatures.

In addition, the test facility should be able to maintain the following air conditions:

• Outside air condition from -20°F to +90°F with 10% RH to 90% RH
• Exhausted air conditions from 70°F to 80°F with 30% to 70%RH

Air by-pass (Carry-over) has to be measured first using SF6 tracer gas which is known not to be transferred by the desiccant surface.
Test rig utilized to investigate the impact of temperature, humidity, pressure, etc. must be designed to allow for the variation in psychrometric conditions and airflows.
Test rig shall have a variable speed drive on the wheel. This drive to be controlled by pressure differential on the wheel on the exhaust side to accept a little condensation and frosting while not having the wheel blocked by frost.

Conditions to be tested:
- For 2 wheels from 2 manufacturers
- For outside air conditions:
  - -20°F : Any RH but RH should be measured and reported
  - -10°F : Any RH but RH should be measured and reported
  - 0°F : Any RH but RH should be measured and reported
  - 10°F : Any RH but RH should be measured and reported
  - 20°F : 50% HR 90% HR
  - 30°F : 50% HR 90% HR
  - 50°F : 50% HR 90% HR
  - 70°F : 50% HR 90% HR
  - 90°F : 50% HR 90% HR

- For exhaust air conditions:
  - 75°F : 30% HR 50% HR 70% HR
- For the 10 chemicals listed on page 7, plus SF-6 Test

Project Milestones:

No.	Major Project Completion Milestone	Deadline Month
1	Literature search (2 Months)	2
2	Results of the validation of the Test Rig (2 months + 2 months in parallel of the literature search)	4
3	First complete series of results with one chemical (2 months)	6
4	Complete datas of results with all chemicals at all temperature and humidity conditions (6 Months)	12
5	Final testing methodology documentation and final report (3 Months)	15

Proposal Evaluation Criteria
Proposals submitted to ASHRAE for this project should include the following minimum information:

No.	Proposal Review Criterion	Weighting Factor
1	Understanding of the Work Statement	15%
2	Proposed methodology	20%
3	Quality of facilities and access	15%
4	Quality of the proposed personnel: PI, researchers, etc..	25%
5	Students involvement 5%	5%
6	Probability of meeting the objectives in the scheduled timeframe 15%	15%
7	Past performance with AHRAE or other similar organizations	5%

References

1. ASHRAE Strategic plan 2014
2. ASHRAE Research Strategic Plan 2010-2018
3. ANSI/ASHRAE Standard 84-2013 “Method of testing Air-to-air Heat/Energy Exchangers
4. 2015 ASHRAE Handbook-HVAC Applications Chapter 16 Laboratories
5. 2016 ASHRAE Handbook-HVAC Systems and equipment Chapter 26, Air-to-air energy recovery equipment
6. 2015 ASHRAE Handbook-HVAC Applications Chapter 18 – Clean spaces
7. ASHRAE Laboratory design guide
8. Fischer, J, ASHRAE 2015 Annual Conference, Seminar 19: Apply ANSI/ASHRAE 62.1 Addendum K for Laboratory Hoods, Applying Total Energy Recovery in Laboratory Environments
9. DOE (Department of energy) report 2008
10. ASHRAE Standard 62.1 Ventilation for acceptable indoor air quality
11. ASHRAE Standard 90.1 Energy standard for buildings except low rise residential
12. Bayer, Charlene W, Total energy recovery wheel contaminant transfer study, submitted to SEMCO, August 31, 2011
13. Bayer, Charlene W. and Hendry, Robert J. The importance of the desiccant in total energy wheel cross-contamination. Prepared for SEMCO, May 17, 1999
14. Total Recovery Desiccant Wheel Pollutant Contaminant Challenge: Ventilation Effectiveness Comparison, The Georgia Tech Research Institute for DOE, Dr. Charlene Bayer, March 2004
15. Downing, Chris, Independent performance verification of SEMCO’s total energy recovery wheels, 1999
16. Kodama, Akio, Cross contamination test of the Seibu-Giken “HI_PANEX-Ion” Enthalpy wheel, Kanazawa University, Japan
17. A Novel Total Heat Exchanger with Little Odor Transfer Using Ion Exchange Resin as a Desiccant, ASHRAE Transactions, Okano et.al,
18. The Effectiveness of a Molecular Sieve Heat Wheel in Maintaining Good Air Quality in a Major Laboratory Research Facility, ASHRAE IAQ 96, Johns Hopkins School of Medicine, Schaefer et.al, 1996
19. Brad Cochran, I2SL, Evaluation of cross-contamination in enthalpy wheel devices in laboratory exhaust system
20. Labs 21, Energy recovery in laboratory facilities Presentation on Hopkins Ross Facility entitled “Applying 3A Molecular Sieve Total Energy Wheels to Laboratory Environments”
21. DOE, a guide to navigating building and fire codes for laboratories

APPENDIX B
GAS CONCENTRATION MEASUREMENT TECHNIQUES

ASHRAE Fundamentals Handbook [11] lists different gaseous contaminant concentration measurement techniques such as gas chromatography (GC), high performance liquid chromatography (HPLC), and infrared (IR) spectroscopy. In the following paragraphs, these gaseous contaminant concentration measurement techniques and their practical applications in energy exchangers will be described.

The GC technique is separation of components of a gaseous sample using a stationary phase and a mobile phase. Mobile phase usually is an inert gas (helium or nitrogen) that does not react with gas samples and the stationary phase is a liquid or solid inside a long column. If the stationary phase is solid, gas components are absorbed into the solid and desorbed to mobile phase. If the stationary phase is liquid, gas components are adsorbed on surface of liquid and desorbed to mobile phase.

Mobile phase, i.e., carrier gas, is used to take gaseous samples to column with the stationary phase. The mobile phase reacts with stationary phase and as the chemical reactions between components of gaseous sample and stationary phase increases, there would be a longer time for the sample to pass through the column. After passing through the column, sample reaches a detector port that is used to identify chemical components and their concentration. Detector produces signals in accordance with components concentration, which are shown by a computer. Figure B.1 shows a schematic of a gas chromatogram. Time period from gas sample injection to detection port is called retention time. The retention time for different components depends on chemical reaction between mobile and stationary phase.

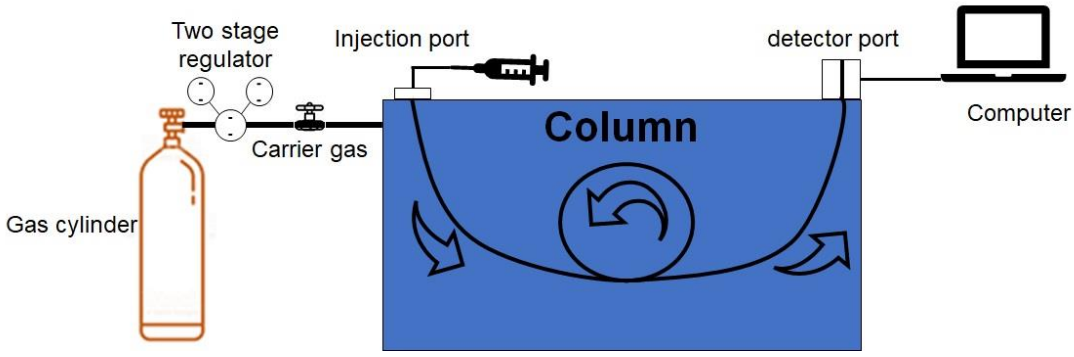

Figure B.1. Schematic diagram of GC instrumentation.

The GC is an accurate, high-speed and high-sensitivity separation technique that is used to determine components of complex materials such as gasoline, smoke, oil, and soil organic matter. However, this separation technique needs another instrument such as mass spectrogram for confirmation of results. Further, the sample for the GC analysis must be volatile, i.e., materials with low boiling point.

Roulet *et al.* [10] used the GC technique to measure concentration of 11 gaseous contaminants (n-decane, n-butanol, hexanol, phenol, 1,6-dicholorhexane, hexanal, benzaldehyde, limonene, m-xylene, mesitylene, and dipropylether). Air samples were collected in a small tube with an absorbing medium. Absorbed contaminants in the small tube were desorbed by heating the tube and stored in a cold trap. A flame ionization detector (FID) was used to detect and measure the amount of each compound, while a mass spectrograph was used to help identify each compound in the cold trap. Wolfrum *et al.* [21] collected air samples into a manifold containing 10 sorbent tubes (100 mg of Tenax TA 35/60) and desorbed the concentrated contaminants in sorbent tubes with a thermal desorption unit (Perkin-Elmer ATD 400). These concentrated gas samples were analyzed by a gas chromatograph (Agile 6890N) with an FID.

Another gaseous contaminant concentration measurement technique is the HPLC. The HPLC is very similar to the GC technique with some modifications. In the HPLC the mobile phase is liquid,

and the stationary phase can be solid or liquid. As sample goes through the column, chemical components of the sample react with stationary phase. The chemical components of the sample are separated and identified by a detector which measures concentration of each component.

Different components of an HPLC instrument include stainless steel columns, absorbent materials coated on surface of column and a pump for driving liquid from a chamber to columns. Further, there are different types of HPLC technique; 1) Normal phase; mobile phase is non-polar and stationary phase is polar, 2) Reverse phase; mobile phase is polar and stationary phase is non-polar, 3) Size exclusion; stationary phase consists of porous beads that allow permeation of small-size molecules, and 4) Ion-exchange; mobile phase has positive or negative electric charge depending on electric charge of stationary phase.

The HPLC technique has been known as an affordable and easy to handle method for measuring gas concentration. Using the HPLC technique, it is possible to identify compounds of limited thermal stability or volatility in short times, i.e., each experiment may take 5 to 10 minutes. However, a disadvantage of the HPLC technique is that availability of different detectors makes it difficult for the operator to choose suitable detector for concentration measurement purpose [39]. Hult *et al.* [24] used the HPLC technique for measuring formaldehyde transfer rate in their experiments. Air samples were drawn using a multichannel peristaltic pump, with a sampling flow rate of 1L/min at 20 mins. Air samples were collected into silica gel cartridges coated with 2,4-dinitrophenylhydrazine (DNPH XPoSure Aldehyde Sampler; Waters corporation). Then, samples were extracted into 2 mL of high purity acetonitrile and analyzed using the HPLC technique (HPLC; 1200 Series; Agilent Technologies).

The IR spectroscopy technique is the absorption measurement of different IR frequencies by a sample exposed to an IR radiation source. A chemical compound can absorb IR light, if frequency

of the light matches with frequency of the chemical compound vibrations. The vibrations of a chemical compound could be described as wagging, bending, and stretching. When frequency of the IR light is equal to the frequency of chemical compound vibrations, the energy from IR waves is absorbed by the chemical group. When the frequency of IR waves is different than that of chemical group vibrations, the energy from IR waves does not absorb by the chemical compound. For example, consider formaldehyde as a gaseous sample with two types of molecular vibrations including wagging (rotational movement) and stretching (translational movement). The frequency for wagging is assumed as 4 Hz and the frequency for stretching is assumed as 2 Hz. When an IR radiation with 2 or 4 Hz hits formaldehyde molecule, formaldehyde absorbs all the energy. When an IR wave with frequency other than 2 or 4 Hz is emitted, the IR wave passes through the chemical compound. To show output data for an IR spectroscopy analysis, frequency is converted to wave number, i.e., reciprocal of wavelength. Different gases absorb the IR radiation in different wave numbers. Carbon dioxide absorbs IR radiations with wave numbers at 2350 cm^{-1}. Water vapor absorbs wave numbers between 1300-1800 and 3500-4000 cm^{-1}.

Andersson *et al.* [19] used an infrared spectrophotometer (MIRAN 1A) to determine the concentration of nitrous oxide. The air samples were collected using a vacuum pump and a metal tube with 45^{o} capped end. The tube was inserted into the duct and placed perpendicular to the air stream such that the inclined capped end of the tube remained in the middle of the duct with the open area facing the air flow. Sparrow *et al.* [20] used a commercially available TSI carbon dioxide meter (Q-TRAK 8550) to measure the concentration of carbon dioxide in the air samples. Fisk *et al.* [4] used infrared analyzers for real-time measurement of propane and sulfur hexafluoride. A microprocessor based solenoid valve system was used which directed the air samples into the analyzers from the air stream.

A literature review on different gas measurement techniques and their uncertainties was done. Table B.1 shows the uncertainty for each gas measurement technique.

Table B.1. Gas measurement techniques and their uncertainties.

Measurement technique	Uncertainty	Reference
1. Gas chromatography	1%	Wolfrum et al. (2008) [21]
	2%	Hult et al. (2014) [24]
2. Gas detector tubes	5-10%	Kodama (2010) [6], Okano et al. (2001) [14]
3. Photoacoustic spectroscopy	1%	Nie et al. (2015) [26]
4. Infrared spectroscopy	2%	Patel (2014) [8]
	3-5%	Kassai (2018) [25]
	3%	Sparrow et al. (2001) [20]

Using the measurement technique uncertainty, EATR and tracer gas concentration difference between the outdoor airstream and the return airstream ($C_3 - C_1$), the EATR uncertainty was calculated using Eq. (2.6). Figure B.1 shows the EATR uncertainty versus gas measurement technique uncertainty. The EATR values were assumed as 1%, 3% and 10%, and ($C_3 - C_1$) values were assumed as 50ppm, 100ppm and 200ppm.

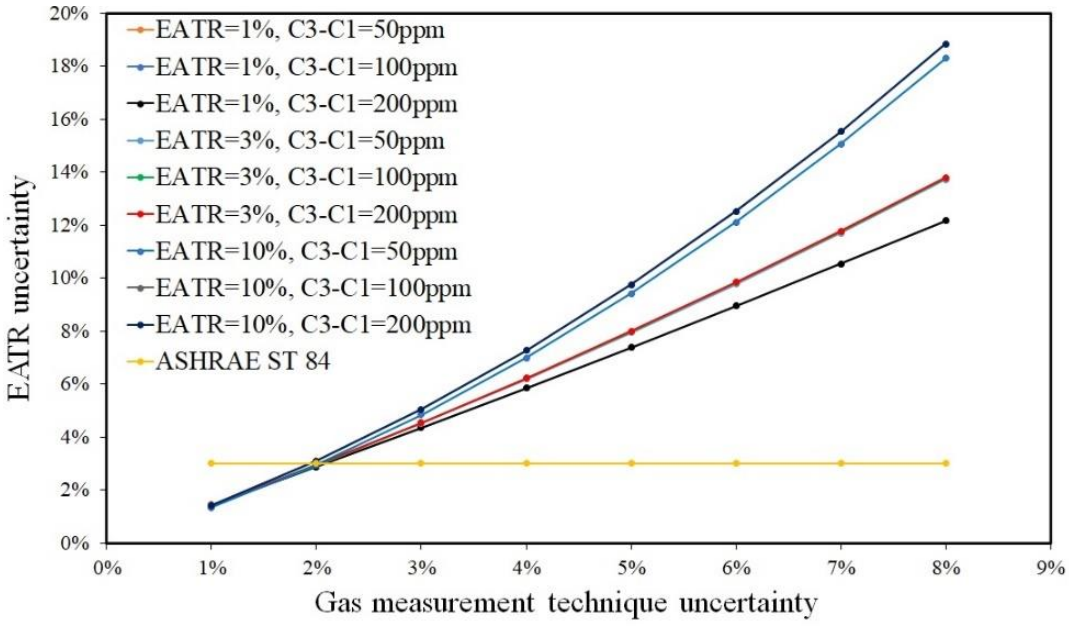

Figure B.1. The EATR uncertainty versus instrument uncertainty for different values of the EATR and ($C_3 - C_1$).

The photoacoustic spectroscopy technique with 1% uncertainty shows the lowest EATR uncertainty of less than 2%. The GC technique with 2% uncertainty shows the EATR uncertainty of less than 3%. The FTIR spectroscopy technique with 2% uncertainty [8] shows the EATR uncertainty less than 3%. However, gas detector tubes with an uncertainty between 5-10% leads to EATR uncertainty more than 3%. Therefore, the three gas measurement techniques, i.e., GC, FTIR spectroscopy, photoacoustic spectroscopy, when EATR is below 10% and $(C_3 - C_1)$ is between 50 to 200 ppm satisfy the EATR uncertainty recommended by ASHRAE Standard 84 [15].